ABSTRACT

KINEMATIC SYNTHESIS OF PLANAR FOUR BAR AND GEARED FIVE BAR MECHANISMS WITH STRUCTURAL CONSTRAINTS

by
Yahia Mohammad Saleh Al-Smadi

In motion generation, the objective is to calculate the mechanism parameters required to achieve or approximate a set of prescribed rigid-body positions. This doctoral dissertation study is aimed to integrate the classical kinematic analysis of a planar four-bar and geared five-bar motion generation with three structural design constraints. These constraints consider driving link static torque, deflection of the crank and buckling of the follower for a given rigid-body load or constant external load.

This kineto-elastostatic analysis is based on the following assumptions to be considered during the analysis; the crank and the follower are elastic members and the coupler is rigid member, friction in the joints is neglected, link weights are neglected compared to a given rigid-body load or constant external load, the cross sectional properties of a link do not vary, and finally the mechanism is moving in quasi static condition.

By incorporating these constraints into conventional planar four-bar and five-bar motion generation models, mechanisms are synthesized to achieve-not only prescribed rigid-body positions-but also satisfy the above mentioned structural constraints for a given rigid-body load or constant external load.

KINEMATIC SYNTHESIS OF PLANAR FOUR BAR AND GEARED FIVE BAR MECHANISMS WITH STRUCTURAL CONSTRAINTS

by
Yahia Mohammad Saleh Al-Smadi

A Dissertation
Submitted to the Faculty of
New Jersey Institute of Technology
in Partial Fulfillment of the Requirements for the Degree of
Doctor of Philosophy in Mechanical Engineering

Department of Mechanical Engineering

January 2009

APPROVAL PAGE

KINEMATIC SYNTHESIS OF PLANAR FOUR BAR AND GEARED FIVE BAR MECHANISMS WITH STRUCTURAL CONSTRAINTS

Yahia Mohammad Saleh Al-Smadi

11/24/08

Dr. Rajpal S. Sodhi, Dissertation Advisor — Date
Professor of Mechanical Engineering, NJIT
Chair of Mechanical Engineering Department, NJIT

11/24/08

Dr. Kevin Russell, Committee Member — Date
Armament Engineering and Technology Center
US Army Research, Development and Engineering Center
Picatinny Arsenal, NJ 07806

11/24/08

Dr. Bernard Koplik, Committee Member — Date
Professor of Mechanical Engineering, NJIT

11/24/2008

Dr. Zhiming Ji, Committee Member — Date
Associate Professor of Mechanical Engineering, NJIT

11/24/08

Dr. Sanchoy K. Das, Committee Member — Date
Professor of Industrial and Management Engineering, NJIT

BIOGRAPHICAL SKETCH

Author: Yahia Mohammad Saleh Al-Smadi

Degree: Doctor of Philosophy

Date: January 2009

Undergraduate and Graduate Education:

- Doctor of Philosophy in Mechanical Engineering,
  New Jersey Institute of Technology, Newark, NJ, USA, 2009

- Master of Science in Manufacturing Systems Engineering,
  New Jersey Institute of Technology, Newark, NJ, USA, 2002

- Bachelor of Science in Mechanical Engineering,
  Jordan University of Science and technology, Irbed, Jordan, 1999

Major: Mechanical Engineering

Presentations and Publications:

Yahia M. Al-Smadi
"Computer Aided Design/Engineering for Trunnion Girder Design on Water Street Bridge,"
Heavy Movable Structures Symposium, Orlando, FL, November 3-6, 2008.

Yahia M. Al-Smadi, Kevin Russell, Raj S. Sodhi
"On the Design of Traveler Parking Brake System,"
Journal of Bridge Engineering, Submitted October, 2008.

Yahia M. Al-Smadi, Kevin Russell, Raj S. Sodhi
"Geared Five-Bar Path Generators with Structural Conditions,"
Journal of Inverse Problems in Science and Engineering, Submitted July, 2008.

Yahia M. Al-Smadi, Qiong Shen, Kevin Russell, Raj S. Sodhi
"Geared Five-Bar Motion Generators with Structural Conditions,"
Journal of Mechanism and Machine Theory, Submitted July, 2008.

Yahia M. Al-Smadi, Kevin Russell, Raj S. Sodhi
"Kinematic Synthesis of Planar Four-Bar Path Generators with Structural Conditions,"
Journal of Mechanical Research Communications, Submitted July, 2008.

Yahia M. Al-Smadi, Kevin Russell, Raj S. Sodhi
"Kinematic Synthesis of Planar Four-Bar Motion Generators with Structural Constraints,"
Journal of Multi Body Dynamics, Submitted June, 2008.

Yahia M. Al-Smadi, Kevin Russell, Raj S. Sodhi
"Planar Four-Bar Path Generators with Structural Conditions,"
JSME Journal of Mechanical Design, Systems, and Manufacturing, Vol. 2, No. 5 2008, 926-936.

Yahia M. Al-Smadi, Kevin Russell, Raj S. Sodhi
"Planar Four-Bar Motion Generators with Structural Conditions,"
ASME Journal of Advanced Machine and Robotics , In-Press, November 2008.

Qiong Shen, Yahia M. Al-Smadi, Kevin Russell, Raj S. Sodhi
"On Planar Five-bar Motion Generation with a Driver Torque Constraint,"
JSME Journal of Mechanical Design, Systems, and Manufacturing, Vol. 2, No. 3, 2008, 408-416.

Qiong Shen, Yahia M. Al-Smadi, Peter J. Martine, Kevin Russell, Raj S. Sodhi
"An Extension of Design Optimization for Motion Generation,"
Journal of Mechanism and Machine Theory, In-Press, 2008.

Yahia M. Al-Smadi, Qiong Shen, Kevin Russell, Raj S. Sodhi
"Planar Four-Bar Motion Generation with Prescribed Static Torque and Rigid-Body Reaction Force,"
Journal of Mechanics Based Design of Structures and Machines, In Press, 2008.

Yahia Al-Smadi and Herbert Protin
"Thinking Outside the Box – Using Small Diameter Sheaves,"
Heavy Movable Structures Symposium, Orlando, FL, November 1-3, 2006.

David Thurnher, Herbert Protin, Yahia Al-Smadi
"Erie Canal Lift Bridges-Historic Towerless Lift Bridges and How They Work,"
Heavy Movable Structures Symposium, Orlando, FL, November 1-3, 2006.

وَقُل رَّبِّ زِدْنِي عِلْمًا ﴿١١٤﴾

القرآن , سورة طه 114

(And say: "My Lord, Increase me in knowledge" Al-Quran, Ta-Ha [20:114]

قال رسول اللّه صَلّى اللّه عليْهِ وسَلّم

« إن الملائكة لتضع أجنحتها لطالب العلم رضا بما يصنع . »

The Messenger of Allah "peace be upon him" said, "Verily, the angels lower their wings for the seeker of knowledge out of pleasure of what he is doing."

أخي لن تنال العلم إلا بستة سأنبيك عن تفصيلها ببيان
ذكاء وحرص واجتهاد وبلغة وصحبة أستاذ وطول زمان

O Brother, you will not acquire knowledge except through six
I will inform you of them precisely
Intelligence, eagerness, studious, and goals
And a company of a master, and a long time

For my beloved mom and dad

For every smile you've brought to my heart… For every wise word of encouragement you've shared… For every time you've been there for me when I needed you most… I'm so thankful for the gift of you in my life. I ask ALLAH (SWT) to grant you Jannah and tranquil life.

For my beloved wife

I will never forget your support and encouragement, the times you stood beside me and still you are. Thank you so much for your effort, love and patience. May ALLAH (SWT) reward you with Jannah.

For my beloved sons Muhammad and AbdulRahman

For you Sons with loving thoughts, how very special you are. May ALLAH (SWT) shower you with mercy and satisfaction; always show him the best of your selves. I love you so much.

For my beloved family

The help and support of was your greatest gift of all. I can not express my gratitude to you. Thank you

ACKNOWLEDGMENT

I would like to thank Almighty Allah (SWT) for His countless blessings throughout my life.

I would like to express my deepest appreciation to Prof. Rajpal S. Sodhi, who not only served as my research supervisor, but also providing insight and intuition. I would also like to acknowledge Dr. Kevin Russell, in giving me constantly support and reassurance. Special thanks are given to Dr. Bernard Koplik, Dr. Zhiming Ji and Dr. Sanchoy K. Das for actively participating in my committee.

I would like to like to express my gratitude to Dr. Mohammad T. Khasawneh and Dr. Mohammad I. Younis for their help and encouragement.

Many thanks for my fellow engineers at Parsons; Omar Khair-Eldin, Ammar Zalt, and Iftekhar Chaudry are deserving recognition for their support.

I would like to sincerely thank my dear friend Bashar I. Dweiri for his support and encouragement throughout my academic career.

TABLE OF CONTENTS

TABLE OF CONTENTS
(Continued)

Chapter **Page**

TABLE OF CONTENTS
(Continued)

Chapter **Page**

LIST OF TABLES

LIST OF FIGURES

LIST OF FIGURES
(Continued)

LIST OF FIGURES
(Continued)

Figure **Page**

LIST OF FIGURES
(Continued)

Figure **Page**

CHAPTER 1

INTRODUCTION

1.1 Mechanism Synthesis and Motion Generation

Mechanism synthesis involves the determination of the particular mechanism variables required to approximate particular (specified) mechanism output. Motion generation is a discipline in mechanism synthesis in which a moving rigid body passes through prescribed positions in sequence, it involves the determination of the particular mechanism variables required to approximate particular (specified) rigid-body orientations. In the formulation of motion generation three points are defined on the coupler of the mechanism and the object is to find the coordinates of moving pivots and fixed pivots. The orientation of the coupler is very important during the mechanism operation. There are so many industrial usage examples for motion generation mechanisms such as tripper/dump truck shown in Figure 1.1 [49], the bucket (coupler) on the truck is moving in a certain desired set of positions in order to elevate, dump the waste, and go back to the initial position. One of the biggest challenges in the mechanism synthesis faces the designer is the space limitation in which the working envelope of the machine is defined, motion generation synthesis is the best option to consider, it detect the right orientation of the rigid body and avoid interference with adjacent objects.

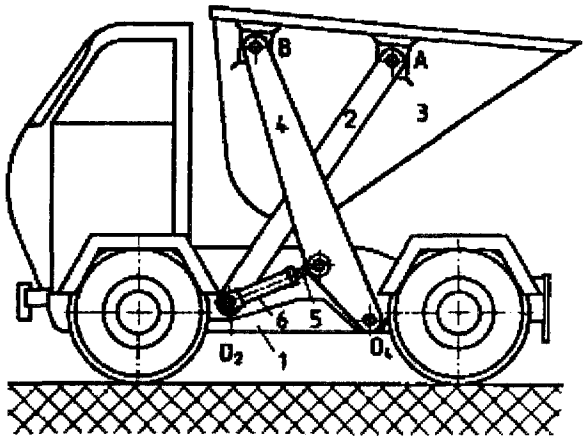

Figure 1.1 Tripper/Dump truck schematic.

Motion generation is different from other classes of mechanism synthesis like path and function generation. In Path generation, the mechanism is synthesized so that the path of the rigid body is a concern regardless the orientation of the coupler. Function generation refers to the mechanism synthesis where the output motion of the rigid body s a function of the input motion.

1.2 Planar Four-Bar Motion Generation

Planar Four-bar motion generation method (as illustrated in Figure 1.2) is very well established field, user can only calculate the mechanism parameters required to achieve or approximate a set of prescribed rigid-body positions. Parameters are two fixed pivots $\mathbf{a}_0$ and $\mathbf{b}_0$ and two moving pivots $\mathbf{a}_1$ and $\mathbf{b}_1$, the crank is the member connects between the fixed pivot $\mathbf{a}_0$ or $\mathbf{f}_0$ and the corresponding moving pivot $\mathbf{a}_1$or $\mathbf{m}_1$ with a link length of R_1. The follower is the mechanism member connects the fixed pivot $\mathbf{b}_0$ and $\mathbf{b}_1$, with a link length of R_2. The last moving member in the mechanism is the coupler that connects the moving pivots $\mathbf{a}_1$ and $\mathbf{b}_1$.

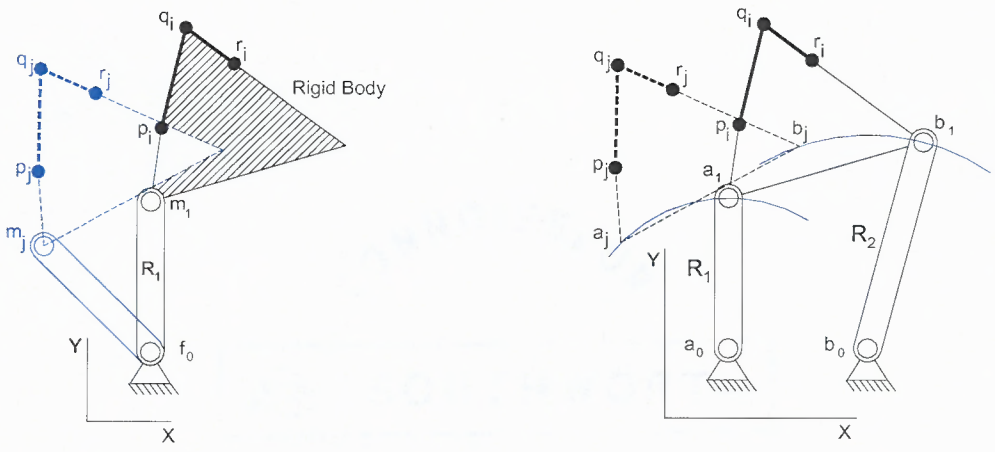

Figure 1.2 Four-bar motion generation mechanism.

When using this conventional planar mechanism synthesis model (constant link model) to calculate the coordinates of the fixed pivot $\mathbf{a}_0$ and the moving pivot $\mathbf{a}_1$ (there are four unknown variables in the crank link $\mathbf{a}_0\mathbf{a}_1$ (a_{0x}, a_{0y}, a_{1x}, a_{1y},)), the user can specify a maximum of four rigid body positions, when the scalar link variables R_1 is prescribed. This is also applicable for the follower link $\mathbf{b}_0\mathbf{b}_1$.

If a range for a_{0x} is specified, a locus of fixed and moving pivot solutions is illustrated in Figure 1.3a, where the upper curve (blue) is for the moving pivots $\mathbf{a}_1$ and $\mathbf{b}_1$, and the lower curve (red) is for the fixed pivots $\mathbf{a}_0$ and $\mathbf{b}_0$. User can choose any two points to represent the fixed pivots $\mathbf{a}_0$ and $\mathbf{b}_0$, and choose the corresponding moving pivots $\mathbf{a}_1$ and $\mathbf{b}_1$ as shown in Figure 1.3b.

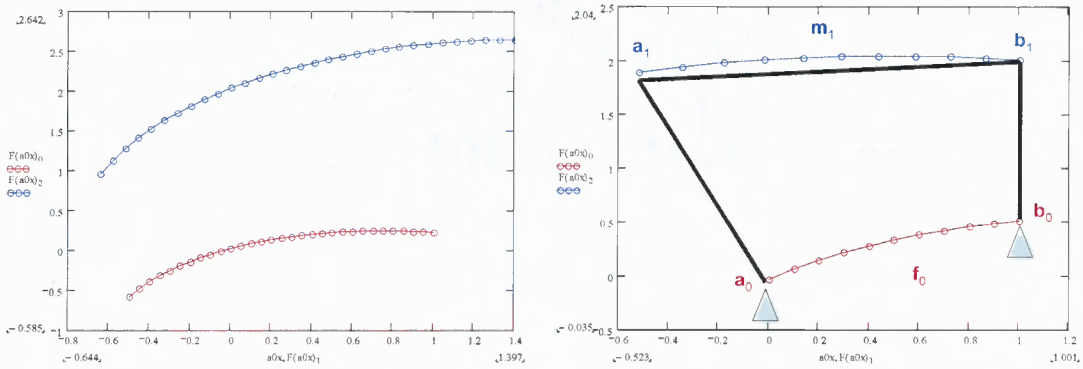

(a) (b)

Figure 1.3 Solutions for four-bar motion generation (a) A locus of fixed and moving pivots (b) Arbitrary four-bar solution.

Industrial applications for motion generation mechanism can be found nearly every where. Loading machine shown in Figure 1.4 [47] is a four-bar mechanism moves the boxes from the upper station to the lower station, so the coupler must move in specific orientation and defined positions in order to perform the job efficiently.

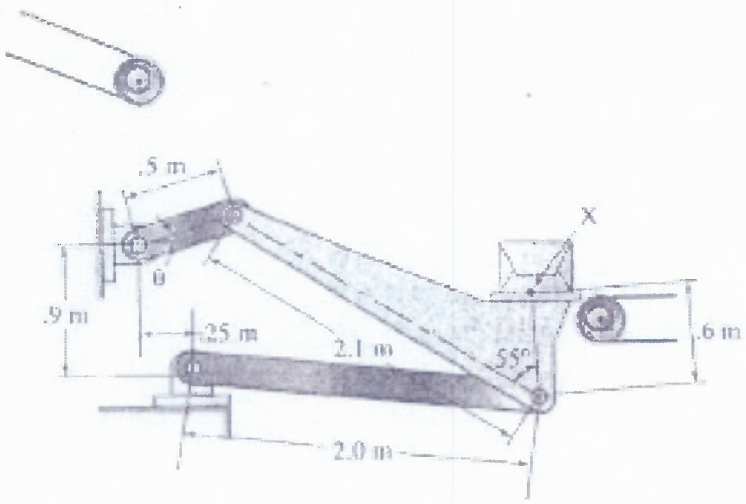

Figure 1.4 Four-bar loading mechanism.

1.3 Planar Five-bar Motion Generation

Figure 1.5 illustrates the planar five-bar motion generator. User can only calculate the mechanism parameters required to achieve or approximate a set of prescribed rigid-body positions. Parameters are two fixed pivots $\mathbf{a}_0$ and $\mathbf{b}_0$ and three moving pivots $\mathbf{a}_1$, $\mathbf{b}_1$, and $\mathbf{c}_1$. The crank is the member connects between the fixed pivot $\mathbf{a}_0$ and the corresponding moving pivot $\mathbf{a}_1$, with a link length of R_1. The follower is the mechanism member connects the fixed pivot $\mathbf{b}_0$ and $\mathbf{b}_1$, with a link length of R_2, link $\mathbf{b}_1\mathbf{c}_1$has two moving pivots $\mathbf{c}_1$ and $\mathbf{b}_1$ with a link length of R_3, the last moving member in the mechanism is the coupler that connects the moving pivots $\mathbf{a}_1$ and $\mathbf{c}_1$.

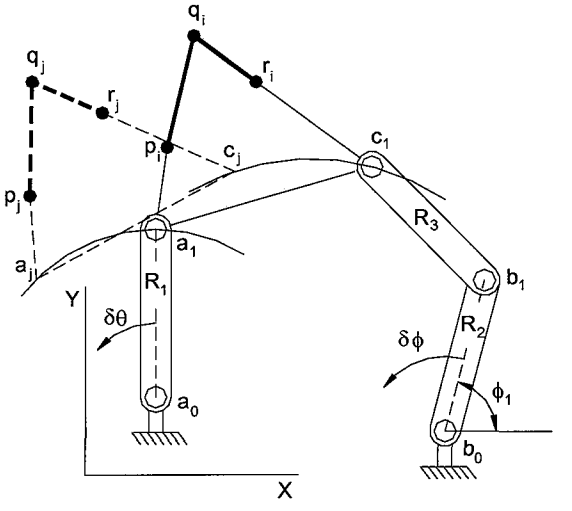

Figure 1.5 Five-bar motion generation.

Links $\mathbf{a}_0\mathbf{a}_1$ and $\mathbf{b}_0\mathbf{b}_1$ are the driving links (denoted by driving link angles θ and ϕ). When using planar mechanism synthesis model (constant link model) to calculate the coordinates of the fixed pivot $\mathbf{a}_0$ and the moving pivot $\mathbf{a}_1$ (there are four unknown variables in the crank link $\mathbf{a}_0\mathbf{a}_1$ (a_{0x}, a_{0y}, a_{1x}, a_{1y}), the user can specify a maximum of four rigid body positions, when a_{0x} and the scalar link variables R_1 are prescribed.

This is also applicable for the follower link $\mathbf{b}_1\mathbf{c}_1$. However, moving pivot $\mathbf{b}_1$ is a function of prescribed value of fixed pivot $\mathbf{b}_0$, scalar link length R_2, and displacement angle ϕ, where ϕ is a function of θ through specific ratio determined by the power transmission system. If gears, chains or belts are used in the mechanism joining links a0a1 and b0b1, $\delta\phi = K.\theta\delta$ where K is the gear (Figure 1.6), sprocket or pulley ratio. If motors are used, $\delta\phi$ can be prescribed independently from $\delta\theta$.

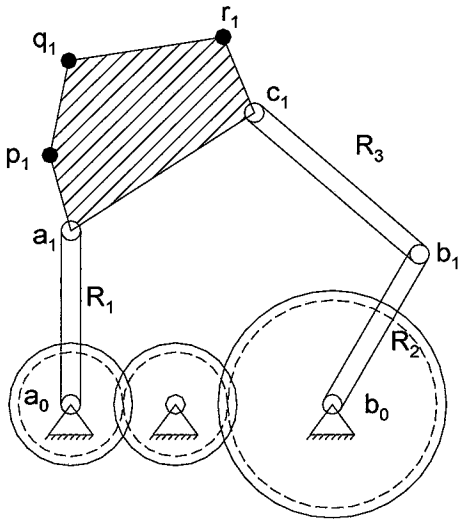

Figure 1.6 Synthesized five-bar mechanism.

Figure 1.7 [47] is a five-bar loading mechanism moves the boxes between two stations, the working envelop and orientations of the carrying block (coupler) throughout the full range of motion are fully defined.

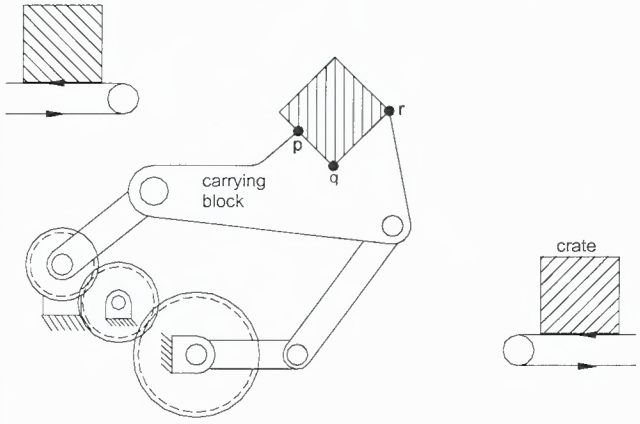

Figure 1.7 Five-bar loading mechanism.

1.4 Research Objectives

The author focuses in this research to follow the path (bold line) described in Figure 1.8 for the mechanism synthesize, the scope in the mechanism synthesize is to analyze single phase planar four-bar motion generation and single phase planar five-bar motion generation using conventional methods with new structural constraints, However the research can be modified to other modules shown in the same figure.

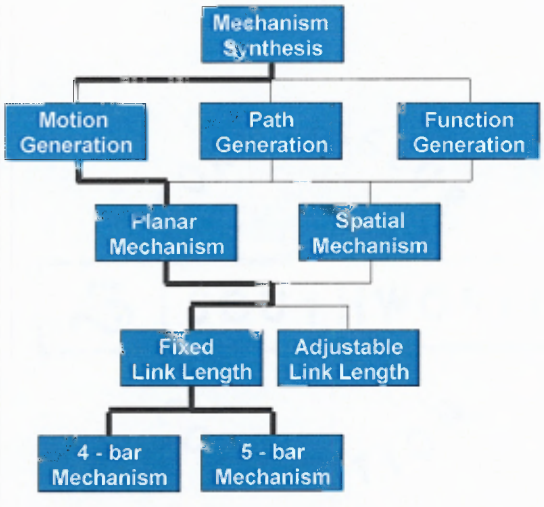

Figure 1.8 Research path in the area of mechanism synthesis.

The focus of this research is to study the mechanism synthesis considering the structural considerations. Usually, the design process for any mechanism as illustrated in Figure 1.9 starts first with calculating the parameters involved in the motion generation model, the fixed and the moving pivots are found as well as the lengths of all links are also found. Then the designer takes the synthesized mechanism step further and apply the loads on the mechanism and calculate for the reaction loads and the required driving torque, the traditional design process is concluded by applying the strength of material principles on the mechanism members which they include, stresses, deflections, buckling, vibration, etc. (third block in Figure 1.9).

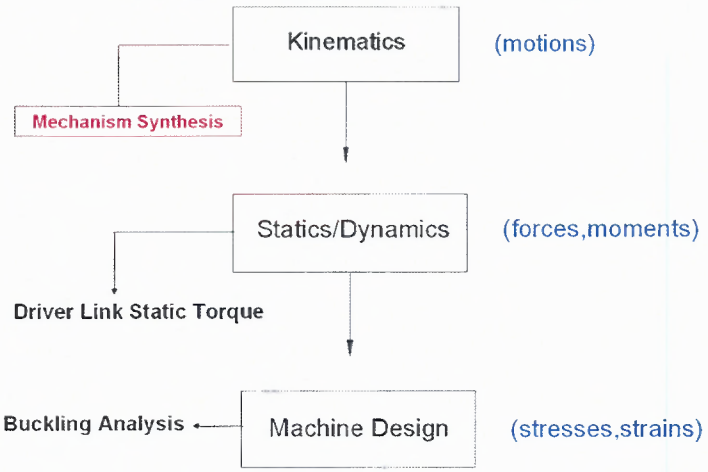

Figure 1.9 Conventional process for mechanism design.

All the design steps described in Figure 1.9 can be grouped together into one genuine and comprehensive model where the mechanism synthesizes is still the core of the new design process. New formulation of driving torque and strength of material will be integrated with the numerical mechanism synthesis algorithms. The target of Chapters 2 and 3 is to synthesis a planar four-bar and five-bar motion generation under external/rigid-body load and driving static torque at certain positions, so the

achieved mechanism will pass through or approximate a set of prescribed position at the same time it will achieve a driving static torque at certain position. These chapters will combine the first two modules of traditional design process described in Figure 1.9.

Chapters 4 and 5 focus on the mechanism synthesis for planar four-bar and five-bar motion generation considering external/rigid-body loads, and the structural constraints are; First, limiting the required driving or motor torque not to go beyond specified torque value. Second, preventing the deflection in the crank exceeds a prescribed deflection value. Finally, designing the follower in four-bar or link $\mathbf{b}_1\mathbf{c}_1$ in five-bar to prevent buckling under the compressive reaction loads. Chapters 4 and 5 bundle all modules shown in Figure 1.9 into one algorithm or design process as shown in Figure 1.10.

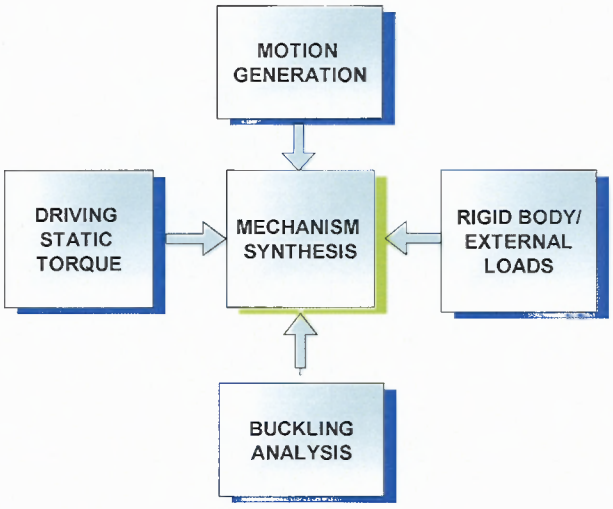

Figure 1.10 New mechanism design process.

1.5 Research Structure

The research is structured to four motion generation topics; Chapters 2 and 3 start with formulation of conventional motion generation model, derivation of torque constraint, example problem then discussion. Chapters 4 and 5 include what has been done in CMMhapters 2 and 3 in addition to formulation of deformation and buckling constraints. An optimization model which consists of the formulation of the structural constraints, followed by a numerical example and finally the results are discussed. Software that are used in the research are MathCAD to codify the synthesis algorithms and extract the mechanism parameters, Solidworks to model the mechanism members, ADAMS dynamic modeler to extract the dynamic parameters such as reactions and torques, and AutoCAD to draw the mechanism in each position.

CHAPTER 2

PLANAR FOUR-BAR MOTION GENERATION WITH PRESCRIBED STATIC TORQUE AND RIGID-BODY REACTION FORCE

2.1 Introduction

2.1.1 Motion Generation

In Figure 2.1, four prescribed rigid-body positions are defined by the x and y-coordinates of variables **p**, **q** and **r** and the calculated mechanism parameters are the x and y-coordinates of fixed pivot variables $\mathbf{a}_0$ and $\mathbf{b}_0$ and moving pivot variables $\mathbf{a}_1$ and $\mathbf{b}_1$. Motion generation for planar four-bar mechanisms is a well-established field. Recent contributions include the work of Yao and Angeles [14] who applied the contour method in the approximate synthesis of planar linkages for rigid-body guidance. Hong and Erdman [11] introduced a new application Burmester curves for adjustable planar four-bar linkages. Zhou and Cheung [16] introduced an optimal synthesis method of adjustable four-bar linkages for multi-phase motion generation. Al-Widyan, Angeles and Jesús Cervantes-Sánchez [7] considered the robust synthesis of planar four-bar linkages for motion generation.

Danieli, Mundo and Sciarra [9] applied Burmester theory in the design of planar four-bar motion generators to reproduce tibia-femur relative motion. Martin, Russell and Sodhi [12] presented an algorithm for selecting planar four-bar motion generators with respect to Grashof, transmission angle and mechanism perimeter conditions. Goehler, Stanisic and Perez [10] applied parameterized T1 motion theory to the synthesis of planar four-bar motion generators. Caracciolo and Trevisani [8] considered rigid-body motion control of flexible four-bar linkages. Zhixing,

Hongying, Dewei and Jiansheng [15] presented a guidance-line rotation method of rigid-body guidance for the synthesis of planar four-bar mechanisms. Sodhi and Russell [13] also considered motion generation of planar four-bar mechanisms with prescribed rigid-body position tolerances.

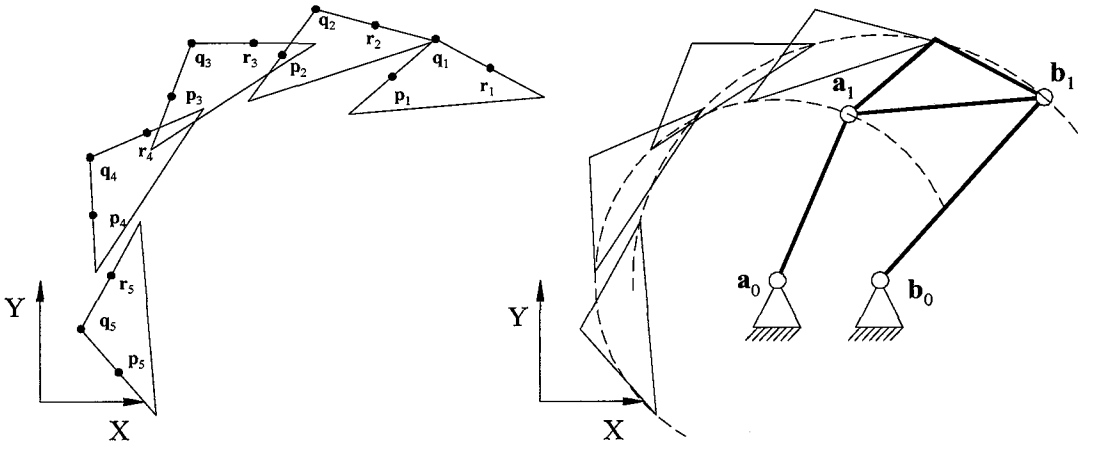

Figure 2.1 Prescribed rigid-body positions and calculated planar four-bar mechanism.

2.1.2 Motivation and Scope of Work

Using conventional motion generation methods (Suh and Radcliffe [1] and Sandor and Erdman, [2]), the user can only calculate the mechanism parameters required to achieve or approximate a set of prescribed rigid-body positions. Although such solutions are useful for preliminary kinematic analyses, other factors (e.g., static loads, dynamic loads, stresses, strains, etc.) must be considered prior to fabricating a physical prototype of the mechanical design. This work considers static driving link torque given a rigid-body load. By incorporating the new static torque constraint into conventional planar four-bar motion generation models (Suh and Radcliffe [1] and Sandor and Erdman [2]), planar four-bar mechanisms are synthesized to achieve-not

only prescribed rigid-body positions-but also satisfy driver static torque for a given rigid-body load.

2.2 Conventional Planar Four-bar Motion Generation

Equations (2.1) through (2.3) encompass the planar four-bar motion generation model presented by Suh and Radcliffe [1]. Equations (2.1) and (2.2) are "constant length" constraints and ensure the constant lengths of links $\mathbf{a}_0\mathbf{a}_1$ and $\mathbf{b}_0\mathbf{b}_1$. Variables L_1 and L_2 in Equations (2.1) and (2.2) are the prescribed scalar lengths of links $\mathbf{a}_0\mathbf{a}_1$ and $\mathbf{b}_0\mathbf{b}_1$, respectvely. Equation (2.3) is a rigid-body planar displacement matrix. When using this conventional planar mechanism synthesis model to calculate the coordinates of the fixed pivots $\mathbf{a}_0$ and $\mathbf{b}_0$ and the moving pivots $\mathbf{a}_1$ and $\mathbf{b}_1$ (where $\mathbf{a}_0 = [a_{0x}, a_{0y}, 1]$, $\mathbf{a}_1 = [a_{1x}, a_{1y}, 1]$, $\mathbf{b}_0 = [b_{0x}, b_{0y}, 1]$ and $\mathbf{b}_1 = [b_{1x}, b_{1y}, 1]$), the user can specify a maximum of four rigid-body positions when the scalar link variables L_1 and L_2 are specified.

$$\left(\left[\mathbf{D}_{1j}\right]\mathbf{a}_1 - \mathbf{a}_0\right)^T \left(\left[\mathbf{D}_{1j}\right]\mathbf{a}_1 - \mathbf{a}_0\right) - L_1^2 = 0 \tag{2.1}$$

$$\left(\left[\mathbf{D}_{1j}\right]\mathbf{b}_1 - \mathbf{b}_0\right)^T \left(\left[\mathbf{D}_{1j}\right]\mathbf{b}_1 - \mathbf{b}_0\right) - L_2^2 = 0 \tag{2.2}$$

$$\left[\mathbf{D}_{1j}\right] = \begin{bmatrix} p_{jx} & q_{jx} & r_{jx} \\ p_{jy} & q_{jy} & r_{jy} \\ 1 & 1 & 1 \end{bmatrix} \begin{bmatrix} p_{1x} & q_{1x} & r_{1x} \\ p_{1y} & q_{1y} & r_{1y} \\ 1 & 1 & 1 \end{bmatrix}^{-1} \tag{2.3}$$

where $j = 1, 2, 3, 4$

In conventional motion generation, three points (**p**, **q**, and **r**) on the coupler body are defined. If the coupler points lie on the same line (prohibited), displacement matrix $[\mathbf{D}_{1j}]$ (Equation (2.3)) becomes proportional with proportional rows, this matrix could not be inverted.

2.3 Driver Link Static Torque

With an external load **F** acting on the rigid-body of the planar four-bar mechanism, a driving link torque **T** achieves static equilibrium. In Figure 2.2, the load **F** is applied at the arbitrary rigid-body point **q**.

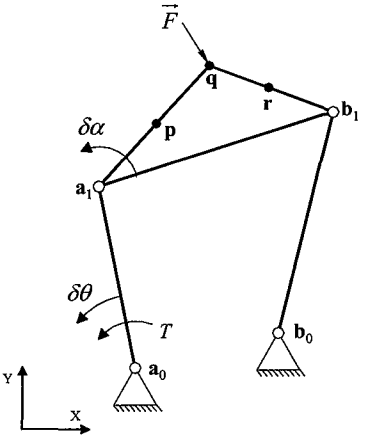

Figure 2.2 Planar four-bar mechanism with applied load.

To formulate the driver link static torque constraint, the moment condition $\Sigma\mathbf{M}=0$ is considered about the moving pivot $\mathbf{a}_1$ as illustrated in Figure 2.3, the moving pivot reaction loads $\mathbf{R}_{a1}$ and $\mathbf{R}_{b1}$ are also considered in the moment condition.

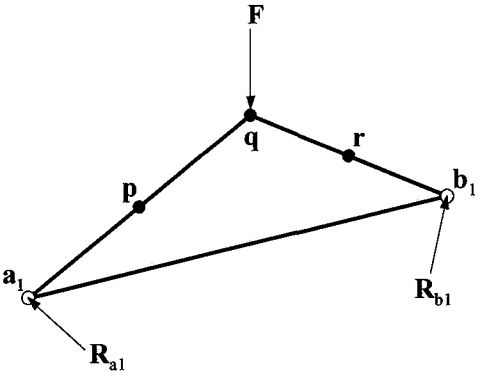

Figure 2.3 Coupler with applied load.

The resulting equilibrium equation of the moments about the moving pivot $\mathbf{a}_1$ is

$$\overrightarrow{a_1b_1} \times \mathbf{R}_{b1} - \overrightarrow{a_1q} \times \mathbf{F} = 0 \tag{2.4}$$

where

$$\mathbf{R}_{b1} = R_b \frac{\overrightarrow{b_0b_1}}{\left|\overrightarrow{b_0b_1}\right|} \tag{2.5}$$

And the reaction load R_b is a real number that varies with the mechanism driver position. By substituting Equation (2.5) into Equation (2.4) and solve for R_b, Equation (2.4) becomes

$$R_b = \frac{\left|\overrightarrow{a_1q} \times \mathbf{F}\right|}{\left|\overrightarrow{a_1b_1} \times \frac{\overrightarrow{b_0b_1}}{\left|\overrightarrow{b_0b_1}\right|}\right|} \tag{2.6}$$

Because link $\mathbf{b}_0\mathbf{b}_1$ is a two-force member, vectors $\mathbf{R}_{b1}$ and $\overrightarrow{b_0b_1}$ are collinear and subsequently result in a zero cross product. Equation (2.5) can be written as

$$\mathbf{R}_{b1} = \frac{\left|\overrightarrow{a_1q} \times \mathbf{F}\right|}{\left|\overrightarrow{a_1b_1} \times \overrightarrow{b_0b_1}\right|} \overrightarrow{b_0b_1} \tag{2.7}$$

Next, the force condition $\Sigma\mathbf{F}=0$ is considered for the coupler as illustrated in Figure 2.2. The resulting equilibrium equation of the forces is

$$\mathbf{R}_{a1} = -\mathbf{R}_{b1} - \mathbf{F} \tag{2.8}$$

Substituting Equation (2.7) into Equation (2.8) and solve for $\mathbf{R}_{a1}$

$$\mathbf{R}_{a1} = -\frac{\left|\overrightarrow{a_1q} \times \mathbf{F}\right|}{\left|\overrightarrow{a_1b_1} \times \overrightarrow{b_0b_1}\right|} \overrightarrow{b_0b_1} - \mathbf{F} \tag{2.9}$$

Next, the moment condition $\Sigma\mathbf{M}=0$ is considered about the fixed pivot $\mathbf{a}_0$ as illustrated in Figure 2.4, the moving pivot reaction loads $\mathbf{R}_{a1}$ is considered in the moment condition.

$$\mathbf{T}-\overrightarrow{a_0a_1}\times(-\mathbf{R}_{a1})=0 \tag{2.10}$$

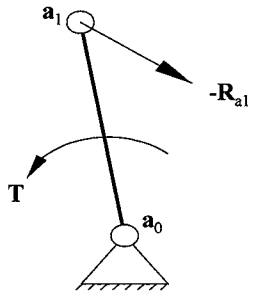

Figure 2.4 Driver link with static torque **T** and reaction load $\mathbf{R}_{a1}$.

The required driving torque to achieved equilibrium of the crank is

$$\mathbf{T}=\overrightarrow{a_0a_1}\times\left(-\frac{\left|\overrightarrow{a_1q}\times\mathbf{F}\right|}{\left|\overrightarrow{a_1b_1}\times\overrightarrow{b_0b_1}\right|}\overrightarrow{b_0b_1}-\mathbf{F}\right) \tag{2.11}$$

where

$$\mathbf{F}=\begin{pmatrix}f_x\\f_y\\0\end{pmatrix},\mathbf{T}=\begin{pmatrix}0\\0\\\tau_j\end{pmatrix},\overrightarrow{a_1q}=\mathbf{q}_j-\left[\mathbf{D}_{1j}\right]\mathbf{a}_1,\overrightarrow{a_0a_1}=\left[\mathbf{D}_{1j}\right]\mathbf{a}_1-\mathbf{a}_0,\ \overrightarrow{b_0b_1}=\left[\mathbf{D}_{1j}\right]\mathbf{b}_1-\mathbf{b}_0,\text{ and}$$

$$\overrightarrow{a_1b_1}=\left[\mathbf{D}_{1j}\right]\left(\mathbf{b}_1-\mathbf{a}_1\right),\ j=1,2,3,4$$

Equation (2.11) calculates the four-bar mechanism driver static torque for a given rigid-body load. Equations (2.1), (2.2) and (2.12) constitute a set of nine simultaneous equations to calculate nine of the 10 possible unknown variables of the planar four-bar mechanism (a_{0x}, a_{0y}, a_{1x}, a_{1y}, b_{0x}, b_{0y}, b_{1x}, b_{1y}, L_1 and L_2).

2.4 Example Problem

Table 2.1 includes the x and y-coordinates (in inches) of four prescribed traveler brake pad mount positions. The brake pad mount is the coupler for a four-bar braking mechanism to be synthesized. To ensure effective braking, the prescribed normal force for the brake pad and mount must reach 1500lbs. A prescribed driver static torque of 1600in-lbs is also prescribed to achieve the corresponding prescribed normal force. The brake pad is to be fully applied at position 4 and fully released at position 2. To ensure that the brake is fully released at position 1, the y-displacement of rigid-body variable **q** between positions 1 and 4 must exceed 0.12 inches.

Using Equations (2.1), (2.2) and (2.11) with a prescribed range of a_{0x} = -6,-5.9...-5 and initial guesses of a_{0y} = -10, $\mathbf{a}_1$ = (-2, -4), L_1 = 20, $\mathbf{b}_0$ = (3, -10), $\mathbf{b}_1$ = (2, -4), L_2 = 20, solution loci for $\mathbf{a}_0$, $\mathbf{a}_1$, $\mathbf{b}_0$, $\mathbf{b}_1$ were calculated and plotted (Figure 2.5). From the braking mechanism solution loci, a multitude of individual four-bar braking mechanisms can be selected. Figure 2.5 also includes a selected mechanism solution where $\mathbf{a}_0$ = (-5.5, -10.3213), $\mathbf{a}_1$ = (-3.7992, -4.1652), $\mathbf{b}_0$ = (0.7583, -11.3729) and $\mathbf{b}_1$ = (2.6765, -3.4786). The achieved rigid-body positions for the selected mechanism are listed in Table 2.2.

To achieve positions 2 through 4 in Table 2.2, link $\mathbf{a}_0$-$\mathbf{a}_1$ rotates counterclockwise 1.3805, 3.3907 and 5.4037 degrees, respectively. A static analysis of the braking mechanism solution using ADAMS (Figure 2.6) confirms that the prescribed 1500lb brake pad normal force and corresponding 1600in-lb driver static torque are achieved. The complete four-bar traveler braking mechanism is illustrated in Figures 2.7 and 2.8. The calculated solution loci for a0, a1, b0, b1 include a

multitude of four-bar braking mechanism solutions. Figure 2.9 includes an alternate mechanism solution where a0 = (-5, -9.1267), a1 = (-3.3073, -2.9803), b0 = (4.7002, -12.1762) and b1 = (6.8351, -2.5639). The achieved rigid-body positions for the alternate mechanism are listed in Table 2.3. To achieve positions 2 through 4 in Table 2.3, link a0a1 rotates counterclockwise 1.3749, 3.3997 and 5.3905 degrees, respectively. For the alternate mechanism selection (like the previous selection) the prescribed 1500lb brake pad normal force and corresponding 1600in-lb driver static torque have been confirmed to be satisfied using ADAMS.

Table 2.1 Prescribed Rigid-body Positions (f=1500lbs, τ_4=1600in-lb)

	p	q	r
Pos 1	-2.0118, -3.6916	0.5833, -2.1864	3.1844, -3.6811
Pos 2	-2.1602, -3.6537	0.4359, -2.1503	3.0359, -3.6469
Pos 3	-2.3781, -3.6045	0.2192, -2.1032	2.8180, -3.6018
Pos 4	-2.5981, -3.5624	0, -2.0624	2.5980, -3.5624

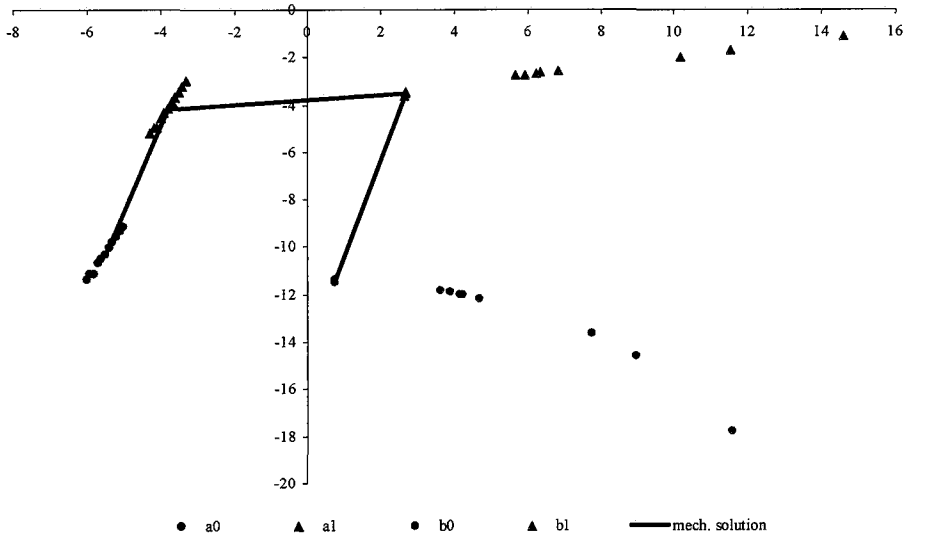

Figure 2.5 Mechanism solution loci and selected mechanism.

Table 2.2 Rigid-body Positions Achieved by Synthesized Planar Four-bar Mechanism

	p	q	r
Pos 1	-2.0118, -3.6916	0.5833, -2.1864	3.1844, -3.6811
Pos 2	-2.1603, -3.6537	0.4359, -2.1503	3.0359, -3.6469
Pos 3	-2.3782, -3.6045	0.2192, -2.1032	2.8180, -3.6018
Pos 4	-2.5981, -3.5624	-0.0000, -2.0625	2.5981, -3.5624

Note: $|q_{1y}-q_{4y}|$=0.1239in which exceeds the 0.12in minimum

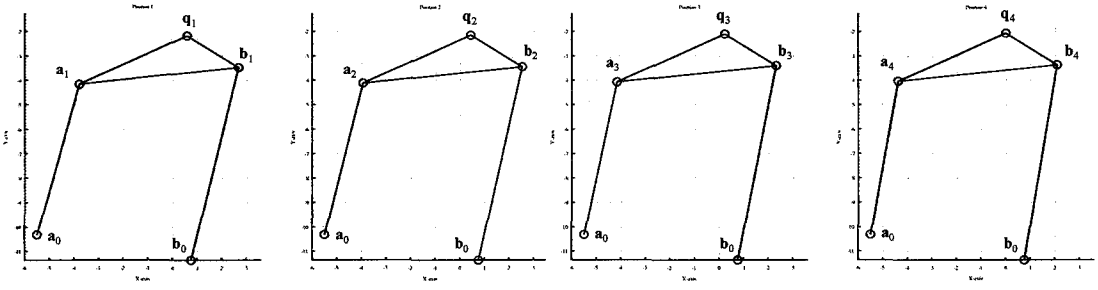

Figure 2.6 Four-bar mechanism positions in static analysis (τ_4=1600 in-lb).

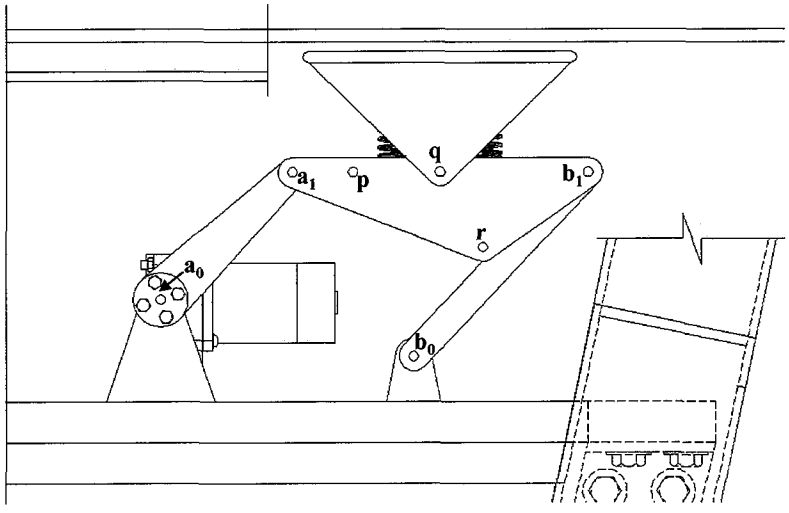

Figure 2.7 Four-bar mechanism and mechanism variables.

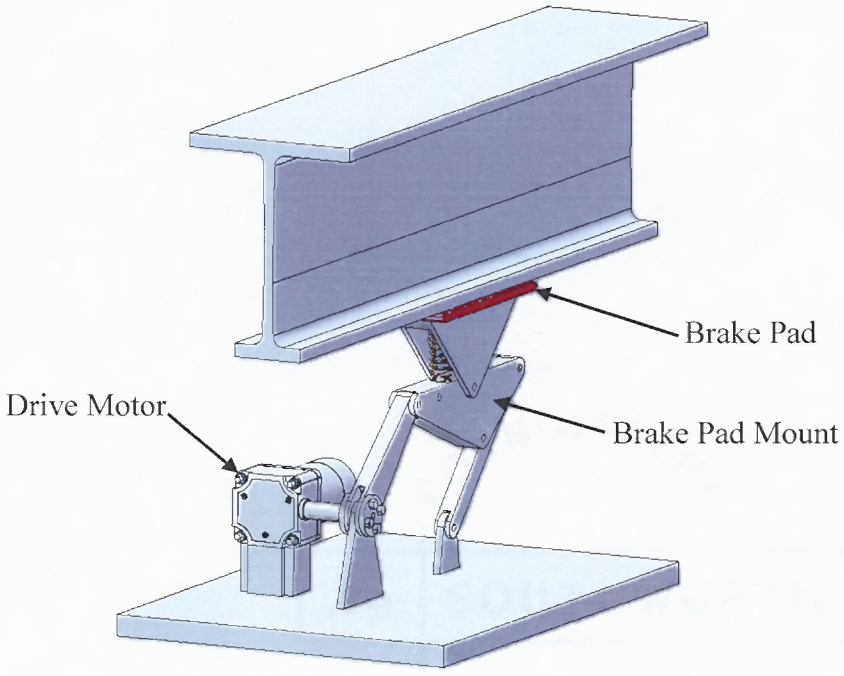

Figure 2.8 Four-bar braking mechanism.

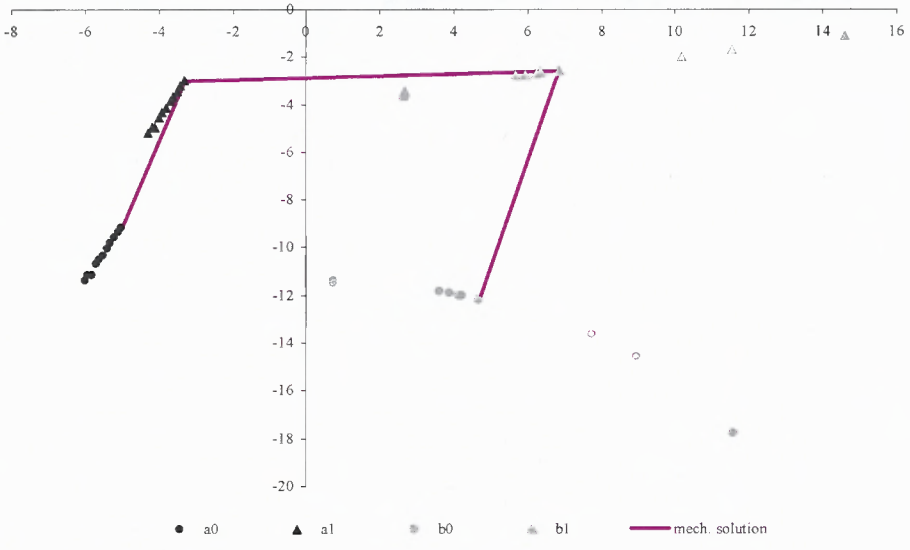

Figure 2.9 Mechanism solution loci and alternate mechanism selection.

Table 2.3 Rigid-body Positions Achieved by Alternate Planar Four-bar Mechanism

	p	q	r
Pos 1	-2.0118, -3.6916	0.5833, -2.1864	3.1844, -3.6811
Pos 2	-2.1603, -3.6537	0.4359, -2.1503	3.0359, -3.6469
Pos 3	-2.3782, -3.6045	0.2192, -2.1032	2.8180, -3.6018
Pos 4	-2.5981, -3.5624	-0.0000, -2.0624	2.5981, -3.5624

Note: $|q_{1y}-q_{4y}|$=0.124in which exceeds the 0.12in minimum

2.5 Discussion

Equation (2.11) becomes invalid when the pivots $\mathbf{a}_1$, $\mathbf{b}_1$ and $\mathbf{b}_0$ are collinear. Such a state is possible when the four-bar mechanism reaches a "lock-up" or binding position. When pivots $\mathbf{a}_1$, $\mathbf{b}_1$ and $\mathbf{b}_0$ are collinear, the denominator in Equation (2.11) becomes zero (making the equation invalid). For the derivation of Equation (2.11), the weights of the crank and follower links are assumed to be negligible. For a four-bar braking mechanism however, the weights of the crank and follower should be minuscule in comparison to the normal braking force *f*. ADAMS dynamic modeler was used to independently confirm the achieved rigid-body positions, brake normal forces and driver static torques of the synthesized mechanisms. The mechanism solution loci were calculated in MathCAD and expressed to four decimal places.

The Proposed designed mechanism is an excellent choice for an application of traveler parking brake. In the application of the traveler parking brake the load is required when the pad touches the rail as shown in Figures 2.5 and 2.6. Coupler selected positions were the choice of the designer who faces many challenges in the design of such application such as the complexity of the location, in other words, the

obstruction of steel support members on the traveler and underneath the rail, compact space limitation, and the suitability of tools required for the application (e.g., the use of hydraulic cylinder has no avail). If the designed mechanism shown in Figures 2.5 and 2.7 is loaded with vertical load of 1500lbf and let to rotate 360°, then the magnitude of the reaction forces R_{a1} , R_{b1} and driver static torque T as function of the crank ($\mathbf{a_1a_0}$) displacement angle (Φ) will be shown in Figures 2.11, 2.12 and 2.13, respectively. The displacement angle (Φ) is illustrated in Figure 2.10.

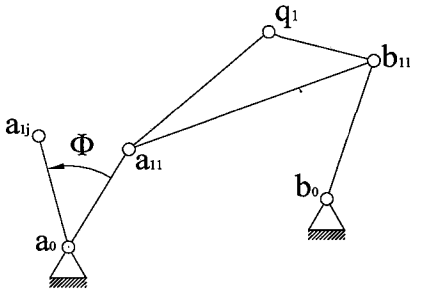

Figure 2.10 Crank displacement angle.

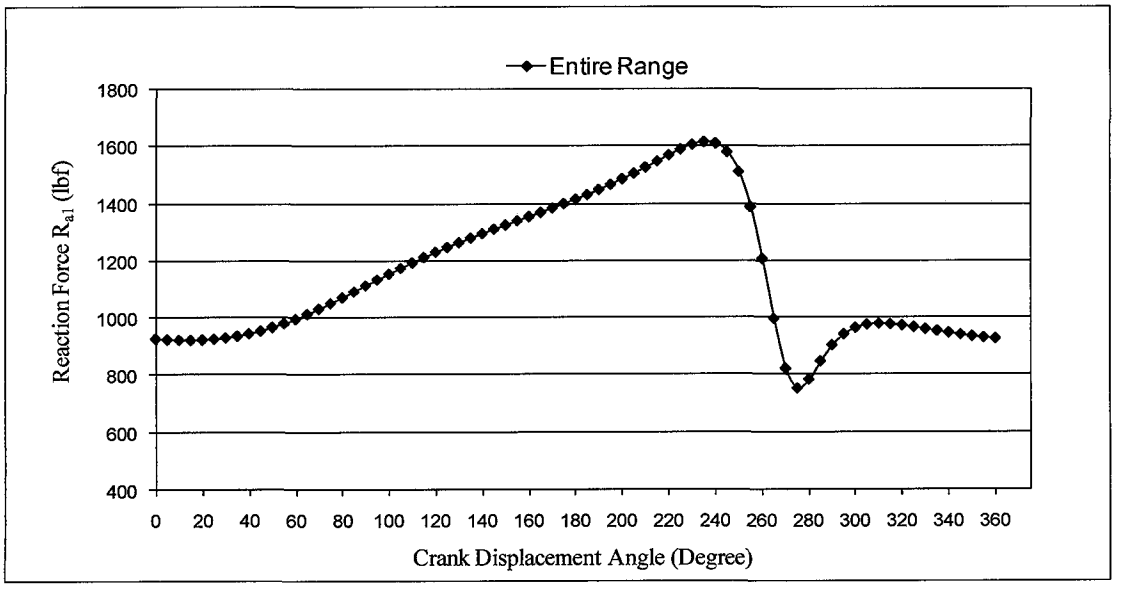

Figure 2.11 Magnitude of the reaction force $\mathbf{R_{a1}}$ for the specified crank rotation.

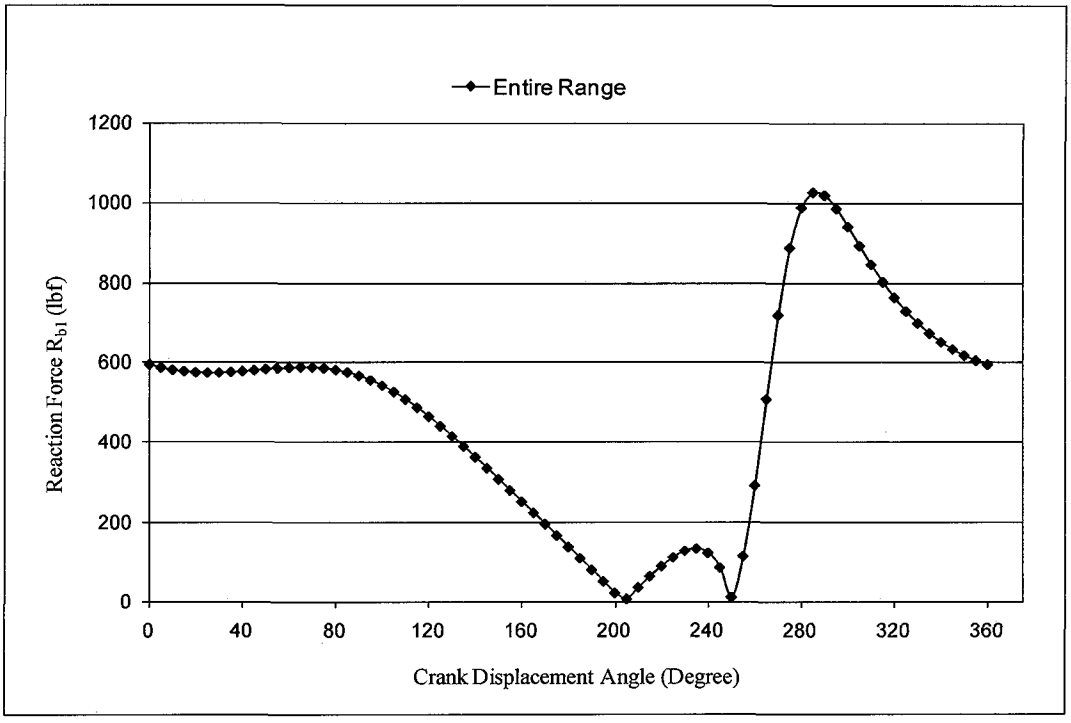

Figure 2.12 Magnitude of the reaction force $\mathbf{R_{b1}}$ for the specified crank rotation.

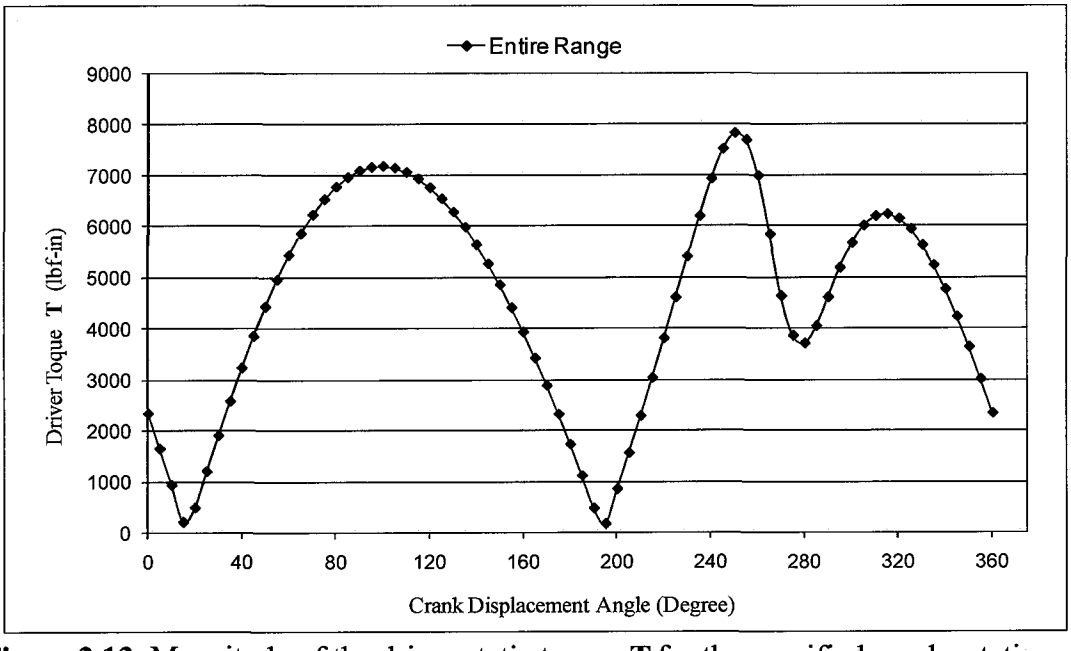

Figure 2.13 Magnitude of the driver static torque **T** for the specified crank rotation.

CHAPTER 3

PLANAR FIVE-BAR MOTION GENERATION WITH PRESCRIBED STATIC TORQUE AND RIGID-BODY REACTION FORCE

3.1 Introduction

3.1.1 Motion Generation

In motion generation, the objective is to calculate the mechanism parameters required to achieve or approximate a set of prescribed rigid-body positions. This mechanism design objective is particularly useful when the rigid-body must achieve a specific displacement sequence for effective operation (e.g., specific tool paths and/or orientations for accurate fabrication operations). In Figure 3.1, four prescribed rigid-body positions are defined by the coordinates of variables **p**, **q** and **r** (motion generation model input) and the model output are the calculated coordinates of the moving pivot variables $\mathbf{a}_1$ and $\mathbf{c}_1$ and scalar link lengths R_1 and R_3. A numerical geared five-bar motion generation model [1, 33-34] is presented in the next section.

Motion generation for planar five-bar mechanisms is a fairly-established field. Recent contributions include the works Sodhi and Russell [33] and Musa et al. [34] that consider motion generation of adjustable geared five-bar motion generators with prescribed rigid-body positions and rigid-body positions with tolerances. The works of Balli and Chand [35-36] introduce a complex number method for the synthesis of a planar five-bar motion generator with prescribed timing and a method to synthesize a planar five-bar mechanism of variable topology type with transmission angle control. Nokleby and Podhorodeski [37] presented an optimization method to synthesize Grashof five-bar mechanisms. Wang and Yan [38] presented an approach for

synthesizing planar five-bar linkages with five prescribed precision positions. Basu and Farhang [39] introduced a mathematical formulation for the approximate analysis and design of two-input, small-crank five-bar mechanisms for function generation. Dou and Ting [40] introduced a method to identify to rotatability and branch condition in linkages containing simple geared five-bar chains. Lin and Chaing [41] extended pole method for use in the synthesis planar, geared five-bar function generators. Ge and Chen [42] introduced a software-based approach for the atlas method on path synthesis of geared five-bar mechanisms. The authors also studied the effect of link length, crank angles and gear tooth ratio on the motion of the geared five-bar linkage [43]. Li and Dao [44] introduced a complex number method for the synthesis for geared, five-bar guidance mechanisms. Huang and Roth [18] considered static force conditions as well as motions in the dimensional synthesis of planar and spatial linkages.

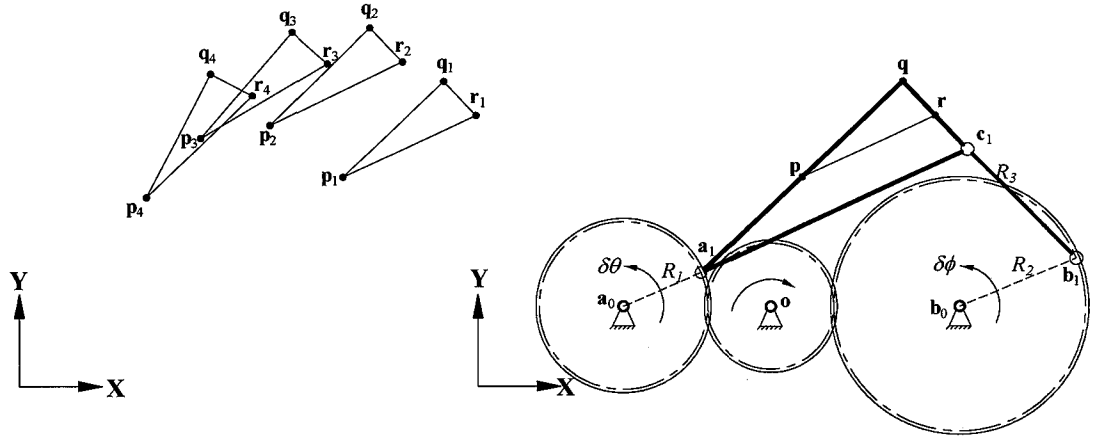

Figure 3.1 Prescribed rigid-body positions and calculated planar five-bar mechanism.

3.1.2 Motivation and Scope of Work

Using conventional motion generation methods, the user can only calculate the mechanism parameters required to achieve or approximate a set of prescribed rigid-body positions. Although such solutions are useful for preliminary kinematic analyses, other factors (e.g., static loads, dynamic loads, stresses, strains, etc.) must be considered prior to fabricating a physical prototype of the mechanical design. This work considers static driving link torque given the load of the rigid-body. By incorporating the new static torque constraint into conventional planar five-bar motion generation models, planar five-bar mechanisms are synthesized to achieve-not only prescribed rigid-body positions-but also achieve driver static torque for a given rigid-body load.

3.2 Conventional Planar Five-bar Motion Generation

Equations (3.1) through (3.3) encompass a conventional planar five-bar motion generation model [1][2][33][34].

$$\left([\mathbf{D}_{1j}]\mathbf{a}_1 - \mathbf{a}_0\right)^T \left([\mathbf{D}_{1j}]\mathbf{a}_1 - \mathbf{a}_0\right) - L_1^2 = 0 \tag{3.1}$$

$$\left([\mathbf{D}(\delta\varphi)_{1j}]\mathbf{b}_1 - \mathbf{b}_0\right)^T \left([\mathbf{D}(\delta\varphi)_{1j}]\mathbf{b}_1 - \mathbf{b}_0\right) - L_2^2 = 0 \tag{3.2}$$

$$\left([\mathbf{D}_{1j}]\mathbf{c}_1 - [\mathbf{D}(\delta\varphi)_{1j}]\mathbf{b}_1\right)^T \left([\mathbf{D}_{1j}]\mathbf{c}_1 - [\mathbf{D}(\delta\varphi)_{1j}]\mathbf{b}_1\right) - L_3^2 = 0 \tag{3.3}$$

where j=1,2,3,4

These equations are "constant length" constraints and ensure the fixed lengths of links $\mathbf{a}_0\mathbf{a}_1$, $\mathbf{b}_0\mathbf{b}_1$ and $\mathbf{b}_1\mathbf{c}_1$ throughout the prescribed rigid-body displacements. Variables L_1, L_2 and L_3 in Equations (3.1) through (3.3) are the prescribed scalar

lengths of links $\mathbf{a}_0\mathbf{a}_1$, $\mathbf{b}_0\mathbf{b}_1$ and $\mathbf{b}_1\mathbf{c}_1$, respectively.

$$\left[\mathbf{D}_{1j}\right]=\begin{bmatrix} p_{jx} & q_{jx} & r_{jx} \\ p_{jy} & q_{jy} & r_{jy} \\ 1 & 1 & 1 \end{bmatrix}\begin{bmatrix} p_{1x} & q_{1x} & r_{1x} \\ p_{1y} & q_{1y} & r_{1y} \\ 1 & 1 & 1 \end{bmatrix}^{-1} \tag{3.4}$$

In conventional motion generation, three points (**p**, **q**, and **r**) on the coupler body are defined. If the coupler points lie on the same line (prohibited), displacement matrix $[\mathbf{D}_{1j}]$ (Equation (3.4)) becomes proportional with proportional rows, this matrix could not be inverted.

$$\left[\mathbf{D}(\delta\varphi)_{1j}\right]=\begin{bmatrix} \cos(\delta\varphi)_{1j} & -\sin(\delta\varphi)_{1j} & -b_{0x}\cos(\delta\phi)_{1j}+b_{0y}\sin(\delta\phi)_{1j}+b_{0x} \\ \sin(\delta\varphi)_{1j} & \cos(\delta\varphi)_{1j} & -b_{0x}\sin(\delta\phi)_{1j}-b_{0y}\cos(\delta\phi)_{1j}+b_{0y} \\ 0 & 0 & 1 \end{bmatrix} \tag{3.5}$$

Equation (3.4) is a rigid-body planar displacement matrix. Equation (3.5) is the angular displacement matrix for link $\mathbf{b}_0$-$\mathbf{b}_1$ where

$$M_{1j}=\left[\begin{array}{c|c|c} 1 & & \\ 1 & \mathbf{a}_1-\mathbf{a}_0 & \left[D_{1j}\right]\mathbf{a}_1-\mathbf{a}_0 \\ 1 & 0 & 0 \end{array}\right]$$

$$\cos(\delta\theta)_{1j}=\frac{(\mathbf{a}_1-\mathbf{a}_0)\cdot(\left[D_{1j}\right]\mathbf{a}_1-\mathbf{a}_0)}{|\mathbf{a}_1-\mathbf{a}_0|\cdot|\left[D_{1j}\right]\mathbf{a}_1-\mathbf{a}_0|},\quad \sin(\delta\theta)_{1j}=\frac{\det\left[M_{1j}\right]}{|\mathbf{a}_1-\mathbf{a}_0|\cdot|\left[D_{1j}\right]\mathbf{a}_1-\mathbf{a}_0|}$$

$$(\delta\theta)_{1j}=\arctan 2\left(\sin(\delta\theta)_{1j},\cos(\delta\theta)_{1j}\right)$$

and $(\delta\varphi)_{1j}=k(\delta\theta)_{1j}$. Variable k represents the gear ratio of the gear train joining grounded links $\mathbf{a}_0$-$\mathbf{a}_1$ and $\mathbf{b}_0$-$\mathbf{b}_1$. From this conventional planar five-bar motion generator model, 12 of the 13 unknown variables $\mathbf{a}_0$, $\mathbf{a}_1$ L_1, $\mathbf{b}_0$, $\mathbf{b}_1$, L_2, $\mathbf{c}_1$, and L_3 are calculated with one arbitrary choice of parameter (where $\mathbf{a}_0=[a_{0x}, a_{0y}, 1]$, $\mathbf{a}_1=[a_{1x}, a_{1y}, 1]$, $\mathbf{b}_0=[b_{0x}, b_{0y}, 1]$, $\mathbf{b}_1=[b_{1x}, b_{1y}, 1]$ and $\mathbf{c}_1=[c_{1x}, c_{1y}, 1]$).

3.3 Driver Link Static Torque

With an external load **F** acting on the rigid-body of the geared five-bar mechanism, a torque **T** applied to the driving shaft of gear mounted at $\mathbf{a}_0$ achieves static equilibrium. In Figure 3.2, the load **F** is applied to rigid-body at point **q**. To formulate the driver static torque constraint, the moment condition for the coupler $\Sigma\mathbf{M}=0$ (Figure 3.3b) is taken about the moving pivot $\mathbf{a}_1$. As illustrated in Figure 3.3b, the moving pivot reaction loads $\mathbf{R}_{a1}$ and $\mathbf{R}_{c1}$ are considered in the moment condition The equilibrium moments equation about moving pivot $\mathbf{a}_1$ is (notice that link $\mathbf{b}_1\mathbf{c}_1$ is a two-force member)

$$\overrightarrow{a_1c_1}\times\mathbf{R}_{c1}+\overrightarrow{a_1q}\times\mathbf{F}=0 \tag{3.6}$$

where

$$\mathbf{R}_{c1}=R_c\frac{\overrightarrow{b_1c_1}}{\left|\overrightarrow{b_1c_1}\right|} \tag{3.7}$$

The reaction load R_c is a real number that varies with the mechanism position. Substituting Equation (3.7) into Equation (3.6) produces

$$R_c=\frac{\left|\overrightarrow{a_1q}\times\mathbf{F}\right|}{\left|\overrightarrow{a_1c_1}\times\dfrac{\overrightarrow{b_1c_1}}{\left|\overrightarrow{b_1c_1}\right|}\right|} \tag{3.8}$$

and substituting Equation (3.8) into Equation (3.6) and solving for $\mathbf{R}_{c1}$ produces

$$\mathbf{R}_{c1}=\frac{\left|\overrightarrow{a_1q}\times\mathbf{F}\right|}{\left|\overrightarrow{a_1c_1}\times\overrightarrow{b_1c_1}\right|}\overrightarrow{b_1c_1} \tag{3.9}$$

The resulting equilibrium of force equation for the rigid-body in Figure 3.3b is

$$\mathbf{R}_{a1} + \mathbf{R}_{c1} + \mathbf{F} = 0 \tag{3.10}$$

Substituting Equation (3.9) into Equation (3.10) and solving for $\mathbf{R}_{a1}$ produces

$$\mathbf{R}_{a1} = -\frac{\left|\overrightarrow{a_1q}\times\mathbf{F}\right|}{\left|\overrightarrow{a_1c_1}\times\overrightarrow{b_1c_1}\right|}\overrightarrow{b_1c_1} - \mathbf{F} \tag{3.11}$$

With the rigid-body reaction load Equations (3.9) and (3.14) formulated, torque equations for the gears about $\mathbf{a}_0$ and $\mathbf{b}_0$ are formulated next. The moment condition $\Sigma\mathbf{M}=0$ is taken about the fixed pivot $\mathbf{a}_0$ for link $\mathbf{a}_0\mathbf{a}_1$ in Figure 3.3a. The resulting equilibrium equation of the moments about $\mathbf{a}_0$ is

$$\mathbf{T}_a - \overrightarrow{a_0a_1}\times\mathbf{R}_{a1} = 0 \tag{3.12}$$

Substituting Equation (3.11) into Equation (3.12) and solving for torque $\mathbf{T}_a$ produces

$$\mathbf{T}_a = \overrightarrow{a_0a_1}\times\left(-\frac{\left|\overrightarrow{a_1q}\times\mathbf{F}\right|}{\left|\overrightarrow{a_1c_1}\times\overrightarrow{b_1c_1}\right|}\overrightarrow{b_1c_1} - \mathbf{F}\right) \tag{3.13}$$

The moment condition $\Sigma\mathbf{M}=0$ is now taken about the fixed pivot $\mathbf{b}_0$ for link $\mathbf{b}_0\mathbf{b}_1$ in Figure 3.3c. The resulting equilibrium equation of the moments about $\mathbf{b}_0$ is

$$\mathbf{T}_b - \overrightarrow{b_0b_1}\times\mathbf{R}_{c1} = 0 \tag{3.14}$$

Substituting Equation (3.9) into Equation (3.14) and solving for torque $\mathbf{T}_b$ produces

$$\mathbf{T}_b = \overrightarrow{b_0b_1}\times\frac{\left|\overrightarrow{a_1q}\times\mathbf{F}\right|}{\left|\overrightarrow{a_1c_1}\times\overrightarrow{b_1c_1}\right|}\overrightarrow{b_1c_1} \tag{3.15}$$

where

$$\mathbf{F}=\begin{pmatrix} f_x \\ f_y \\ 0 \end{pmatrix}, \overrightarrow{\mathrm{a_1q}}=\mathbf{q}_i-[\mathbf{D}_{1i}]\mathbf{a}_1,\ \overrightarrow{\mathrm{a_0a_1}}=[\mathbf{D}_{1i}]\mathbf{a}_1-\mathbf{a}_0,\ \overrightarrow{\mathrm{b_1c_1}}=[\mathbf{D}_{1i}]\mathbf{c}_1-\left[\mathbf{D}(\delta\phi)_{1i}\right]\mathbf{b}_1 \text{ and}$$

$\overrightarrow{\mathrm{a_1c_1}}=[\mathbf{D}_{1i}]\mathbf{c}_1-[\mathbf{D}_{1i}]\mathbf{a}_1$.

As mentioned earlier, the gear mounted to the driving shaft at $\mathbf{a}_0$, is the designated driver in this work. Neglecting power loss, the static equilibrium driver torque is

$$\mathbf{T}=\mathbf{T}_a+k_1^{-1}\mathbf{T}_b \tag{3.16}$$

where

$k_1=\frac{r_a}{r_b}$ .Variables r_a and r_b are the pitch radii of the gears centered at $\mathbf{a}_0$ and $\mathbf{b}_0$, respectively (Figure 3.2). Equation (3.16) calculates the five-bar mechanism driver static torque for a given rigid-body load.

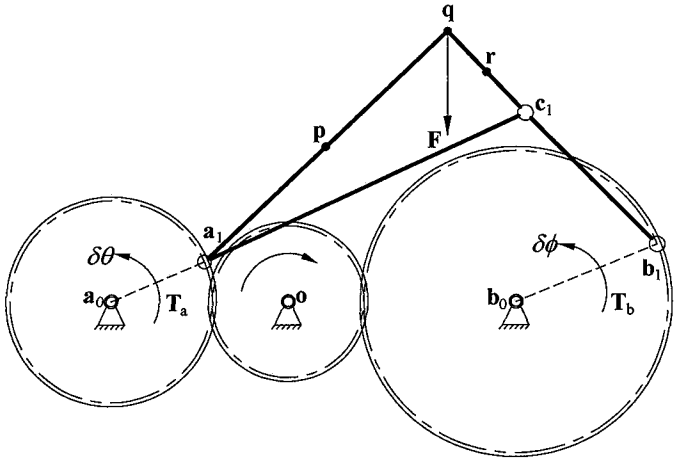

Figure 3.2. Geared five-bar mechanism in static equilibrium.

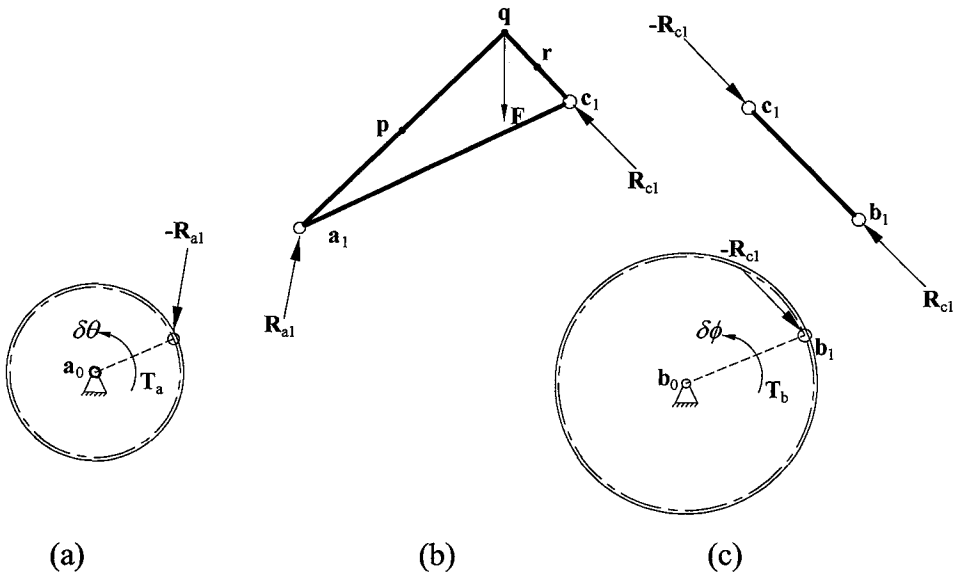

Figure 3.3 Geared five-bar mechanism in static equilibrium (a) link $\mathbf{a}_0\mathbf{a}_1$ (b) rigid-body and (c) link $\mathbf{b}_0\mathbf{b}_1$.

3.4 Example Problem

Table 3.1 includes the x and y-coordinates (in inches) of four prescribed rigid-body positions. The prescribed normal force to the coupler at point **q** must reach 1000lbs. A prescribed driver static torque of 416in-lbs is also prescribed to achieve the corresponding prescribed normal force. The force is to be fully applied at position 4. The gears pitch radii r_a, r_b, and r of 2, 3, and 1.5 inches, respectively.

Using the motion generation Equations (3.1), (3.2) and torque constant Equation (3.16) with prescribed values of $\mathbf{a}_0$=(0, 0), $\mathbf{b}_0$=(5.3223, -2.1759), $\mathbf{b}_1$=(8.1414, -1.1498), and R_2=3, and initial guesses of $\mathbf{a}_1$=(2, 0.5), R_1=2, $\mathbf{c}_1$=(8, 1), and R_3=3 the calculated solution is $\mathbf{a}_1$=(1.9314, 0.51202), R_1= 2.0000, $\mathbf{c}_1$=(7.81328, 0.64456), and R_3= 1.82427. The achieved rigid-body positions for the selected mechanism are listed in Table 3.2. To achieve positions 2 through 4 in Table 3.2, link $\mathbf{a}_0\mathbf{a}_1$ rotates counterclockwise 39.8516, 59.9332, and 89.9864 degrees, respectively.

Figure 4 illustrates the synthesized geared five-bar motion generator. As illustrated in this figure, the moving pivot $\mathbf{b}_1$ is on the pitch circle of the gear centered at the fixed pivot $\mathbf{b}_0$. the prescribed 1000lb coupler normal force and corresponding 416in-lb driver static torque have been confirmed to be satisfied using ADAMS.

Table 3.1 Prescribed Rigid-body Positions (w=1000lbs)

	p	**q**	**r**
Pos 1	4.7020, 2.1783	5.8557, 2.8699	6.7741, 2.0766
Pos 2	4.3023, 2.9462	5.4560, 3.6377	6.3743, 2.8444
Pos 3	3.7561, 3.4159	4.9039, 4.1172	5.8290, 3.3317
Pos 4	2.6890, 3.7891	3.8089, 4.5343	4.7635, 3.7850

Table 3.2 Rigid-body Positions Achieved by Synthesized Planar Five-bar Mechanism

	p	**q**	**r**
Pos 1	4.7020, 2.1783	5.8557, 2.8699	6.7741, 2.0766
Pos 2	4.3047, 2.9465	5.4583, 3.6381	6.3767, 2.8448
Pos 3	3.7577, 3.4186	4.9055, 4.1198	5.8305, 3.3343
Pos 4	2.6899, 3.7924	3.8099, 4.5373	4.7645, 3.7880

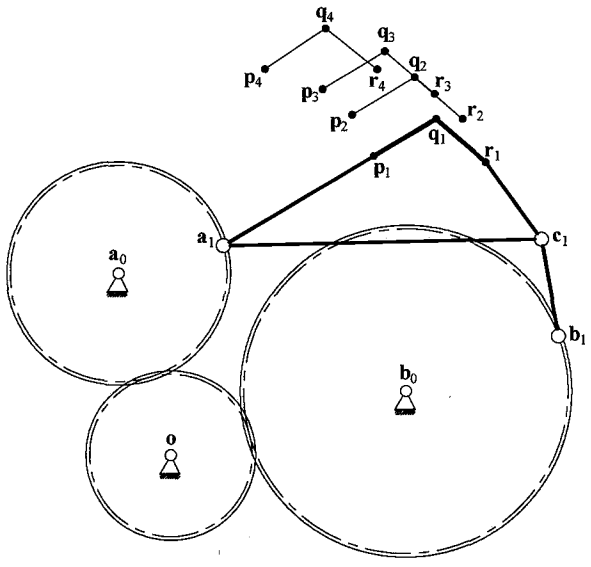

Figure 3.4. Synthesized geared five-bar motion generator.

3.5 Discussion

Equation (3.16) becomes invalid when the pivots $\mathbf{a}_1$, $\mathbf{b}_1$ and $\mathbf{c}_1$ are collinear. Such a state is possible when the five-bar mechanism reaches a "lock-up" or binding position. When pivots $\mathbf{a}_1$, $\mathbf{b}_1$ and $\mathbf{c}_1$ are collinear, the denominator in Equation (3.16) becomes zero (making the equation invalid). The specific geared five-bar mechanism design considered in this work is one where $\mathbf{a}_1$ is a moving pivot on the gear centered at $\mathbf{a}_0$ and $\mathbf{b}_1$ is a moving pivot on the gear centered at $\mathbf{b}_0$. The mathematical analysis software MathCAD was used to codify and solve the formulated algorithm. ADAMS dynamic modeler was used to independently confirm the achieved rigid-body positions, normal forces and driver static torques of the synthesized mechanisms.

If the designed mechanism shown in Figures 3.4 is loaded with vertical load of 1000lbf and let to rotate from initial position to the final position, then the magnitude of the reaction forces R_{a1} , R_{b1} and driver static torque T will be shown in Figures 3.5, 3.6, and 3.7, respectively.

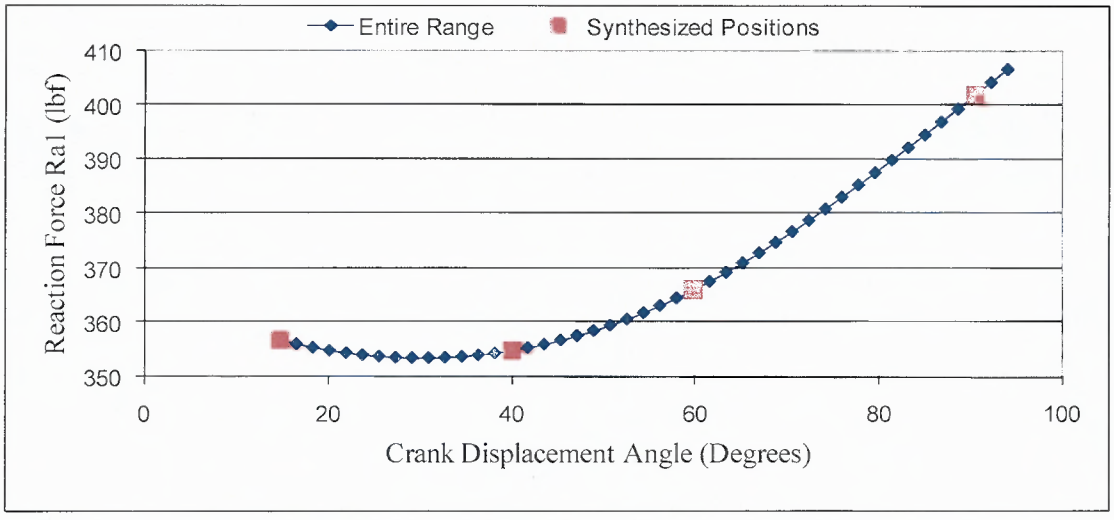

Figure 3.5 Magnitude of the reaction force $\mathbf{R_{a1}}$ for the specified crank rotation.

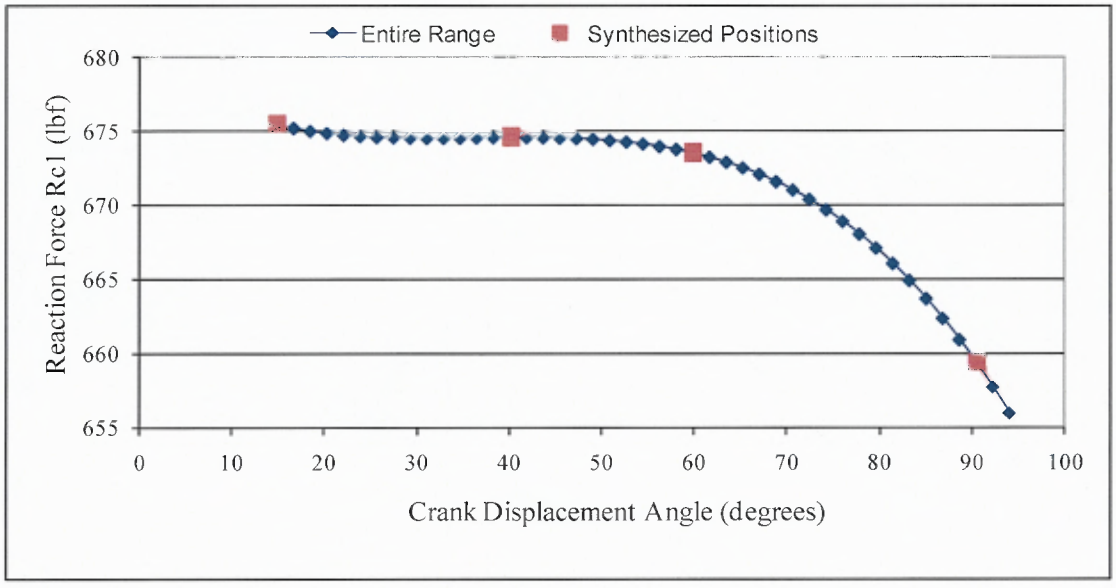

Figure 3.6 Magnitude of the reaction force $\mathbf{R_{c1}}$ for the specified crank rotation.

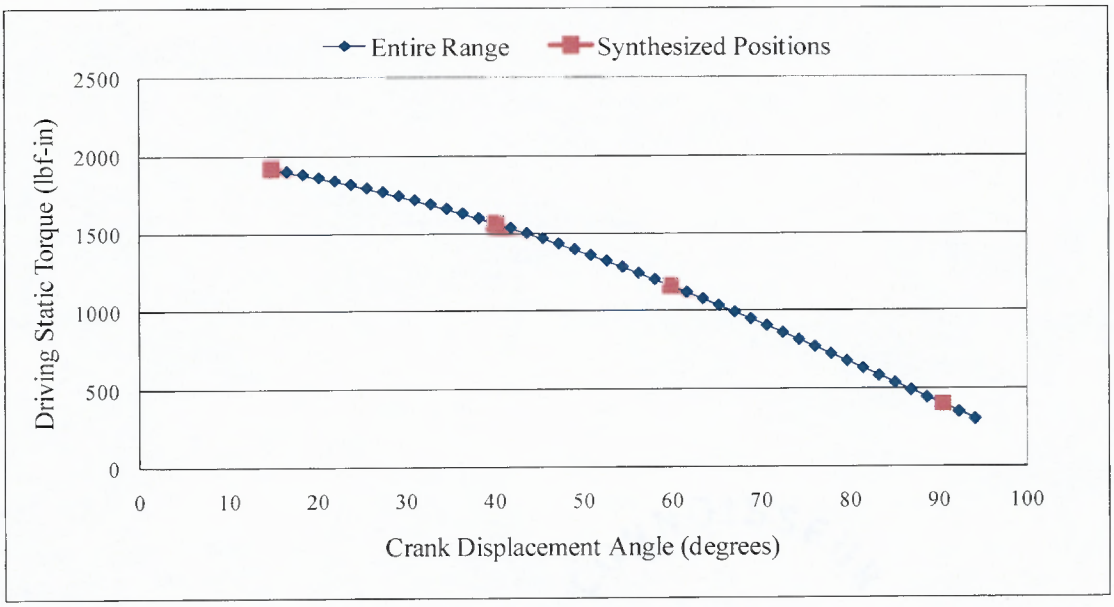

Figure 3.7 Magnitude of the driver static torque **T** for the specified crank rotation.

CHAPTER 4

PLANAR FOUR-BAR MOTION GENERATION WITH STATIC STRUCTURAL CONDITIONS

4.1 Introduction

In motion generation, the objective is to calculate the mechanism parameters required to achieve or approximate a set of prescribed rigid-body positions by using a well known constant link constraints. This novel work is based on an integration of classical kinematic analysis of a planar four-bar motion generation and three structural design constraints. These structural design constraints are the driving link static torque, the deflection of the crank and the buckling of the follower for a given rigid-body load or constant external load. This work presented in this chapter paper focuses on applied vertical load. However, the same procedure can be done for any given constant external load vector.

This kineto-elastostatic analysis is based on the following assumptions considered during the analysis; the crank and the follower are elastic members and the coupler is rigid member, friction in the joints is neglected, link weights are neglected compared to the applied load, the cross sectional properties of a link do not vary, and finally the mechanism is moving in quasi static condition. The numerical example was performed for four-bar mechanism to achieve eight prescribed coupler positions.

4.1.1 Motion Generation

In motion generation, the objective is to calculate the mechanism parameters required to achieve or approximate a set of prescribed rigid-body positions. This mechanism design objective is particularly useful when the rigid-body must achieve a specific displacement sequence for effective operation (e.g., specific tool paths and orientations for accurate fabrication operations). In Figure 4.1, four prescribed rigid-body positions are defined by the x and y-coordinates of variables **p**, **q** and **r** and the calculated mechanism parameters are the x and y-coordinates of fixed pivot variables $\mathbf{a}_0$ and $\mathbf{b}_0$ and moving pivot variables $\mathbf{a}_1$ and $\mathbf{b}_1$.

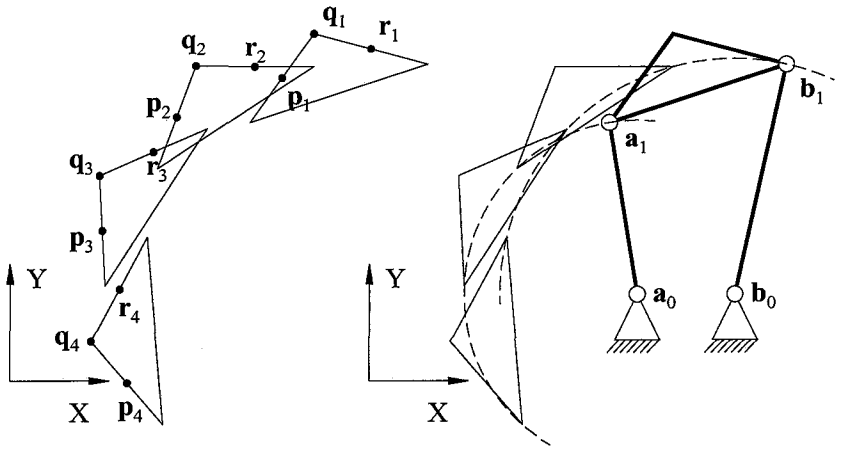

Figure 4.1 Prescribed rigid-body positions and calculated planar four-bar mechanism.

Motion generation for planar four-bar mechanisms is a well-established field. Zhou and Cheung [16] introduced an optimal synthesis method of adjustable four-bar linkages for multi-phase motion generation. Al-Widyan, Angeles and Jesús Cervantes-Sánchez [7] considered the robust synthesis of planar four-bar linkages for motion generation. Sodhi and Russell [13] also considered motion generation of planar four-bar mechanisms with prescribed rigid-body position tolerances.

A prevalent assumption that has been made in a classical kinamatic analysis of four-bar motion generation which is all links are considered rigid during the operation of the mechanism without consideration of driving torque or applied loads. This study work considers the elasticity of the input and output links and their deformation during the operation of the mechanism under driving static torque and large applied force vector. A survey has been performed for force motion mechanisms and the elastic deformation of the mechanisms. These mechanisms are referred to as flexible mechanisms or flexible link mechanisms.

C. Huang, and R. Roth [18] investigated kinematic synthesis of a mechanism using constant link constraints by using dimensional analysis and static analysis to support a specified external load at each position by using virtual work principle. The maximum number of positions specified for four-bar mechanism was three positions. James R. Senft [19] introduced a general mathematical model for force-linear machines and classified and quantified how, when and where these machines suffer frictional losses. Brian Tavis Rundgren [20] presented synthesis technique gives the designer the ability to design linkages having a desired resistance profiles under an assumed motion profile through calculating the resistance forces by using both the static and the anticipated dynamic effects of the resistance loading. Y. B. Mehta, and C. Bagci [21] presented the matrix displacement-direct element method, a finite element method (FEM) with line elements, of force and torque analysis of statically indeterminate, as well as statically determinate. Force and torque distributions and the deformed geometries of these spatial mechanisms are determined.

Static analysis of the mechanism always leads to deformation of the links which is also another area of research. Michal Hac [22], Behrooz Fallahi [23], Koon-Ho Yang, and Youn-Sik Park [24], and R. Caracciolo and A. Trevisani [25] performed a dynamic analysis and derived equations of motions for large displacement mechanisms and also performed a vibration analysis to predict the mechanism response and its stability during operation. J. Mayo, and J. Dominguez [26] performed a dynamic analysis based on introduction of non-linear elastic forces into the motion equations (formulated by using FEM).

Achieving the prescribed positions depends on the mechanism mobility and the elasticity of the input and output links, B.R. Sriram and T.S. Mruthyunjaya [27] performed an optimization process to solve a kinematic mechanism synthesis using path generation for flexible mechanism under static condition, displacement analysis was performed using FEM. Two assumptions were made; the output link (follower) was assumed flexible and no external force was applied other than the external torque applied at the input link (crank). Mohammad H.F. Dado [28] presented flexible link mechanism synthesis procedure for specified limit positions and the associated stored elastic strain energies for the compliant four-bar mechanism. The compliant output link (follower) is modeled using the variable parametric pseudo-rigid-body model and the mechanism is not subject to an external force. S. Venanzi, P. Giesen, and V. Parenti-Castelli [29] presented an iterative technique to perform the non-linear position analysis of planar compliant mechanism, input link deflection was assigned. There was no external force applied on the mechanism, and a fixed moment was applied to get the position required.

When an axial compressive force is applied to a link, that link is subject to buckle. Generally, links shall be designed to have adequate strength in order to prevent buckling and deflection. Ümit Sönmez [30], and Raymond H. Plaut, Laurie A. Alloway and Lawrence N. Virgin [31] used straight flexible beams in compliant mechanism which incorporates the buckling motion. Anwen Wang, and Wenying Tian [32] used the finite difference method to govern the elastic dynamic of post-buckling deformations of slender beams. It is shown from the previous survey that no work has not been done for a mechanism synthesis using rigid body prescribed position analysis utilizes different structural constraints including toque, deflection and buckling.

4.1.2 Motivation and Scope of Work

Using conventional motion generation methods (Suh and Radcliffe [1] and Sandor and Erdman, [2]), the user can only calculate the mechanism parameters required to achieve or approximate a set of prescribed rigid-body positions. This work takes an advantage of quasi static process of applied constant external or body loads to introduce driving static torque constraint which will be incorporated in the conventional kinematic synthesis of four-bar motion generation. The first purpose of this analysis is to synthesize a mechanism in order not to exceed a specified driving static torque during the operation of the mechanism.

Elastic analysis is also considered by assuming that the input and the output links (crank and follower) are elastic which means they are subject to deformation and buckling under constant external loads. The second purpose is to synthesize a

mechanism so that the deflection of the crank does not exceed a specified value during the operation of the mechanism. A formulation for the crank deflection is established based on Euler deflection equation.

The final constraint formulation was also based on elastica theory, it is the buckling of the follower under compressive loads using Euler buckling equation. The buckling constraint for the follower was added to the conventional kinamtic synthesis of four-bar motion generation. The third purpose of this paper is to synthesize a mechanism so that the follower is designed to prevent buckling during the normal operation of the mechanism. An optimization model was formulated to achieve the kinto-elastostatic conditions and numerical example is also presented for eight prescribed coupler positions.

4.1.3 Problem Description

The mechanism shown in Figure. 4.2a is pin jointed elastic link planar mechanism. A constant force **F** (external or body load) applied on point **q** on the coupler and motor driving toque applied on the crank at point $\mathbf{a}_0$. While the crank is rotating counter clock wise to achieve the certain positions, the load is changing its position vector relative to fixed pivot pin $\mathbf{a}_0$, hence the required motor driving torque is changing. there is a continuous change in reaction load vectors at pin joints $\mathbf{a}_1$ and $\mathbf{b}_1$ (moving pivots) in order to achieve the static equilibrium.

The big advantage of pin joints is that they eliminate release moment reaction. The components of the reaction on joint $\mathbf{a}_1$ will be normal and coaxial relative to the crank conform a combination of deflection and buckling (Figure 4.2b). The

components of the reaction on joint $\mathbf{b}_1$ will be always coaxial relative to the follower, because the follower is a two force member; this reaction tends to buckle the follower as shown in Figure. 4.2b.

There is a set of eight unknown variables of the planar four-bar mechanism (a_{0x}, a_{0y}, a_{1x}, a_{1y}, b_{0x}, b_{0y}, b_{1x}, b_{1y}). An optimization algorithm will be structured to involve the position synthesis with a specified motor driving motor torque, the cross section area for the crank is constant and must keep crank deflection below a specified deflection and finally the cross section of the follower is constant and must prevent buckling.

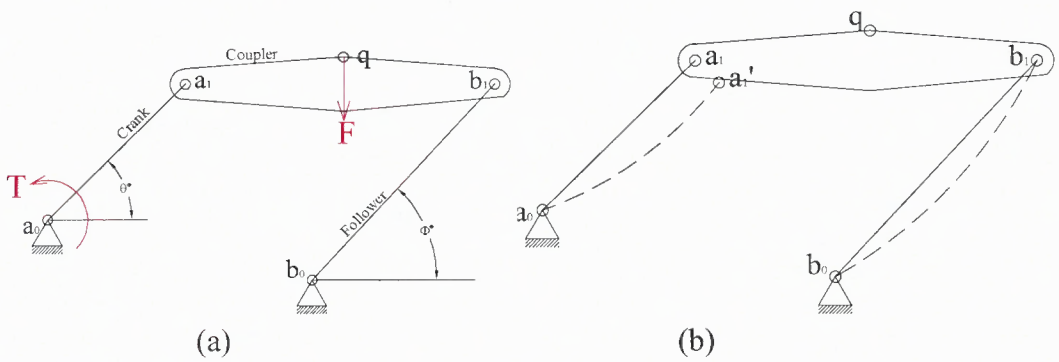

Figure 4.2 Planar four-bar mechanism (a) applied force and motor driving toque. (b) elastic behavior of the crank and the follower.

4.2 Planar Four-bar Motion Generation

4.2.1 Conventional Planar Four-Bar Motion Generation

Equations (4.1) through (4.3) encompass the planar four-bar motion generation model presented by Suh and Radcliffe [1]. Equations (4.1) and (4.2) are "constant length" constraints and ensure the constant lengths of links $\mathbf{a}_0\mathbf{a}_1$ and $\mathbf{b}_0\mathbf{b}_1$. Variables L_1 and L_2 in Equations. (4.1) and (4.2) are the prescribed scalar lengths of links $\mathbf{a}_0\mathbf{a}_1$ and $\mathbf{b}_0\mathbf{b}_1$, respectively. Equation. (4.3) is a rigid-body planar displacement matrix.

When using this conventional planar mechanism synthesis model to calculate the coordinates of the fixed pivots $\mathbf{a}_0$ and $\mathbf{b}_0$ and the moving pivots $\mathbf{a}_1$ and $\mathbf{b}_1$ (where $\mathbf{a}_0=[a_{0x},\ a_{0y},\ 1]$, $\mathbf{a}_1=[a_{1x},\ a_{1y},\ 1]$, $\mathbf{b}_0=[b_{0x},\ b_{0y},\ 1]$ and $\mathbf{b}_1=[b_{1x},\ b_{1y},\ 1]$), the user can specify a maximum of four rigid-body positions when the scalar link variables L_1 and L_2 are specified.

$$\left(\left[\mathbf{D}_{1j}\right]\mathbf{a}_1-\mathbf{a}_0\right)^T\left(\left[\mathbf{D}_{1j}\right]\mathbf{a}_1-\mathbf{a}_0\right)-L_1^{\,2}=0 \tag{4.1}$$

$$\left(\left[\mathbf{D}_{1j}\right]\mathbf{b}_1-\mathbf{b}_0\right)^T\left(\left[\mathbf{D}_{1j}\right]\mathbf{b}_1-\mathbf{b}_0\right)-L_2^{\,2}=0 \tag{4.2}$$

$$\left[\mathbf{D}_{1\mathrm{j}}\right]=\begin{bmatrix} p_{jx} & q_{jx} & r_{jx} \\ p_{jy} & q_{jy} & r_{jy} \\ 1 & 1 & 1 \end{bmatrix}\begin{bmatrix} p_{1x} & q_{1x} & r_{1x} \\ p_{1y} & q_{1y} & r_{1y} \\ 1 & 1 & 1 \end{bmatrix}^{-1} \tag{4.3}$$

where j = 1, 2, 3, 4

In conventional motion generation, three points (**p**, **q**, and **r**) on the coupler body are defined. If the coupler points lie on the same line (prohibited), displacement matrix $[\mathbf{D}_{1j}]$ (Equation (4.3)) becomes proportional with proportional rows, this matrix could not be inverted.

4.2.2 Objective Function Formulation

In order to overcome the limitation in the maximum number of prescribed body positions, Wen-Tzong Lee et al. (2008) developed an objective function for adjustable spherical four-bar motion generation for expanded prescribed positions. This objective function which needs to be minimized is based on the method of least squares. This principle will be used and modified for planar four-bar mechanism. For the first position the constant link equations for the crank (L_1) and for the follower (L_2) can be written as

$$L_1^2 = (\mathbf{a}_1 - \mathbf{a}_0)^T (\mathbf{a}_1 - \mathbf{a}_0) \tag{4.4}$$

$$L_2^2 = (\mathbf{b}_1 - \mathbf{b}_0)^T (\mathbf{b}_1 - \mathbf{b}_0) \tag{4.5}$$

Substitute Equations (4.4) and (4.5) in Equations (4.1) and (4.2)

$$\left([\mathbf{D}_{1j}]\mathbf{a}_1 - \mathbf{a}_0\right)^T \left([\mathbf{D}_{1j}]\mathbf{a}_1 - \mathbf{a}_0\right) - (\mathbf{a}_1 - \mathbf{a}_0)^T (\mathbf{a}_1 - \mathbf{a}_0) = 0 \tag{4.6}$$

$$\left([\mathbf{D}_{1j}]\mathbf{b}_1 - \mathbf{b}_0\right)^T \left([\mathbf{D}_{1j}]\mathbf{b}_1 - \mathbf{b}_0\right) - (\mathbf{b}_1 - \mathbf{b}_0)^T (\mathbf{b}_1 - \mathbf{b}_0) = 0 \tag{4.7}$$

where

j = 1, 2, …, N and N is the number of prescribed positions

The objective function which will be used and minimized is the summation square of Equations (4.6) and (4.7)

$$F(x) = \sum_{j=1}^{N} \left(\left([\mathbf{D}_{1j}]\mathbf{a}_1 - \mathbf{a}_0\right)^T \left([\mathbf{D}_{1j}]\mathbf{a}_1 - \mathbf{a}_0\right) - (\mathbf{a}_1 - \mathbf{a}_0)^T (\mathbf{a}_1 - \mathbf{a}_0) \right)^2 + \sum_{j=1}^{N} \left(\left([\mathbf{D}_{1j}]\mathbf{b}_1 - \mathbf{b}_0\right)^T \left([\mathbf{D}_{1j}]\mathbf{b}_1 - \mathbf{b}_0\right) - (\mathbf{b}_1 - \mathbf{b}_0)^T (\mathbf{b}_1 - \mathbf{b}_0) \right)^2 \tag{4.8}$$

4.3 Planar Four-bar Mechanism Under Rigid-body Loading and Static Torque

With an external load **F** acting on the rigid-body of the planar four-bar mechanism, a driving link torque **T** achieves static equilibrium. In Figure 4.3a, the load **F** is applied at the arbitrary rigid-body point **q**. To formulate the driver link static torque constraint, the moment condition $\Sigma\mathbf{M}=0$ is considered about the fixed pivot $\mathbf{a}_0$. As illustrated in Figure 4.3b, the fixed pivot reaction loads $\mathbf{R}_{a0}$ and $\mathbf{R}_{b0}$ are also considered in the moment condition. The resulting equilibrium equation of the moments about the fixed pivot $\mathbf{a}_0$ is

$$\overrightarrow{a_0b_0}\times\mathbf{R}_{b_0}+\overrightarrow{a_0q}\times\mathbf{F}+\mathbf{T}=0 \tag{4.9}$$

where

$$\mathbf{R}_{b_0}=R_b\frac{\overrightarrow{b_0b_1}}{\left|\overrightarrow{b_0b_1}\right|} \tag{4.10}$$

and the reaction load R_b is a real number that varies with the mechanism driver position. By expanding the vectors $\overrightarrow{a_0b_0}$ and $\overrightarrow{a_0q}$, Equation (4.9) becomes

$$\left(\overrightarrow{a_0a_1}+\overrightarrow{a_1b_1}+\overrightarrow{b_1b_0}\right)\times\mathbf{R}_{b_0}+\left(\overrightarrow{a_0a_1}+\overrightarrow{a_1q}\right)\times\mathbf{F}+\mathbf{T}=0 \tag{4.11}$$

Because link $\mathbf{b_0b_1}$ is a two-force member, vectors $\mathbf{R}_{b0}$ and $\overrightarrow{b_0b_1}$ are collinear and subsequently result in a zero cross product. As a result Equation (4.11) is simplified as

$$\left(\overrightarrow{a_0a_1}+\overrightarrow{a_1b_1}\right)\times\mathbf{R}_{b_0}+\left(\overrightarrow{a_0a_1}+\overrightarrow{a_1q}\right)\times\mathbf{F}+\mathbf{T}=0 \tag{4.12}$$

Next, the moment condition $\Sigma\mathbf{M}=0$ is considered about the moving pivot $\mathbf{a}_1$ considering all of the links and joints to the right of $\mathbf{a}_1$. As illustrated in Figure 4.3c, the fixed pivot reaction loads $\mathbf{R}_{a1}$ and $\mathbf{R}_{b0}$ are also considered in the moment

condition. The resulting equilibrium equation of the moments about the moving pivot $\mathbf{a}_1$ is

$$\overrightarrow{a_1b_1} \times \mathbf{R}_{b_0} + \overrightarrow{a_1q} \times \mathbf{F} = 0 \tag{4.13}$$

Substituting Equation (4.13) into Equation (4.12) produces

$$\overrightarrow{a_0a_1} \times \mathbf{R}_{b_0} + \overrightarrow{a_0a_1} \times \mathbf{F} + \mathbf{T} = 0 \tag{4.14}$$

Substituting Equation (4.10) into Equations (4.13) and (4.14) produces

$$\frac{R_b}{\left|\overrightarrow{b_0b_1}\right|} \overrightarrow{a_1b_1} \times \overrightarrow{b_0b_1} = \mathbf{F} \times \overrightarrow{a_1q} \tag{4.15}$$

$$\frac{R_b}{\left|\overrightarrow{b_0b_1}\right|} \overrightarrow{a_0a_1} \times \overrightarrow{b_0b_1} = \mathbf{F} \times \overrightarrow{a_0a_1} - \mathbf{T} \tag{4.16}$$

Combining Equations (4.15) and (4.16) produces

$$\mathbf{T} = \left(\frac{\left(\mathbf{F} \times \overrightarrow{a_1q}\right)_3}{\left(\overrightarrow{a_1b_1} \times \overrightarrow{b_0b_1}\right)_3} \overrightarrow{b_0b_1} + \mathbf{F} \right) \times \overrightarrow{a_0a_1} \tag{4.17}$$

where

$$\mathbf{F} = \begin{pmatrix} f_x \\ f_y \\ 0 \end{pmatrix}, \mathbf{T} = \begin{pmatrix} 0 \\ 0 \\ \tau_j \end{pmatrix}, \overrightarrow{a_1q} = \mathbf{q}_j - \left[\mathbf{D}_{1j}\right]\mathbf{a}_1, \overrightarrow{a_0a_1} = \left[\mathbf{D}_{1j}\right]\mathbf{a}_1 - \mathbf{a}_0, \overrightarrow{b_0b_1} = \left[\mathbf{D}_{1j}\right]\mathbf{b}_1 - \mathbf{b}_0, \text{ and}$$

$$\overrightarrow{a_1b_1} = \left[\mathbf{D}_{1j}\right]\left(\mathbf{b}_1 - \mathbf{a}_1\right), \text{j} = 1, 2, 3, 4$$

In Equation (4.17) the terms $\left(\mathbf{F} \times \overrightarrow{a_1q}\right)_3$ and $\left(\overrightarrow{a_1b_1} \times \overrightarrow{b_0b_1}\right)_3$ are the third elements of the corresponding vectors. Equation (4.17) calculates the four-bar mechanism driver static torque for a given rigid-body load.

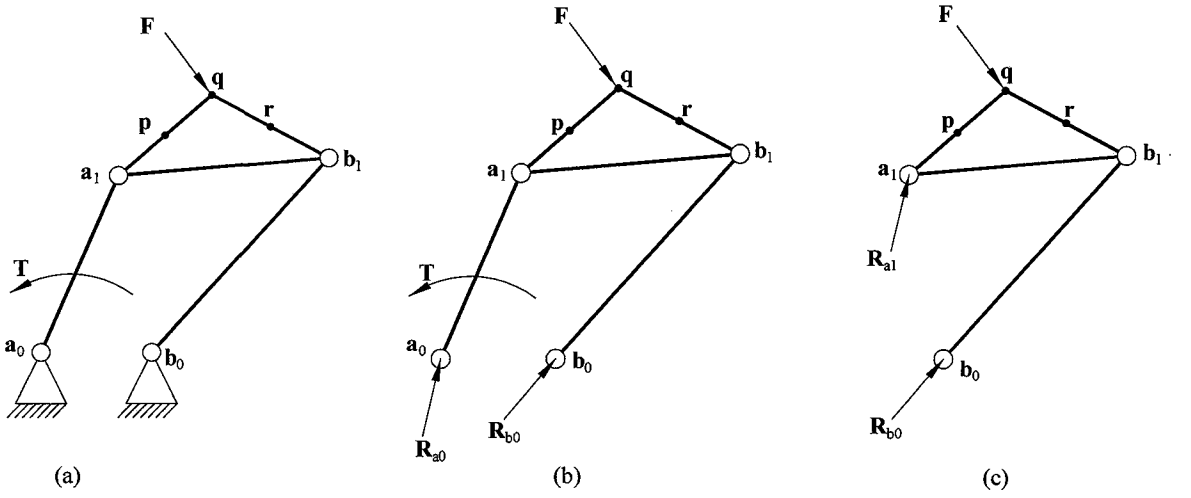

Figure 4.3 Planar four-bar mechanism (a) in static equilibrium (b) with reaction loads $\mathbf{R_{a0}}$, $\mathbf{R_{b0}}$ and (c) with reaction loads $\mathbf{R_{b0}}$ and $\mathbf{R_{a1}}$.

In order to use Equation (4.17) as a torque constraint to minimize the objective function Equation (4.8), a magnitude of the torque will be taken into account without the torque direction, the mechanism will be designed so that through the operation of the mechanism the motor driving torque shall not exceed the prescribed torque value which is an input to the optimization algorithm. So the Equation (4.17) will be modified as

$$\left[\left(\frac{\left(\mathbf{F}\times\overrightarrow{a_1q}\right)_3}{\left(\overrightarrow{a_1b_1}\times\overrightarrow{b_0b_1}\right)_3}\overrightarrow{b_0b_1}+\mathbf{F}\right)\times\overrightarrow{a_0a_1}\right]^2-T^2\le 0 \tag{4.18}$$

where

j= 1,2,..., N and N is the number of the prescribed positions.

Equation (4.18) is the first derived constraint (Driver link static torque constraint).

4.4 Formulation of Structural Constraints

4.4.1 Stiffness Matrix of Planar Four-bar Mechanism Under Rigid-body Load

This section establishes the stiffness model of the mechanism, since the mechanism will move in quasi static process; the reaction moment at $\mathbf{a}_0$ would be the required torque to stabilize the mechanism statically at that specified position. So node or joint $\mathbf{a}_0$ would be fixed and all other joints are hinged. The coupler can be modeled as a rigid frame structure where $\mathbf{a}_1\mathbf{q}$ is one member pinned at $\mathbf{a}_1$ and fixed at $\mathbf{q}$, the other piece of the frame would be $\mathbf{q}\mathbf{b}_1$ where it is fixed at $\mathbf{q}$ and pinned at $\mathbf{b}_1$. The reactions of the model will be as shown in Figure 4.4.

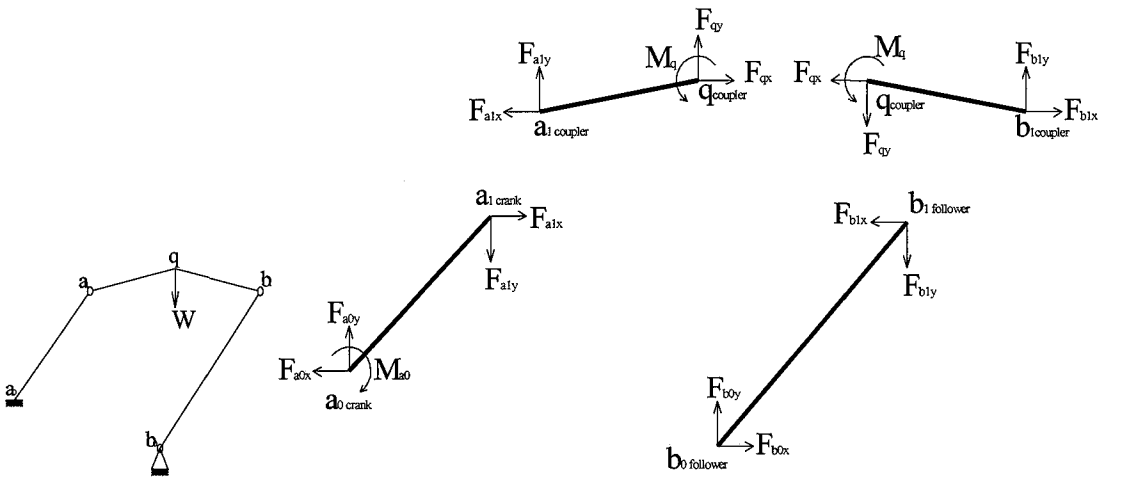

Figure 4.4 Reactions on the model of planar four-bar mechanism.

Notice that the pin joint releases the moment. All the links are modeled as planar beam elements with three degree of freedom at each joint connecting two beams together. Beam element is well described in many FEM books. Saeed Moaveni [3] describes the horizontal and vertical displacement of the beam and frame elements as shown in Figure 4.5. Charles E. Knight [4] describes the stiffness matrix for 3D beam and frame elements.

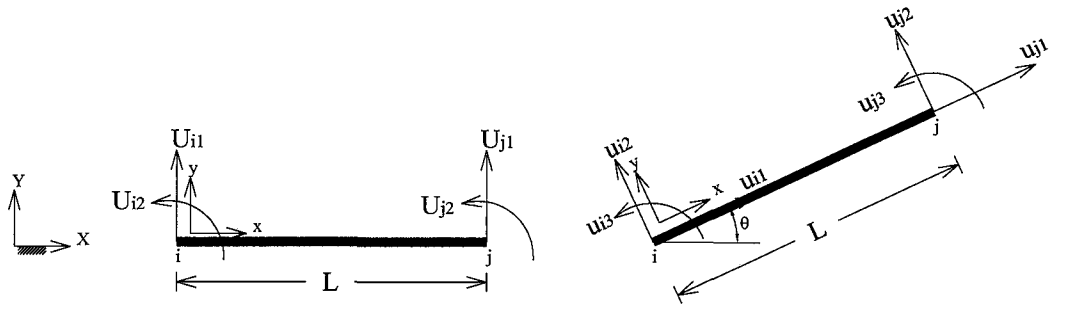

(a) (b)

Figure 4.5 Deflections of (a) Beam Element, (b) Frame Element.

All links are modeled as single beam or frame elements. The element equilibrium and deformation equations are given by

$$\{f\} = [k]\{u\} \tag{4.19a}$$

$$\{U\} = [T]\{u\} \tag{4.19b}$$

$$[K] = [T][k][T]^{-1} \tag{4.19c}$$

$$\{F\} = [K]\{U\} \tag{4.19.d}$$

{u}, [T], and [k] are the element deflection, transformation and stiffness matrices, respectively. They are defined in the as shown in the Equations 4.20a through 4.20d, the stiffness matrix of any element shall show the boundary conditions of the element. For example, the follower is pinned-pinned element, and the reactions are axial to the element. So the stiffness matrix [k] would be modified as shown in Equation (4.20d).

There are four links and five joints, each element stiffness matrix would be 6x6 and the global stiffness matrix for the mechanism would be the number of joints times the number of degrees of freedom for each joint, which would be 15x15. Since

the global stiffness matrix [K] and the global applied load vector {F} are known, the global element deformations can be found by using Equation. (4.19d).

In Figure 4.6 variables E_j, A_j, I_j and L_j (where j=1,2,3,4) are the modulus of elasticity, cross-sectional area, moment of inertia and length of each link, respectively. Because the coupler is to be a uniform rigid-body in this study, E_2=E_3, A_2=A_3, I_2=I_3 and its modulus of elasticity is one million times higher than those of the crank and follower. The angular orientation of each link (using the positive x-axis as reference) is denoted by angle θ_j (where j=1,2,3,4). These angles are used in Equation (4.20b).

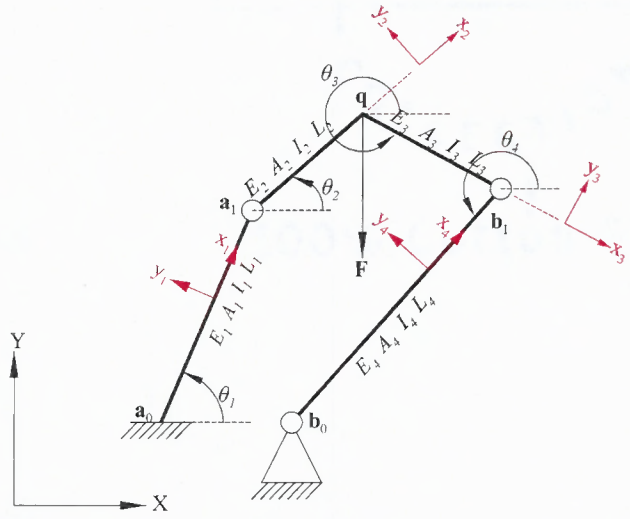

Figure 4.6 Statically-loaded planar four-bar mechanism.

$$\{u\} = \begin{bmatrix} u_{i1} \text{ (Local Axial Deformation at node i)} \\ u_{i2} \text{ (Local Lateral Deformationat node i)} \\ u_{i3} \text{ (Local Angular Deformationat node i)} \\ u_{j1} \text{ (Local Axial Deformation at node j)} \\ u_{j2} \text{ (Local Lateral Deformationat node j)} \\ u_{j3} \text{ (Local Angular Deformationat node j)} \end{bmatrix} \quad (4.20a)$$

$$[T] = \begin{bmatrix} \cos\theta & \sin\theta & 0 & 0 & 0 & 0 \\ -\sin\theta & \cos\theta & 0 & 0 & 0 & 0 \\ 0 & 0 & 1 & 0 & 0 & 0 \\ 0 & 0 & 0 & \cos\theta & \sin\theta & 0 \\ 0 & 0 & 0 & -\sin\theta & \cos\theta & 0 \\ 0 & 0 & 0 & 0 & 0 & 1 \end{bmatrix} \tag{4.20b}$$

$$[k] = \begin{bmatrix} \frac{AE}{L} & 0 & 0 & -\frac{AE}{L} & 0 & 0 \\ 0 & \frac{12EI}{L^3} & \frac{6EI}{L^2} & 0 & -\frac{12EI}{L^3} & \frac{6EI}{L^2} \\ 0 & \frac{6EI}{L^2} & \frac{4EI}{L} & 0 & -\frac{6EI}{L^2} & \frac{2EI}{L} \\ -\frac{AE}{L} & 0 & 0 & \frac{AE}{L} & 0 & 0 \\ 0 & -\frac{12EI}{L^3} & -\frac{6EI}{L^2} & 0 & \frac{12EI}{L^3} & -\frac{6EI}{L^2} \\ 0 & \frac{6EI}{L^2} & \frac{2EI}{L} & 0 & -\frac{6EI}{L^2} & \frac{4EI}{L} \end{bmatrix} \tag{4.20c}$$

$$[k_{Axial}] = \begin{bmatrix} \frac{AE}{L} & 0 & 0 & -\frac{AE}{L} & 0 & 0 \\ 0 & 0 & 0 & 0 & 0 & 0 \\ 0 & 0 & 0 & 0 & 0 & 0 \\ -\frac{AE}{L} & 0 & 0 & \frac{AE}{L} & 0 & 0 \\ 0 & 0 & 0 & 0 & 0 & 0 \\ 0 & 0 & 0 & 0 & 0 & 0 \end{bmatrix} \tag{4.20d}$$

4.4.2 Follower Link Buckling Constraint

A conventional planar four-bar mechanism as shown in Figure. 4.1 have pins or hinges in fixed and moving pivots in order to move and rotate. Links $\mathbf{a}_0\mathbf{a}_1$ and $\mathbf{b}_0\mathbf{b}_1$ are pinned-pinned. Figure 4.7 shows the free body for the mechanism members under quasi static condition. Note that reactions $\mathbf{R}_A$ on the crank and $\mathbf{R}_B$ on the follower are opposite to the same reactions found on the coupler.

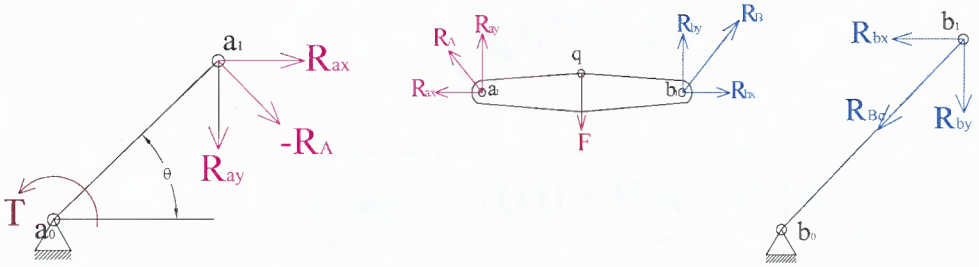

(a) (b) (c)

Figure 4.7 Deflections Schematic diagram for (a) The crank with reaction loads $\mathbf{R}_A$.(b) The coupler with external load F and reaction loads $\mathbf{R}_A$ and $\mathbf{R}_B$. (c) The follower with reaction $\mathbf{R}_{Bc}$.

The follower tends to buckle about the axis for which moment of inertia is minimum. Buckling analysis for columns utilizes Euler equation for long columns Equation (4.21) and Johnson's equations for short columns Equation (4.22). These equations are used to find the critical load on the column for any given column geometrical and material parameters. A comparison between the slenderness ratio and column constant shall be made prior to choosing the applicable critical load equation as described herein [48]:

$$\text{Slenderness Ratio} = \frac{L_e}{r} \qquad \text{and} \qquad \text{Column Constant} = \sqrt{\frac{2\pi^2 E}{\sigma_y}}$$

where

$$r = \sqrt{\frac{I}{A}} \qquad \text{and} \qquad L_e = kL$$

A: Column cross section area

E: Modulus of elasticity of the column material

I: Moment of inertia of the cross section of the column

k: Effective length factor.

L_e: Column effective length

L: Column Length

r: Radius of gyration

σ_y: Yield strength of column material

Walter D. Pilkey [5] describes the conditions in which the ends of the column are supported presented different values for k factor

$$\textit{Effective Length Factor } (k) = \begin{vmatrix} 2.0 & \textit{Fixed – Free} \\ 1.0 & \textit{Free – Pinned} \\ 1.0 & \textit{Pinned – Pinned} \\ 0.7 & \textit{Fixed – Pinned} \\ 0.5 & \textit{Fixed – Fixed} \\ 1.0 & \textit{Fixed – Guided} \\ 2.0 & \textit{Guided – Pinned} \end{vmatrix}$$

A.Ghali et al. [6], illustrates the end support conditions as shown in Figure 4.8

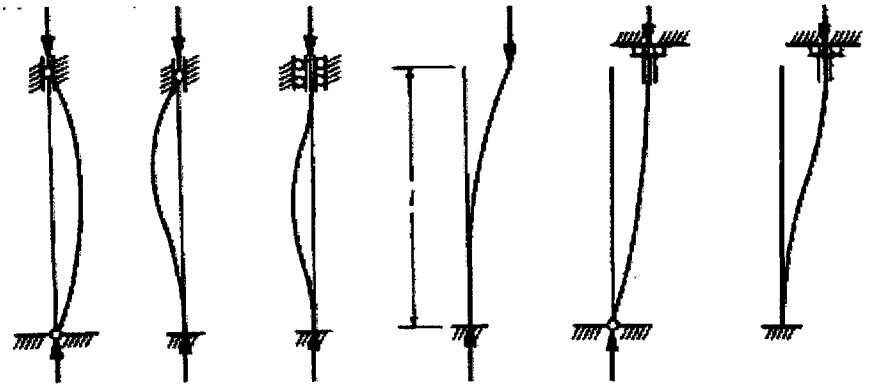

Figure 4.8 Illustration for column end support conditions.

Euler equation is used only if slenderness ratio is bigger than column constant. Otherwise, Johnson equation is applied.

Euler formula for critical buckling load $$P_{cr} = \frac{\pi^2 EI}{(kL)^2} \tag{4.21}$$

Johnson equation for critical buckling load $$P_{cr} = \sigma_y \times \left(A - \frac{\sigma_y L_e^{\,2}}{4\pi^2 EI} \right) \tag{4.22}$$

As shown in Equations (4.21) and (4.22) the critical load is a function of column length. In this research, for simplicity, Euler equation will be used for analysis. However, the same analysis approach can be used if Johnson equation is involved. The follower end conditions are pinned-pinned, Hence, the column effective length factor k = 1. Buckling of the follower should not occur unless the compressive forces R_b Equation (1.6) equals to the critical buckling load P_{cr} Equation (4.21).

$$\frac{\pi^2 EI}{(kL)^2_{k=1}} = \frac{\left|\overrightarrow{qa_1} \times \vec{F}\right|}{\left|\overrightarrow{a_1b_1} \times \overrightarrow{b_0b_1}\right|} \tag{4.23}$$

Rearrange Equation (4.23) produces

$$L^2_{Follower} = \frac{\pi^2 \times E_{Follower} \times I_{Follower}}{\dfrac{\left|\overrightarrow{qa_1} \times \vec{F}\right|}{\left|\overrightarrow{a_1b_1} \times \overrightarrow{b_0b_1}\right|}} \tag{4.24}$$

To make a buckling constraint of the follower, Equation (4.24) shall be substituted in the conventional mechanism synthesis model Equation (4.2)

$$\left([\mathbf{D}_{1j}]\mathbf{b}_1 - \mathbf{b}_0\right)^T \left([\mathbf{D}_{1j}]\mathbf{b}_1 - \mathbf{b}_0\right) - \frac{\pi^2 \times E_{Follower} \times I_{Follower}}{\left| \dfrac{\left|\overrightarrow{q_ja_1} \times \vec{F}\right|}{\left|\overrightarrow{a_1b_1} \times \overrightarrow{b_0b_1}\right|} . \overrightarrow{b_0b_1} \right|} < 0 \tag{4.25}$$

where $j = 1, 2, \ldots, N$

Equation (4.25) is the second derived constraint (Follower link buckling constraint)

4.4.3 Crank Link Deflection Constraint

Figure 4.6 shows the crank with reaction loads $\mathbf{R}_A$ which tends to deflect the crank linearly as shown in Figure. 4.2b. The crank shall be designed so that the deflection is below the specified deflection value. Under static condition, it is assumed that joint $\mathbf{a}_0$ is fixed which means six degrees of freedom (DOF) are restrained, but since the mechanism is a planar, then only 3 DOF are involved; translations in x and y axes and rotation about z axis. Joint $\mathbf{a}_1$ is a free end with a load $\mathbf{R}_A$ applied. So the model which will be analyzed is a cantilever beam fixed at one end with a load applied at the free end. Therefore, Euler beam formula will be used in the derivation of the deflection of the crank.

A comparison between the results of deflection of joint $\mathbf{a}_1$ using Euler beam formula versus matrix approach using mechanism global stiffness matrix Sub-section 4.4.1 and also using FEA package (COSMOSworks). The results are very close and the comparison proves that Euler beam formula will be very feasible to be used in the deflection constraint derivation. A numerical example shows the results of three methods. See Table 4.6 in Sections 4.7

From Torque Equation (4.17)

$$\overrightarrow{R_A} = \left(\frac{\left(\mathbf{F} \times \overrightarrow{a_1 q_j}\right)_3}{\left(\overrightarrow{a_1 b_1} \times \overrightarrow{b_0 b_1}\right)_3} \overrightarrow{b_0 b_1} + \mathbf{F} \right) \tag{4.26}$$

The normal component of force $\mathbf{R}_A$ to the crank is

$$\overrightarrow{R_{AN}} = \left(\frac{\left(\mathbf{F} \times \overrightarrow{a_1 q_j}\right)_3}{\left(\overrightarrow{a_1 b_1} \times \overrightarrow{b_0 b_1}\right)_3} \overrightarrow{b_0 b_1} + \mathbf{F} \right) \times \frac{\overrightarrow{a_0 a_1}}{\left|\overrightarrow{a_0 a_1}\right|} \tag{4.27}$$

The deflection described by Euler beam formula

$$\delta = \frac{PL^3}{3EI} \quad \text{or} \quad P = \frac{3EI\delta}{L^3} \tag{4.28}$$

where

P: Normal Load acting on the free end

E: Modulus of elasticity of the crank material

I: Moment of inertia of the cross section of the crank

L: Crank length

By tanking the magnitude of the reaction force Equation (4.27) and make it equal to Equation (4.28) and rearrange

$$L^2_{Crank} = \left(\frac{3 \times E_{Crank} \times I_{Crank} \times \delta}{\left| \left(\frac{\left(\mathbf{F} \times \overrightarrow{a_1 q_j} \right)_3}{\left(\overrightarrow{a_1 b_1} \times \overrightarrow{b_0 b_1} \right)_3} \overrightarrow{b_0 b_1} + \mathbf{F} \right) \times \frac{\overrightarrow{a_0 a_1}}{\left| \overrightarrow{a_0 a_1} \right|} \right|} \right)^{\frac{2}{3}} \tag{4.29}$$

Substitute Equation (4.29) in the conventional model Equation (4.1)

$$\left(\left[\mathbf{D}_{1j} \right] \mathbf{a}_1 - \mathbf{a}_0 \right)^T \left(\left[\mathbf{D}_{1j} \right] \mathbf{a}_1 - \mathbf{a}_0 \right) - \left(\frac{3 \times E_{Crank} \times I_{Crank} \times \delta}{\left| \left(\frac{\left(\mathbf{F} \times \overrightarrow{a_1 q_j} \right)_3}{\left(\overrightarrow{a_1 b_1} \times \overrightarrow{b_0 b_1} \right)_3} \overrightarrow{b_0 b_1} + \mathbf{F} \right) \times \frac{\overrightarrow{a_0 a_1}}{\left| \overrightarrow{a_0 a_1} \right|} \right|} \right)^{\frac{2}{3}} < 0 \tag{4.30}$$

where

j = 1, 2,…, ..N and N is number of prescribed positions

Equation (4.30) is the third derived constraint (Crank link deflection constraint)

4.5 Goal Program

Constitute an optimization algorithm to minimize the objective function Equation (4.8). A set of N Equations (4.17), (4.25), and (4.30) are grouped to calculate eight possible unknown variables of the planar four-bar mechanism (a_{0x}, a_{0y}, a_{1x}, a_{1y}, b_{0x}, b_{0y}, b_{1x}, *and* b_{1y}). The construction of the optimization process is described herein;

- The objective function to be minimized

$$F(x)=\sum_{j=1}^{N}\left(\left(\left[\mathbf{D}_{1j}\right]\mathbf{a}_1-\mathbf{a}_0\right)^T\left(\left[\mathbf{D}_{1j}\right]\mathbf{a}_1-\mathbf{a}_0\right)-\left(\mathbf{a}_1-\mathbf{a}_0\right)^T\left(\mathbf{a}_1-\mathbf{a}_0\right)\right)^2 + \sum_{j=1}^{N}\left(\left(\left[\mathbf{D}_{1j}\right]\mathbf{b}_1-\mathbf{b}_0\right)^T\left(\left[\mathbf{D}_{1j}\right]\mathbf{b}_1-\mathbf{b}_0\right)-\left(\mathbf{b}_1-\mathbf{b}_0\right)^T\left(\mathbf{b}_1-\mathbf{b}_0\right)\right)^2 \tag{4.31}$$

- The driver link static torque constraint

$$\left[\left(\frac{\left(\mathbf{F}\times\overrightarrow{\mathrm{a_1q_j}}\right)_3}{\left(\overrightarrow{\mathrm{a_1b_1}}\times\overrightarrow{\mathrm{b_0b_1}}\right)_3}\overrightarrow{\mathrm{b_0b_1}}+\mathbf{F}\right)\times\overrightarrow{\mathrm{a_0a_1}}\right]^2-T^2\le 0$$

- Buckling constraint of the follower Constraint

$$\left(\left[\mathbf{D}_{1j}\right]\mathbf{b}_1-\mathbf{b}_0\right)^T\left(\left[\mathbf{D}_{1j}\right]\mathbf{b}_1-\mathbf{b}_0\right)-\frac{\pi^2\times \mathrm{E}_{Follower}\times \mathrm{I}_{Follower}}{\left|\frac{\left|\overrightarrow{\mathrm{q_ja_1}}\times\vec{\mathrm{F}}\right|}{\left|\overrightarrow{\mathrm{a_1b_1}}\times\overrightarrow{\mathrm{b_0b_1}}\right|}\right|}<0$$

- Deflection constraint of the crank constraint

$$\left(\left[\mathbf{D}_{1j}\right]\mathbf{a}_1-\mathbf{a}_0\right)^T\left(\left[\mathbf{D}_{1j}\right]\mathbf{a}_1-\mathbf{a}_0\right)-\left(\frac{3\times \mathrm{E}_{Crank}\times \mathrm{I}_{Crank}\times\delta}{\left|\left(\frac{\left(\mathbf{F}\times\overrightarrow{\mathrm{a_1q_j}}\right)_3}{\left(\overrightarrow{\mathrm{a_1b_1}}\times\overrightarrow{\mathrm{b_0b_1}}\right)_3}\overrightarrow{\mathrm{b_0b_1}}+\mathbf{F}\right)\times\frac{\overrightarrow{\mathrm{a_0a_1}}}{\left|\overrightarrow{\mathrm{a_0a_1}}\right|}\right|}\right)^{\frac{2}{3}}<0$$

where j = 1, 2, ..., N

Equation (4.31) and inequality constraints (4.18), (4.25) and (4.30) constitute a goal program from which mechanism solutions that approximate the prescribed rigid-body positions and satisfy maximum static torque, maximum elastic deflection and buckling conditions are calculated.

The algorithm employed for solving this goal program (a nonlinear constraints problem) is SQP (Sequential Quadratic Programming) which uses Quasi-Newton approach to solve its QP (Quadratic Programming) subproblem and line search approach to determine iteration step. The merit function used by Han [45] and Powell [46] is used in the following form:

$$\Psi(\mathbf{X}) = f(\mathbf{X}) + \sum_{k=1}^{m} r_k \max\left[0, g_k(\mathbf{X})\right] \tag{4.32}$$

where $g_k(\mathbf{X})$ represents each inequality constraint, m is the total number of inequality constraints and the inequality constraint penalty parameter is

$$(r_{l+1})_k = \max_k \left\{ \lambda_k, \frac{1}{2}\left((r_l)_k + \lambda_k\right) \right\} \tag{4.33}$$

In Equation (4.33) λ_k are estimates of the Lagrange multipliers and l is the iteration index for calculating the penalty parameter r_k for each inequality constraint (l=0, 1, 2, 3,...). After specifying initial guesses for the unknown variables in the goal program $(\mathbf{X})$, the following SQP steps were employed to calculate the unknown variables:

1. calculate λ_k and $(r_{l+1})_k$, (where l=0 and k=1...m)

2. solve Equation (4.32) using Quasi-Newton method

3. calculate $(r_{l+1})_k$ using Equation (4.33) (where l=l+1 and k=1…m)

4. repeat step 2 with newly-calculated r_k

Steps 2 through 4 constitute a loop that is repeated until the penalty term in Equation (4.32), $\sum_{k=1}^{m} r_k \max[0, g_k(\mathbf{X})]$, is less than a specified penalty term residual ε.

4.6 Example Problem

4.6.1 Optimization Analysis and Mechanism Synthesis

Table 4.1 includes the x and y-coordinates of eight prescribed coupler positions (in inches). The prescribed normal force for the coupler is constant 1000lbs. A prescribed driver static torque of 2200 in-lbs is also prescribed to achieve the corresponding prescribed normal force.

Table 4.1 Prescribed Rigid-body Positions

	p	q	r
Pos 1	4.9321, 5.0005	5.0928, 5.1172	5.3858, 4.9969
Pos 2	4.3190, 5.1880	4.4827, 5.3005	4.7724, 5.1725
Pos 3	3.6288, 5.2262	3.7943, 5.3360	4.0820, 5.2034
Pos 4	2.9202, 5.0989	3.0866, 5.2074	3.3732, 5.0722
Pos 5	0.9153, 3.4691	1.0778, 3.5833	1.3689, 3.4584
Pos 6	0.4745, 2.4116	0.6227, 2.5438	0.9263, 2.4535
Pos 7	1.4479, 1.6811	1.4700, 1.8785	1.7564, 2.0138
Pos 8	2.8512, 2.7056	2.8761, 2.9026	3.1643, 3.0340

The crank and the follower are made of steel with modulus of elasticity E = 29000000 psi, the coupler is assumed rigid. The crank has circular cross section of 3/4 inch diameter, and the follower has circular cross section of 3/16 inch diameter.

The maximum crank deflection shall not exceed 0.013inch. Using the motion generation goal program (where N=8 results in m=24 in Equation (4.32)) with initial guesses as $\mathbf{a}_0 = (0, 0)$, $\mathbf{a}_1 = (1.5, 2.5)$, $\mathbf{b}_0 = (6.5, 0.5)$, and $\mathbf{b}_1 = (7.5, 4)$.

Solution loci for $\mathbf{a}_0$, $\mathbf{a}_1$, $\mathbf{b}_0$, $\mathbf{b}_1$ were calculated, the solution is $\mathbf{a}_0 = (0.3627, 0.0188)$, $\mathbf{a}_1 = (1.7838, 2.3355)$, $\mathbf{b}_0 = (6.4932, 1.1458)$ and $\mathbf{b}_1 = (7.5874, 4.4303)$. The achieved rigid-body positions for the selected mechanism are listed in Table 4.2. The positions achieved assuming all links in the synthesized mechanism are rigid.

Table 4.2 Rigid-body Positions Achieved by Rigid Links Synthesis

	p	q	r
Pos 1	4.9321, 5.0005	5.0928, 5.1172	5.3858, 4.9969
Pos 2	4.28545, 5.22276	4.44925, 5.33506	4.73889, 5.20687
Pos 3	3.61452, 5.27427	3.77974, 5.38449	4.06772, 5.25262
Pos 4	2.92365, 5.16549	3.08941, 5.27489	3.37674, 5.14159
Pos 5	0.90705, 3.54612	1.06692, 3.66396	1.36077, 3.54576
Pos 6	0.48539, 2.39159	0.62834, 2.52947	0.93520, 2.45100
Pos 7	1.45883, 1.58633	1.48157, 1.78363	1.76836, 1.91807
Pos 8	2.86439, 2.74024	2.8874, 2.93751	3.17437, 3.07156

Because the crank and follower links are flexible, the deflections of these links simultaneously compromise the accuracy of the rigid-body positions achieved by the synthesized mechanism. Table 4.3 includes the rigid-body positions calculated after incorporating the parameters of the synthesized mechanism in the four-bar mechanism deflection model in Sub-section 4.4.1 (global stiffness matrix for position 1 is shown in Figure 4.19. Rigid-body positions 1 through 8 correspond to crank angles of θ_1= 58.4734, 74.0997, 89.6799, 105.0001, 162.0001, 194.9997, 289.4605

and 328.7140 degrees, respectively. Figure 4.9 illustrates the synthesized four-bar motion generator.

Table 4.3 Rigid-body Positions Achieved by Elastic Links Synthesis

	p	q	r
Pos 1	4.9377, 4.9965	5.0984, 5.1132	5.3914, 4.9929
Pos 2	4.3275, 5.2127	4.4911, 5.3252	4.7809, 5.1973
Pos 3	3.6297, 5.2734	3.7949, 5.3836	4.0829, 5.2518
Pos 4	2.9209, 5.1631	3.0866, 5.2725	3.3740, 5.1392
Pos 5	0.9034, 3.5350	1.0633, 3.6528	1.3572, 3.5347
Pos 6	0.4862, 2.3841	0.6291, 2.5219	0.9360, 2.4435
Pos 7	1.4561, 1.5843	1.4789, 1.7816	1.7657, 1.9161
Pos 8	2.8516, 2.7300	2.8746, 2.9272	3.1616, 3.0614

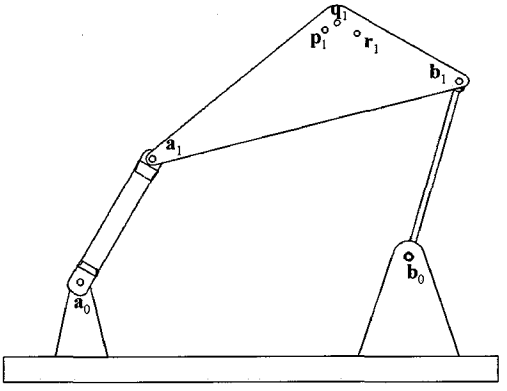

Figure 4.9 Synthesized planar four-bar motion generator.

The achieved positions of the synthesized mechanism are shown schematically in Figure 4.10. ADAMS was used to get the motion of the synthesized mechanism. AutoCAD is used to edit the footprint of each position performed by ADAMS.

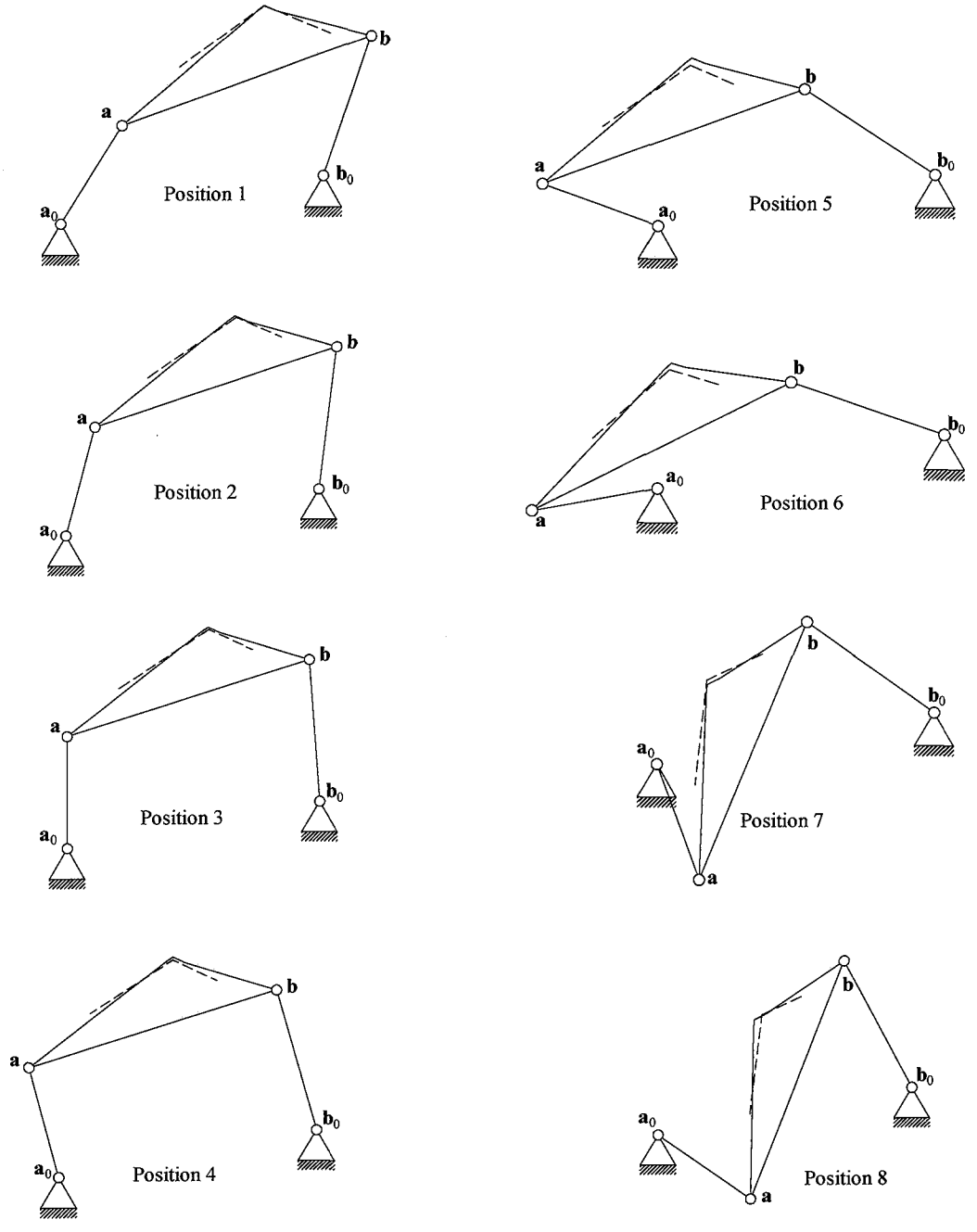

Figure 4.10 Achieved rigid-body positions of motion generator (in ADAMS).

Tables 4.4 and 4.5 include the resulting static torque and deflection of the crank link as well as the resulting follower link columnar loads. The crank and the follower buckling loads are 601820 and 1464 pounds, respectively.

Table 4.4 Crank Static Torques, Reaction Loads and Deflections

	Crank Static Torque [in-lb]	Force $_{a1}$ (lbf)			Crank Deflection [in]
		x	y	Resultant	
Pos 1	1000	216	-352	413	0.0055
Pos 2	497	75	-401	408	0.0027
Pos 3	111	-41	-432	434	0.0006
Pos 4	724	-151	-465	489	0.0040
Pos 5	2134	-568	-641	857	0.0117
Pos 6	1662	-626	-801	1017	0.0091
Pos 7	978	-26	-982	982	0.0053
Pos 8	2178	-18	-960	961	0.0124

Table 4.5 Follower Reaction Loads and Columnar Loads

	Force$_{b1}$ (lbf)			
	x	y	Resultant	$P_{cr\_Follower}$ (lbf)
Pos 1	-216	-648	683	1464
Pos 2	-75	-599	604	1464
Pos 3	41	-568	569	1464
Pos 4	151	-535	556	1464
Pos 5	568	-359	672	1464
Pos 6	626	-199	657	1464
Pos 7	26	-18	31	1464
Pos 8	18	-40	43	1464

The direction of reaction forces on the crank and the follower is illustrated in Figure 4.11. ADAMS is also used to attain the force vectors and trace the trajectory of a point on the coupler during the operation of the mechanism.

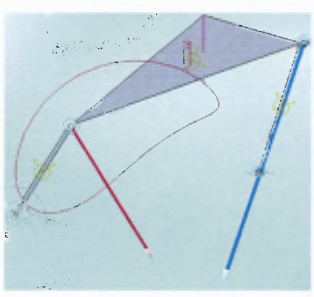

Position 1

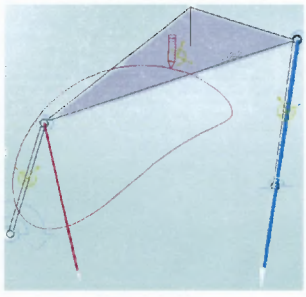

Position 2

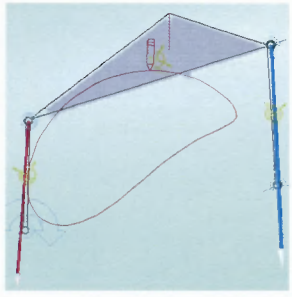

Position 3

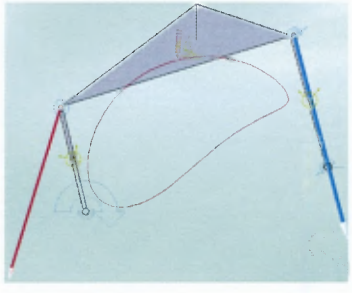

Position 4

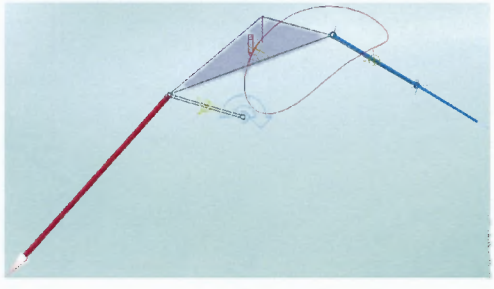

Position 5

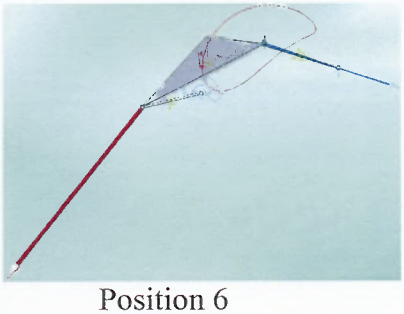

Position 6

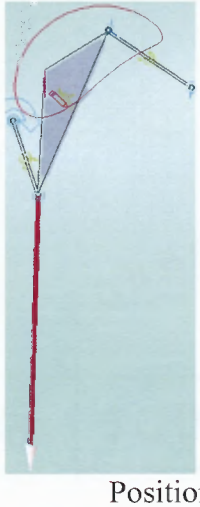

Position 7

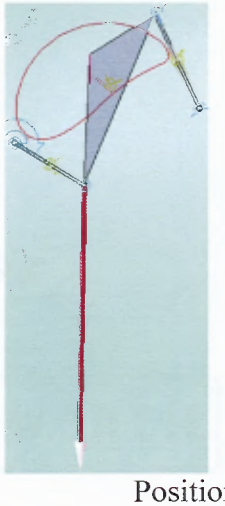

Position 8

Figure 4.11 The reaction loads $\mathbf{R}_A$, the external load F and reaction loads $\mathbf{R}_B$.

The magnitude of the reaction forces and the driving torque for the entire operation of the synthesized mechanism are plotted as a function of the crank displacement angle (Φ) illustrated in Figure 1.10. The driving torque, reaction loads $\mathbf{R}_A$ and reaction loads $\mathbf{R}_B$ are shown in Figures 4.12, 4.13 and 4.14, respectively.

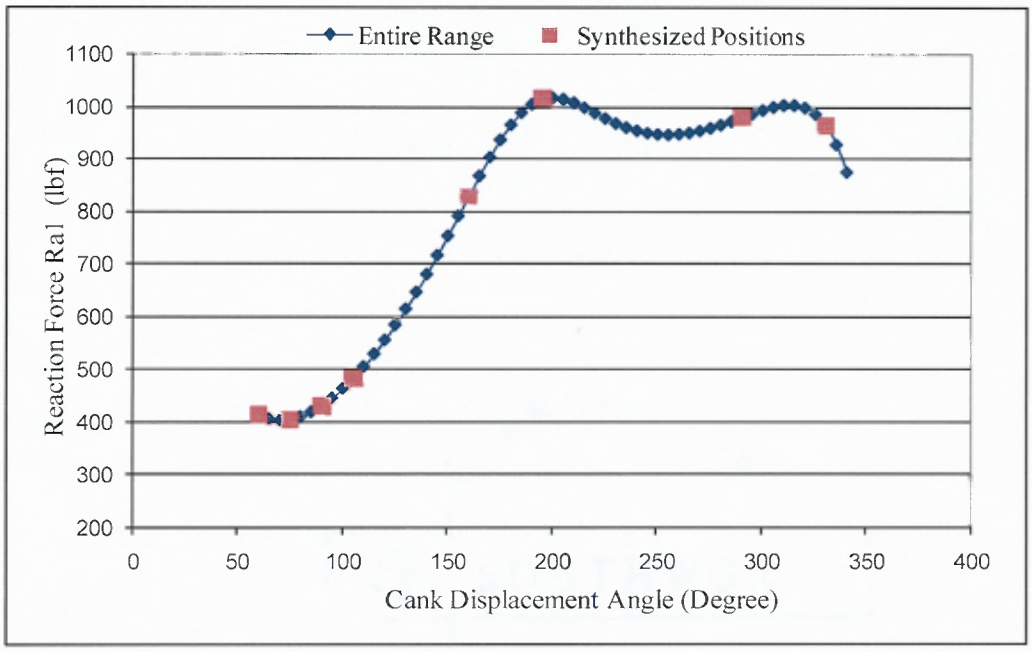

Figure 4.12 Magnitude of the reaction load $\mathbf{R}_A$ as a function of crank rotation.

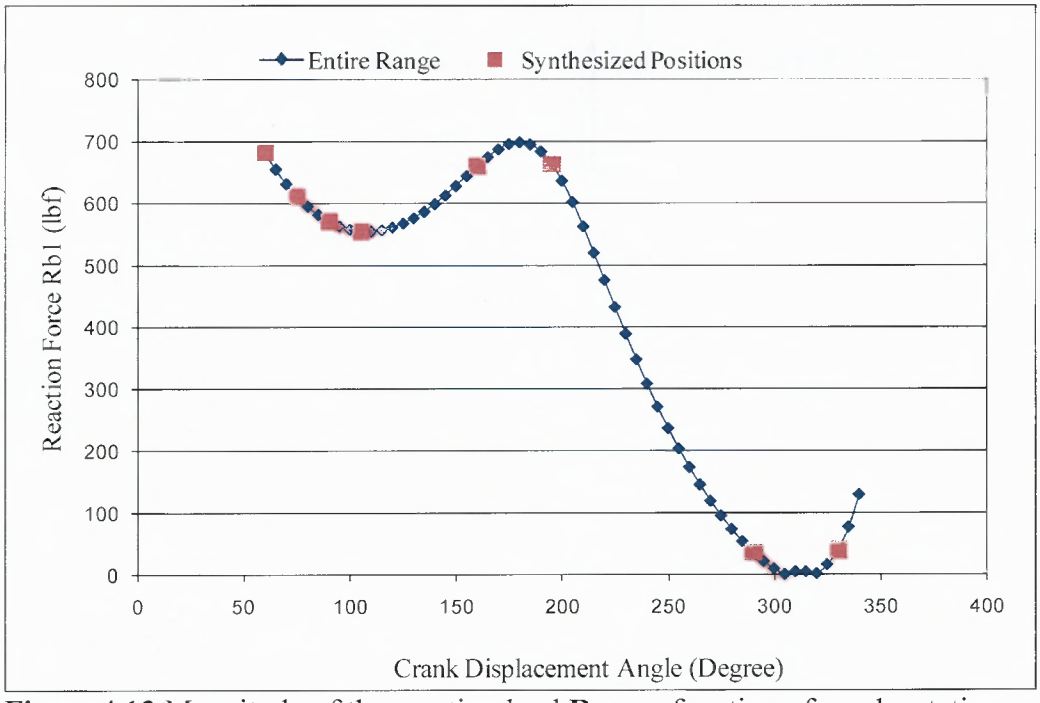

Figure 4.13 Magnitude of the reaction load $\mathbf{R}_B$ as a function of crank rotation.

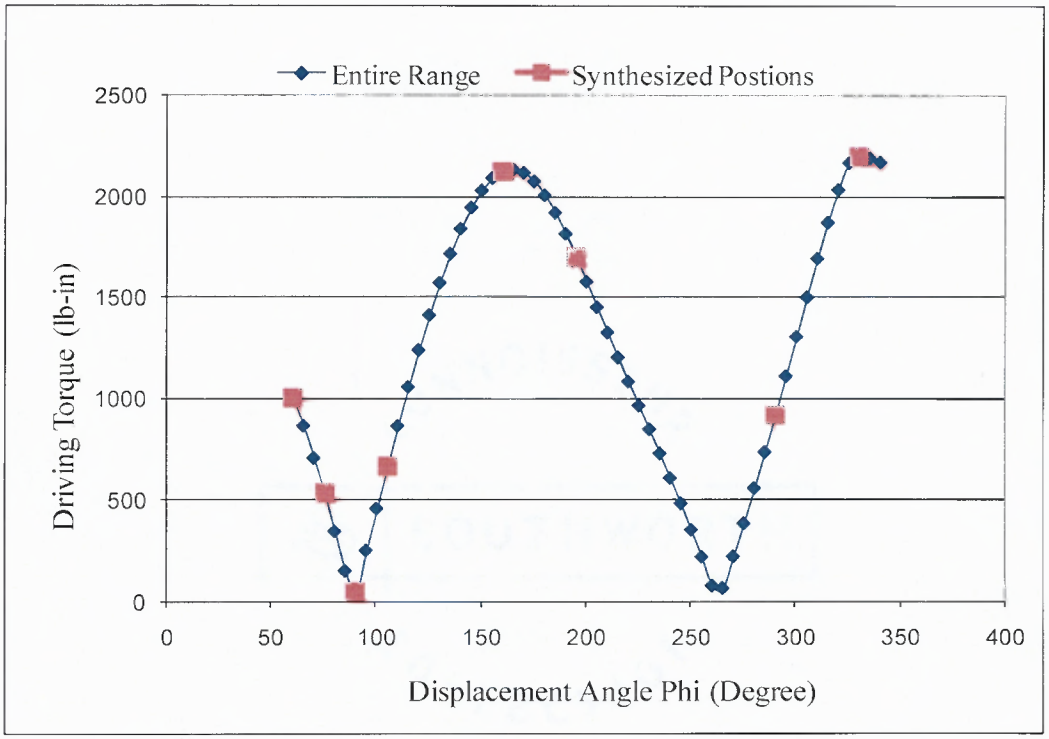

Figure 4.14 Magnitude of the driving static torque **T** as a function of crank rotation.

4.6.2 Calculation Sample and Verification

In this Section, the calculations are presented to verify the results obtained by ADAMS, these calculations are done for the initial position of the synthesized mechanism, the goal of this calculation is to find the result of the driving static torque, reaction loads and the crank deflection. Calculations for other positions were performed similarly as part of the verification process. The units for the reaction loads is lbf, the torque is in lbf-in, and the deflection is inches. The calculations are performed in MathCAD.

Input Values

$$a0 := \begin{pmatrix} 0.36270 \\ 0.01881 \\ 1.0000 \end{pmatrix} \quad a1 := \begin{pmatrix} 1.78383 \\ 2.33547 \\ 1 \end{pmatrix} \quad b0 := \begin{pmatrix} 6.49316 \\ 1.14576 \\ 1.0000 \end{pmatrix} \quad b1 := \begin{pmatrix} 7.58739 \\ 4.4303 \\ 1 \end{pmatrix} \quad q1 := \begin{pmatrix} 5.0928 \\ 5.1172 \\ 1 \end{pmatrix} \quad W := \begin{pmatrix} 0 \\ -1000 \\ 0 \end{pmatrix}$$

- **Analysis of Coupler**

Since Link $\mathbf{b_0b_1}$ is a two force member, Force R_B is always collinear to link $\mathbf{b_0b_1}$

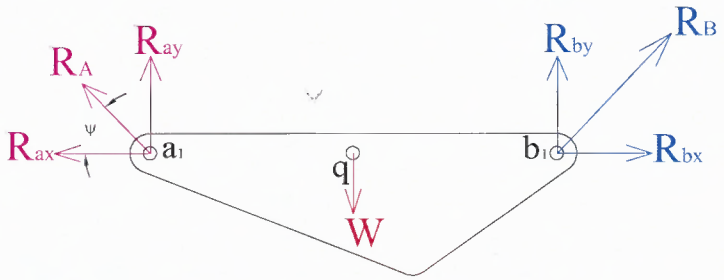

Figure 4.15 Free body diagram for coupler with rigid-body load W and reaction loads $\mathbf{R_A}$ and $\mathbf{R_B}$.

Use Equations (2.5) and (2.6) to find the columnar load in the follower.

$$R_b := \frac{|qa1 \times W|}{\left|a1b1 \times \frac{b1b0}{|b1b0|}\right|} \qquad R_b = 683.115$$

$$R_B := R_b \cdot \frac{b1b0}{|b1b0|} \qquad R_B = \begin{pmatrix} 216 \\ 648 \\ 0 \end{pmatrix} \qquad |R_B| = 683$$

$$-R_B = \begin{pmatrix} -216 \\ -648 \\ 0 \end{pmatrix}$$

Use Sub-section 2.2.1 Equation (1.8) to find the load $\mathbf{R_A}$ on the crank.

$$R_A := -R_B - W \qquad R_A := -\left(\frac{|qa1 \times W|}{\left|a1b1 \times \frac{b1b0}{|b1b0|}\right|} \cdot \frac{b1b0}{|b1b0|}\right) - W \qquad R_A = \begin{pmatrix} -216 \\ 352 \\ 0 \end{pmatrix} \qquad |R_A| = 413$$

$$-R_A = \begin{pmatrix} 216 \\ -352 \\ 0 \end{pmatrix}$$

- **Driver Link Static Torque**

Torque is a result of perpendicular Force to the arm times the arm length.

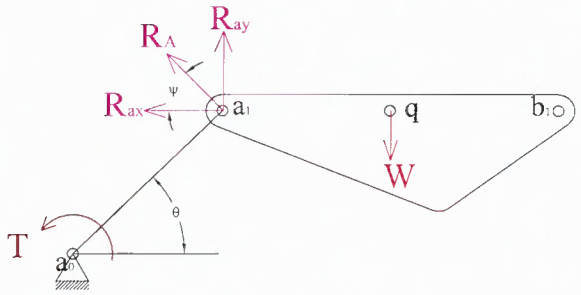

Figure 4.16 Free body diagram for the coupler and the crank with rigid-body load W, reaction load $\mathbf{R}_A$ and driving torque **T**.

$$\overrightarrow{T} = \overrightarrow{a1a0} \times \overrightarrow{R_A}$$

$$T := a1a0 \times \left[-\left(\frac{|qa1 \times W|}{\left| a1b1 \times \frac{b1b0}{|b1b0|} \right|} \cdot \frac{b1b0}{|b1b0|} \right) - W \right] \qquad T = \begin{pmatrix} 0 \\ 0 \\ 1000.292 \end{pmatrix} \qquad |T| = 1000$$

- **Crank Deflection**

Crank Link is link $\mathbf{a}_1\mathbf{a}_0$, the forces acting on crank is the same as $\mathbf{R}_A$ but opposite direction.

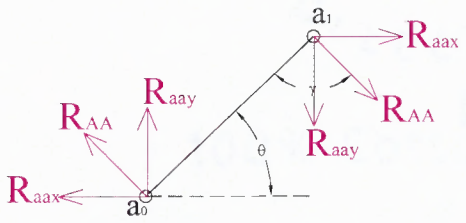

Figure 4.17 Crank with reaction load $\mathbf{R}_{AA}$.

$$R_{AA} := -R_A \qquad R_{AA} = \begin{pmatrix} 215.91 \\ -351.904 \\ 0 \end{pmatrix} \qquad |R_{AA}| = 412.86$$

$$\gamma := \operatorname{acos}\left(\frac{-a1a0 \cdot R_{AA}}{|a1a0| \cdot |R_A|} \right) \cdot \frac{180}{\pi} \qquad \gamma = 63.058$$

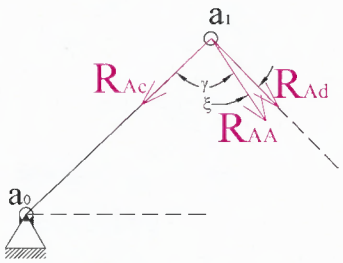

Figure 4.18 Crank with normal reaction load $\mathbf{R}_{Ad}$.

$$s := \frac{a1a0}{|a1a0|} \qquad s = \begin{pmatrix} 0.523 \\ 0.852 \\ 0 \end{pmatrix} \qquad E := 29000000 \qquad I_a := \frac{\pi}{64} \cdot .75^4$$

$$R_{Ac} := R_{AA} \cdot s \qquad R_{Ac} = -187.064$$

$$R_{Ad} := R_{AA} \times s \qquad |R_{Ad}| = 368.05$$

$$R_{Ad} := \left[-\left(\frac{|qa1 \times W|}{\left| a1b1 \times \frac{b1b0}{|b1b0|} \right|} \cdot \frac{b1b0}{|b1b0|} \right) - W \right] \times \frac{a1a0}{|a1a0|} \qquad R_{Ad} = \begin{pmatrix} 0 \\ 0 \\ -368.05 \end{pmatrix}$$

$$\delta_W = \frac{Wl^3}{3EI} \qquad \delta := \left| \frac{R_{Ad} \cdot L_1^{\,3}}{3 \cdot E \cdot I_a} \right|$$

$$\delta := \left| \frac{\left[-\left(\frac{|qa1 \times W|}{\left| a1b1 \times \frac{b1b0}{|b1b0|} \right|} \cdot \frac{b1b0}{|b1b0|} \right) - W \right] \times \frac{a1a0}{|a1a0|} \cdot (|a1a0|)^3}{3 \cdot E \cdot I_a} \right|$$

$$\delta = 0.005468$$

4.7 Discussion

Equation (4.17) becomes invalid when the pivots $\mathbf{a}_1$, $\mathbf{b}_1$ and $\mathbf{b}_0$ are collinear. Such a state is possible when the four-bar mechanism reaches a "lock-up" or binding position. When pivots $\mathbf{a}_1$, $\mathbf{b}_1$ and $\mathbf{b}_0$ are collinear, the denominator in Equation (4.17) becomes zero (making the equation and subsequent constraint invalid). The

mathematical analysis software MathCAD was used to codify and solve the formulated goal program.

It was necessary to perform stiffness model and finite element model for the synthesized mechanism to verify the formulation of the deflection constraint which is used in the goal program. This verification is performed for the first position using two methods which they are; First, a formulation of global stiffness matrix. Stiffness model for the deflection of pivots $\mathbf{a}_1$, $\mathbf{q}$ and $\mathbf{b}_1$ at each position (Table 4.6) is built using the approach discussed in Sub-section 4.4.1. Figure 4.19 shows the global stiffness matrix for the mechanism in position 1, other positions are constructed in the same manner discussed in Sub-section 4.4.1. Second method is a finite element analysis which was performed using COSMOS Designer to verify the deflection of the moving pivot $\mathbf{a}_1$ (Figure 4.20). The results from both methods are very close to the deflection of the crank using Euler deflection equation.

The deflection of the moving pivot $\mathbf{a}_1$ using global stiffness matrix approach discussed in Sub-section 4.4.1 is 0.005457 inch, while the deflection of the same pivot using FEA method is 0.005467 inch. Finally, the deflection of the moving pivot $\mathbf{a}_1$ using Euler equation, assuming the crank is a cantilever beam with force at the free end, is 0.005468 inch. These results are shown in Table 4.7.

$[K_{global}] =$

1	0	0	0	0	0	0	0	0	0	0	0	0	0	0
0	1	0	0	0	0	0	0	0	0	0	0	0	0	0
0	0	1	0	0	0	0	0	0	0	0	0	0	0	0
0	0	0	24303145064	20168302606	0	-24301806948	-20166230979	-871525996	0	0	0	0	0	0
0	0	0	20168302606	17269736792	0	-20166230979	-17266292317	1036713567	0	0	0	0	0	0
0	0	0	0	0	1	0	0	0	0	0	0	0	0	0
0	0	0	-24301806948	-20166230979	0	88473518153	2898520283	1875185661	-64171711205	17267710697	0	0	0	0
0	0	0	-20166230979	-17266292317	0	2898520283	23482219040	2608242547	17267710697	-6215926724	0	0	0	0
0	0	0	-871525996	1036713567	0	1875185661	2608242547	15636788338	-1003659665	-3644956113	0	0	0	0
0	0	0	0	0	0	-64171711205	17267710697	-1003659665	64171734432	-17267641360	0	0	0	0
0	0	0	0	0	0	17267710697	-6215926724	-3644956113	-17267641360	6216134978	0	0	0	0
0	0	0	0	0	0	0	0	0	0	0	1	0	0	0
0	0	0	0	0	0	0	0	0	0	0	0	1	0	0
0	0	0	0	0	0	0	0	0	0	0	0	0	1	0
0	0	0	0	0	0	0	0	0	0	0	0	0	0	1

Figure 4.19 Global stiffness matrix for the synthesized mechanism in the first position.

Table 4.6 Deflection of Joints $\mathbf{a}_1$, **q**, and $\mathbf{b}_1$ Using Stiffness Matrix Approach

Position 1								
Joint a_1 Deflection			**Joint q Deflection**			**Joint b_1 Deflection**		
Ux	Uy	δ	Ux	Uy	δ	Ux	Uy	δ
0.0046	-0.0029	0.0055	-0.0040	0.0068	0.0068	-0.0040	0.0068	0.0068
Position 2								
Joint a_1 Deflection			**Joint q Deflection**			**Joint b_1 Deflection**		
Ux	Uy	δ	Ux	Uy	δ	Ux	Uy	δ
0.0025	-0.0007	0.0026	0.0035	-0.0020	0.0041	0.0032	-0.0030	0.0044
Position 3								
Joint a_1 Deflection			**Joint q Deflection**			**Joint b_1 Deflection**		
Ux	Uy	δ	Ux	Uy	δ	Ux	Uy	δ
-0.0006	-0.0001	0.0006	0.0004	-0.0015	0.0015	0.0001	-0.0024	0.0024
Position 4								
Joint a_1 Deflection			**Joint q Deflection**			**Joint b_1 Deflection**		
Ux	Uy	δ	Ux	Uy	δ	Ux	Uy	δ
-0.0037	-0.0011	0.0039	-0.0027	-0.0024	0.0036	-0.0030	-0.0033	0.0045
Position 5								
Joint a_1 Deflection			**Joint q Deflection**			**Joint b_1 Deflection**		
Ux	Uy	δ	Ux	Uy	δ	Ux	Uy	δ
-0.0036	-0.0110	0.0116	-0.0036	-0.0111	0.0116	-0.0036	-0.0111	0.0117
Position 6								
Joint a_1 Deflection			**Joint q Deflection**			**Joint b_1 Deflection**		
Ux	Uy	δ	Ux	Uy	δ	Ux	Uy	δ
0.0021	-0.0088	0.0090	0.0007	-0.0075	0.0075	0.0009	-0.0064	0.0065
Position 7								
Joint a_1 Deflection			**Joint q Deflection**			**Joint b_1 Deflection**		
Ux	Uy	δ	Ux	Uy	δ	Ux	Uy	δ
-0.0048	-0.0019	0.0052	-0.0027	-0.0020	0.0033	-0.0020	-0.0031	0.0037
Position 8								
Joint a_1 Deflection			**Joint q Deflection**			**Joint b_1 Deflection**		
Ux	Uy	δ	Ux	Uy	δ	Ux	Uy	δ
-0.0063	-0.0105	0.0123	-0.0128	-0.0102	0.0164	-0.0149	-0.0069	0.0164

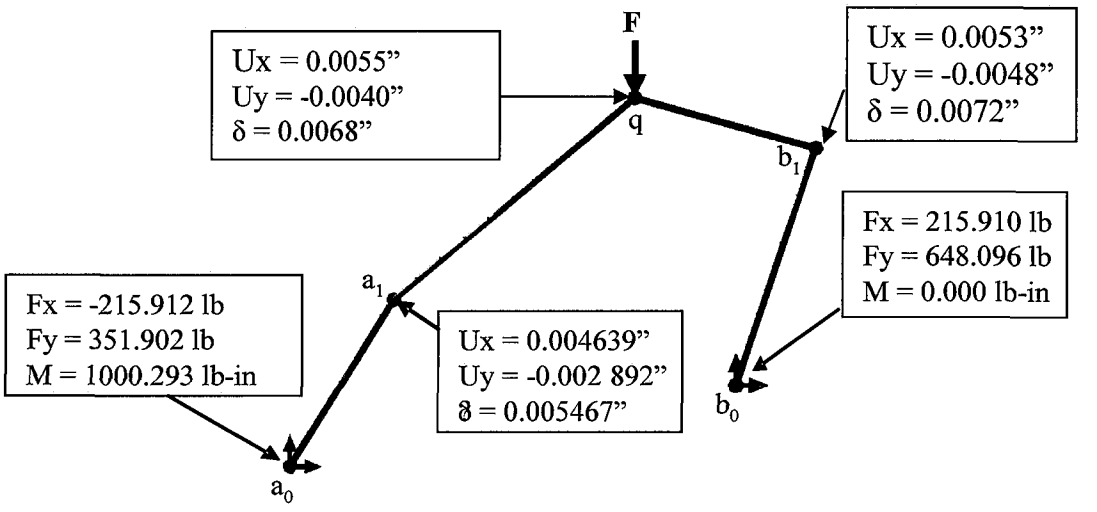

Figure 4.20 Deflections and reaction loads using FEA CosmosDesigner.

Table 4.7 Comparison of Stiffness Matrix Approach Vs FEA for the First Position

Joint a_1 Deflection					
Stiffness Matrix Approach			FEA Approach		
Ux	Uy	δ	Ux	Uy	δ
0.00463	-0.0028	0.0054	0.0046	-0.0028	0.0054
Joint q Deflection					
Stiffness Matrix Approach			FEA Approach		
Ux	Uy	δ	Ux	Uy	δ
0.0055	-0.0040	0.0068	0.0055	-0.0040	0.0068
Joint b_1 Deflection					
Stiffness Matrix Approach			FEA Approach		
Ux	Uy	δ	Ux	Uy	δ
0.00535	-0.0048	0.0072	0.0053	-0.0048	0.0072
Joint a_0 Reaction Loads					
Stiffness Matrix Approach			FEA Approach		
Fx	Fy	Moment	Fx	Fy	Resultant
-214.903	352.262	998.456	215.912	351.902	1000.293
Joint b_0 Reaction Loads					
Stiffness Matrix Approach			FEA Approach		
Fx	Fy	Moment	Fx	Fy	Resultant
214.903	647.738	2.919	215.910	648.096	0.000

Another comparison point is that the value of the driving torque and reaction loads. The results of the reaction loads on the crank and the follower shown in Tables 4.4 and 4.5 obtained by the same calculations performed in Sub-section 4.6.2 are very close to the results of the reactions loads obtained by matrix approach Table 4.7 and FEA model Figure 4.20 for the first position (only first position is shown, others are constructed similarly). This comparison of reaction loads and moment leads to the conclusion that using Euler equation as a deflection constraint Equation (4.30) is adequate.

The synthesized mechanism can be applied in many fields, one of the industrial applications that can utilize this mechanism is the vehicles lifting mechanism as shown in Figure 4.21.

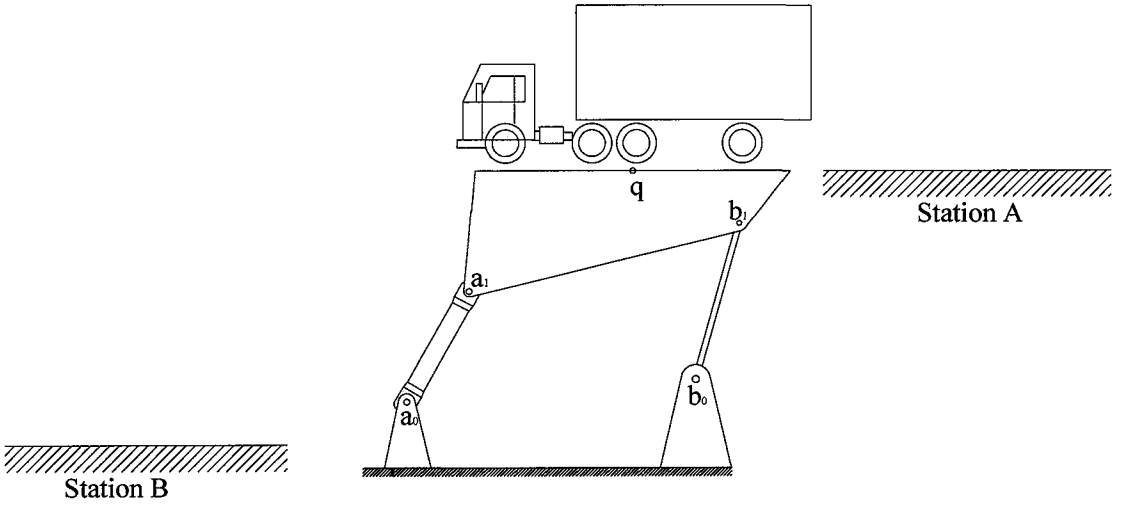

Figure 4.21 Vehicles lifting mechanism.

CHAPTER 5

GEARED FIVE-BAR MOTION GENERATION WITH STRUCTURAL CONDITIONS

5.1 Introduction

5.1.1 Motion Generation

In motion generation, the objective is to calculate the mechanism parameters required to achieve or approximate a set of prescribed rigid-body positions. This mechanism design objective is particularly useful when the rigid-body must achieve a specific displacement sequence for effective operation (e.g., specific tool paths and/or orientations for accurate fabrication operations). In Figure 5.1, four prescribed rigid-body positions are defined by the coordinates of variables **p**, **q** and **r** (motion generation model input) and the model output are the calculated coordinates of the moving pivot variables $\mathbf{a}_1$ and $\mathbf{c}_1$ and scalar link lengths R_1 and R_3. A numerical geared five-bar motion generation model [1, 33-34] is presented in the next section.

Motion generation for planar five-bar mechanisms is a fairly-established field. Recent contributions include the works Sodhi and Russell [33] and Musa et al. [34] that consider motion generation of adjustable geared five-bar motion generators with prescribed rigid-body positions and rigid-body positions with tolerances. The works of Balli and Chand [35-36] introduce a complex number method for the synthesis of a planar five-bar motion generator with prescribed timing and a method to synthesize a planar five-bar mechanism of variable topology type with transmission angle control. Nokleby and Podhorodeski [37] presented an optimization method to synthesize Grashof five-bar mechanisms. Wang and Yan [38] presented an approach for

synthesizing planar five-bar linkages with five prescribed precision positions. Basu and Farhang [39] introduced a mathematical formulation for the approximate analysis and design of two-input, small-crank five-bar mechanisms for function generation. Dou and Ting [40] introduced a method to identify to rotatability and branch condition in linkages containing simple geared five-bar chains. Lin and Chaing [41] extended pole method for use in the synthesis planar, geared five-bar function generators. Ge and Chen [42] introduced a software-based approach for the atlas method on path synthesis of geared five-bar mechanisms. The authors also studied the effect of link length, crank angles and gear tooth ratio on the motion of the geared five-bar linkage [43]. Li and Dao [44] introduced a complex number method for the synthesis for geared, five-bar guidance mechanisms.

Although a substantial number of contributions have been made regarding planar five-bar motion generation (and motion generation in general), the concept of including structural conditions in motion generation is not nearly as established. With the exception of Huang and Roth [18] whose work includes analytical motion generation models for planar four-bar mechanisms with a prescribed rigid-body load, most other works that investigate the structural behavior of mechanisms under load do not consider the structural behavior in the context of motion generation. The works of Mohammad [28], Venanzi et al. [29], Sonmez [30], Plaut et al. [31] and Siriam and Mruthyunjaya [27] do consider flexible links and/or buckling in mechanism design, but they consider the design of compliant mechanisms as opposed to classical linkage-based mechanisms.

The specific contribution this work makes regarding motion generation with structural conditions for geared five-bar mechanism is the formulation of a motion generation goal program that includes elastic deflection, static torque and buckling constraints. Being a goal program, an indefinite number of prescribed rigid-body positions can be incorporated. As demonstrated in the included example, using the goal program formulated in this work, a geared five-bar mechanism is synthesized to approximate a set of prescribed rigid-body positions and also satisfy specified elastic deflection, static torque and buckling conditions for a given rigid-body load.

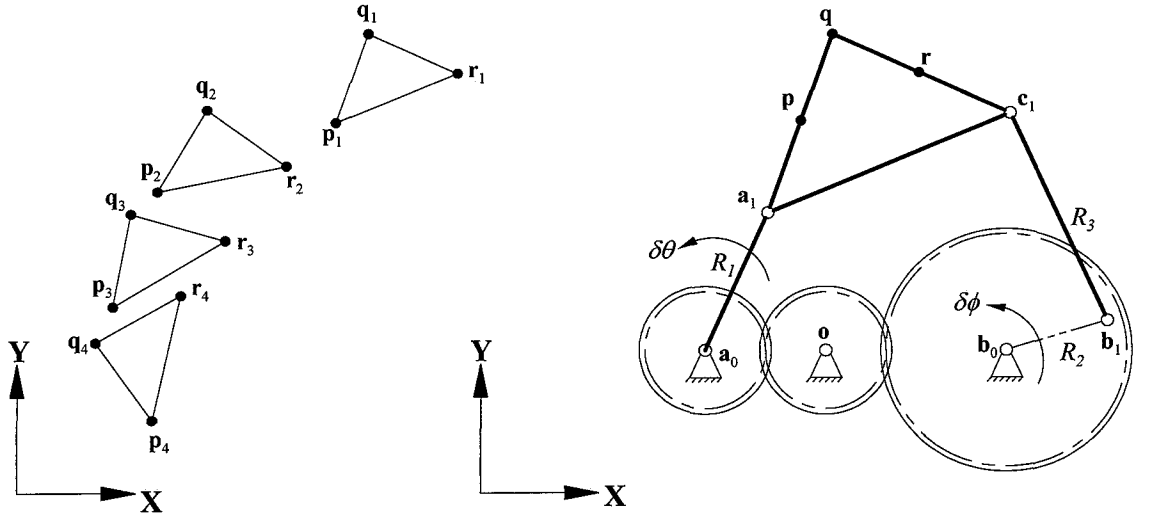

Figure 5.1 Prescribed rigid-body positions and calculated geared five-bar mechanism.

5.1.2 Motivation and Scope of Work

Using conventional motion generation methods the user can only calculate the mechanism parameters required to achieve or approximate a set of prescribed rigid-body positions. Although such solutions are useful for preliminary kinematic analyses, other factors (e.g., static loads, dynamic loads, stresses, strains, etc.) must

be considered prior to fabricating a physical prototype of the mechanical design. This work considers static driving link torque does not to exceed a given torque value. The second purpose is to synthesis a mechanism so that the deflection of the crank does not exceed a specified value during the operation of the mechanism. The third purpose of is to prevent buckling of the follower during the normal mechanism operation. An optimization model was formulated to achieve the kinto-elastostatic conditions and numerical example is also presented for eight prescribed coupler positions.

5.2 Geared Five-bar Motion Generation

Equations (5.1) through (5.3) encompass a conventional geared five-bar motion generation model [1][33][34].

$$\left([\mathbf{D}_{1i}]\mathbf{a}_1 - \mathbf{a}_0\right)^T \left([\mathbf{D}_{1i}]\mathbf{a}_1 - \mathbf{a}_0\right) - R_1^{\,2} = 0 \tag{5.1}$$

$$\left([\mathbf{D}(\delta\phi)_{1i}]\mathbf{b}_1 - \mathbf{b}_0\right)^T \left([\mathbf{D}(\delta\phi)_{1i}]\mathbf{b}_1 - \mathbf{b}_0\right) - R_2^{\,2} = 0 \tag{5.2}$$

$$\left([\mathbf{D}_{1i}]\mathbf{c}_1 - [\mathbf{D}(\delta\phi)_{1i}]\mathbf{b}_1\right)^T \left([\mathbf{D}_{1i}]\mathbf{c}_1 - [\mathbf{D}(\delta\phi)_{1i}]\mathbf{b}_1\right) - R_3^{\,2} = 0 \tag{5.3}$$

These equations are "constant length" constraints and ensure the fixed lengths of links $\mathbf{a}_0\mathbf{a}_1$, $\mathbf{b}_0\mathbf{b}_1$ and $\mathbf{b}_1\mathbf{c}_1$ throughout the prescribed rigid-body displacements. Variables R_1, R_2 and R_3 in Equations (5.1) through (5.3) are the prescribed scalar lengths of links $\mathbf{a}_0\mathbf{a}_1$, $\mathbf{b}_0\mathbf{b}_1$ and $\mathbf{b}_1\mathbf{c}_1$, respectively.

$$[\mathbf{D}_{1i}] = \begin{bmatrix} p_{ix} & q_{ix} & r_{ix} \\ p_{iy} & q_{iy} & r_{iy} \\ 1 & 1 & 1 \end{bmatrix} \begin{bmatrix} p_{1x} & q_{1x} & r_{1x} \\ p_{1y} & q_{1y} & r_{1y} \\ 1 & 1 & 1 \end{bmatrix}^{-1} \tag{5.4}$$

In conventional motion generation, three points (**p**, **q**, and **r**) on the coupler body are defined. If the coupler points lie on the same line (prohibited), displacement matrix $[\mathbf{D}_{1j}]$ (Equation (5.4)) becomes proportional with proportional rows, this matrix could not be inverted.

$$\left[\mathbf{D}(\delta\phi)_{1i}\right]=\begin{bmatrix}\cos(\delta\phi)_{1i} & -\sin(\delta\phi)_{1i} & -b_{0x}\cos(\delta\phi)_{1i}+b_{0y}\sin(\delta\phi)_{1i}+b_{0x}\\ \sin(\delta\phi)_{1i} & \cos(\delta\phi)_{1i} & -b_{0x}\sin(\delta\phi)_{1i}-b_{0y}\cos(\delta\phi)_{1i}+b_{0y}\\ 0 & 0 & 1\end{bmatrix} \tag{5.5}$$

Equation (5.4) is a rigid-body planar displacement matrix. Equation (5.5) is the angular displacement matrix for link $\mathbf{b}_0\mathbf{b}_1$ where i=1,2,3,4 and

$$\left[\mathbf{M}_{1i}\right]=\left[\begin{array}{c|c|c}1 & & \\ 1 & \mathbf{a}_1-\mathbf{a}_0 & \left[\mathbf{D}_{1i}\right]\mathbf{a}_1-\mathbf{a}_0\\ 1 & 0 & 0\end{array}\right]$$

$$\cos(\delta\theta)_{1i}=\frac{(\mathbf{a}_1-\mathbf{a}_0)\cdot(\left[\mathbf{D}_{1i}\right]\mathbf{a}_1-\mathbf{a}_0)}{|\mathbf{a}_1-\mathbf{a}_0|\cdot|\left[\mathbf{D}_{1i}\right]\mathbf{a}_1-\mathbf{a}_0|}$$

$$\sin(\delta\theta)_{1i}=\frac{\det\left[\mathbf{M}_{1i}\right]}{|\mathbf{a}_1-\mathbf{a}_0|\cdot|\left[\mathbf{D}_{1i}\right]\mathbf{a}_1-\mathbf{a}_0|}$$

$$(\delta\theta)_{1i}=\arctan 2\left(\sin(\delta\theta)_{1i},\cos(\delta\theta)_{1i}\right)$$

and $(\delta)_{1i}=k(\delta\theta)_{1i}$. Variable k represents the gear ratio of the gear train joining links $\mathbf{a}_0\mathbf{a}_1$ and $\mathbf{b}_0\mathbf{b}_1$. From this conventional planar five-bar motion generator model, 12 of the 13 unknown variables $\mathbf{a}_0$, $\mathbf{a}_1$ R_1, $\mathbf{b}_0$, $\mathbf{b}_1$, R_2, $\mathbf{c}_1$, and R_3 are calculated with one arbitrary choice of parameter for four prescribed rigid-body positions (where $\mathbf{a}_0 = [a_{0x}, a_{0y}, 1]$, $\mathbf{a}_1 = [a_{1x}, a_{1y}, 1]$, $\mathbf{b}_0 = [b_{0x}, b_{0y}, 1]$, $\mathbf{b}_1 = [b_{1x}, b_{1y}, 1]$ and $\mathbf{c}_1 = [c_{1x}, c_{1y}, 1]$).

5.3 Geared Five-bar Mechanism Under Rigid-body Load

In this work, the moving pivot $\mathbf{b}_1$ is affixed to the gear centered at the fixed pivot $\mathbf{b}_0$ (Figure 5.1). The moving pivot does not extend beyond the pitch circle. Also, the gears are considered rigid and subsequently not subject to deflection due to rigid-body loading. Figure 5.2 illustrates a statically-loaded geared five-bar mechanism. In this work, link $\mathbf{a}_0\mathbf{a}_1$ is only connected to its corresponding gear at $\mathbf{a}_0$. Because of this condition, link $\mathbf{a}_0\mathbf{a}_1$ is illustrated in Figure 5.2 as having a single connection to the ground. A load $\{\mathbf{F}\}$ is applied to the mechanism (in this work, at rigid-body point **q**). An analytical model to calculate the deflections $\{\mathbf{U}\}$ at any element node on this mechanism is formulated using Equation (5.6) where the 15x15 global stiffness matrix $[\mathbf{K}_{global}]$ for the mechanism is comprised of Equation (5.7)-the element stiffness matrix for each mechanism link. The element stiffness matrix for link $\mathbf{a}_0\mathbf{a}_1$ and the rigid-body (link $\mathbf{a}_1\mathbf{q}\mathbf{c}_1$) is Equation. (5.8). Because link $\mathbf{b}_1\mathbf{c}_1$ is a two-force member (and therefore under columnar loading only) its element stiffness matrix $[\mathbf{k}_{axial}]$ is Equation. (5.9). Equation (5.10) is the element local-to-global coordinate frame transformation matrix.

In Figure 5.2 variables E_j, A_j, I_j and L_j (where j = 1,2,3,4) are the modulus of elasticity, cross-sectional area, moment of inertia and length of each link, respectively. Because link $\mathbf{a}_1\mathbf{q}\mathbf{c}_1$ is to be a uniform rigid-body in this study, $E_2 = E_3$, $A_2 = A_3$, $I_2 = I_3$ and its modulus of elasticity is one million times higher than those of the link $\mathbf{a}_0\mathbf{a}_1$ and link $\mathbf{b}_1\mathbf{c}_1$. The angular orientation of each link (using the positive x-

axis as reference) is denoted by angle θ_k (where j=1,2,3,4). These angles are used in Equation (5.10).

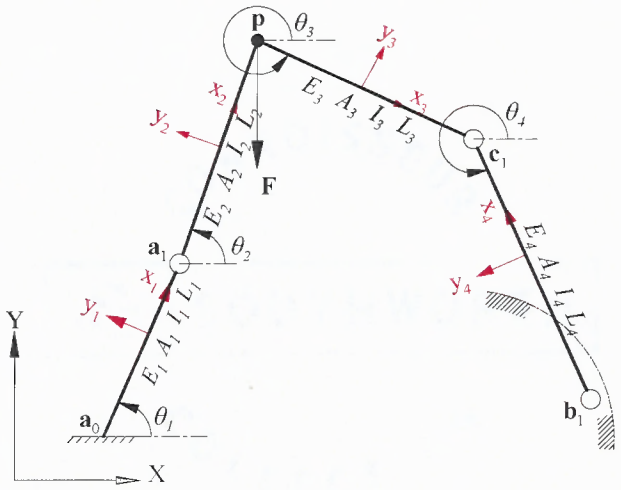

Figure 5.2 Statically-loaded geared five-bar mechanism.

$$\{\mathbf{F}\} = \left[\mathbf{K}_{global}\right]\{\mathbf{U}\} \tag{5.6}$$

$$\left[\mathbf{K}_j\right] = \left[\mathbf{T}_j\right]\left[\mathbf{k}_j\right]\left[\mathbf{T}_j\right]^{-1} \tag{5.7}$$

$$\left[\mathbf{k}_j\right] = \begin{bmatrix} \frac{A_jE_j}{L_j} & 0 & 0 & -\frac{A_jE_j}{L_j} & 0 & 0 \\ 0 & \frac{12E_jI_j}{L_j^3} & \frac{6E_jI_j}{L_j^2} & 0 & -\frac{12E_jI_j}{L_j^3} & \frac{6E_jI_j}{L_j^2} \\ 0 & \frac{6E_jI_j}{L_j^2} & \frac{4E_jI_j}{L_j} & 0 & -\frac{6E_jI_j}{L_j^2} & \frac{2E_jI_j}{L_j} \\ -\frac{A_jE_j}{L_j} & 0 & 0 & \frac{A_jE_j}{L_j} & 0 & 0 \\ 0 & -\frac{12E_jI_j}{L_j^3} & -\frac{6E_jI_j}{L_j^2} & 0 & \frac{12E_jI_j}{L_j^3} & -\frac{6E_jI_j}{L_j^2} \\ 0 & \frac{6E_jI_j}{L_j^2} & \frac{2E_jI_j}{L_j} & 0 & -\frac{6E_jI_j}{L_j^2} & \frac{4E_jI_j}{L_j} \end{bmatrix} \tag{5.8}$$

$$[\mathbf{k}_{axial}] = \begin{bmatrix} \frac{A_4E_4}{L_4} & 0 & 0 & -\frac{A_4E_4}{L_4} & 0 & 0 \\ 0 & 0 & 0 & 0 & 0 & 0 \\ 0 & 0 & 0 & 0 & 0 & 0 \\ -\frac{A_4E_4}{L_4} & 0 & 0 & \frac{A_4E_4}{L_4} & 0 & 0 \\ 0 & 0 & 0 & 0 & 0 & 0 \\ 0 & 0 & 0 & 0 & 0 & 0 \end{bmatrix} \tag{5.9}$$

$$[\mathbf{T}_j] = \begin{bmatrix} \cos\theta_j & \sin\theta_j & 0 & 0 & 0 & 0 \\ -\sin\theta_j & \cos\theta_j & 0 & 0 & 0 & 0 \\ 0 & 0 & 1 & 0 & 0 & 0 \\ 0 & 0 & 0 & \cos\theta_j & \sin\theta_j & 0 \\ 0 & 0 & 0 & -\sin\theta_j & \cos\theta_j & 0 \\ 0 & 0 & 0 & 0 & 0 & 1 \end{bmatrix} \tag{5.10}$$

5.4 Driver Link Static Torque Constant

With an external load **F** acting on the rigid-body of the geared five-bar mechanism, a torque **T** applied to the driver (which is the intermediate gear in this work) achieves static equilibrium. In Figure 5.3, the load **F** is applied to rigid-body at point **q**. To formulate the driver static torque constraint, the moment condition $\Sigma\mathbf{M} = 0$ (Figure 5.4b) is taken about the fixed pivot $\mathbf{a}_1$. The equilibrium moments equation about the fixed pivot $\mathbf{a}_1$ is

$$\overrightarrow{a_1c_1} \times \mathbf{R}_{c1} + \overrightarrow{a_1q} \times \mathbf{F} = 0 \tag{5.11}$$

where

$$\mathbf{R}_{c1} = R_c \frac{\overrightarrow{b_1c_1}}{\left|\overrightarrow{b_1c_1}\right|} \tag{5.12}$$

The reaction load R_c is a real number that varies with the mechanism position. Substituting Equation (5.12) into Equation (5.11) produces

$$R_c = \frac{\left|\overrightarrow{a_1q}\times\mathbf{F}\right|}{\left|\overrightarrow{a_1c_1}\times\frac{\overrightarrow{b_1c_1}}{\left|\overrightarrow{b_1c_1}\right|}\right|} \tag{5.13}$$

and substituting Equation (5.13) into Equation (5.11) and solving for $\mathbf{R}_{c1}$ produces

$$\mathbf{R}_{c1} = \frac{\left|\overrightarrow{a_1q}\times\mathbf{F}\right|}{\left|\overrightarrow{a_1c_1}\times\overrightarrow{b_1c_1}\right|}\overrightarrow{b_1c_1} \tag{5.14}$$

The resulting equilibrium of force equation for the rigid-body in Figure 5.4b is

$$\mathbf{R}_{a1} + \mathbf{R}_{c1} + \mathbf{F} = 0 \tag{5.15}$$

Substituting Equation (5.14) into Equation (5.15) and solving for $\mathbf{R}_{a1}$ produces

$$\mathbf{R}_{a1} = -\frac{\left|\overrightarrow{a_1q}\times\mathbf{F}\right|}{\left|\overrightarrow{a_1c_1}\times\overrightarrow{b_1c_1}\right|}\overrightarrow{b_1c_1} - \mathbf{F} \tag{5.16}$$

With the rigid-body reaction load Equations (5.14) and (5.16) formulated, torque equations for the gears about $\mathbf{a}_0$ and $\mathbf{b}_0$ are formulated next. The moment condition $\Sigma\mathbf{M}=0$ is taken about the fixed pivot $\mathbf{a}_0$ for link $\mathbf{a}_0\mathbf{a}_1$ in Figure 5.4a. The resulting equilibrium equation of the moments about $\mathbf{a}_0$ is

$$\mathbf{T}_a - \overrightarrow{a_0a_1}\times\mathbf{R}_{a1} = 0 \tag{5.17}$$

Substituting Equation (5.16) into Equation (5.17) and solving for torque $\mathbf{T}_a$ produces

$$\mathbf{T}_a = \overrightarrow{a_0a_1}\times\left(-\frac{\left|\overrightarrow{a_1q}\times\mathbf{F}\right|}{\left|\overrightarrow{a_1c_1}\times\overrightarrow{b_1c_1}\right|}\overrightarrow{b_1c_1} - \mathbf{F}\right) \tag{5.18}$$

The moment condition $\Sigma\mathbf{M}=0$ is now taken about the fixed pivot $\mathbf{b}_0$ for link $\mathbf{b}_0\mathbf{b}_1$ in Figure 5.4c. The resulting equilibrium equation of the moments about $\mathbf{b}_0$ is

$$\mathbf{T}_b - \overrightarrow{b_0b_1} \times \mathbf{R}_{c1} = 0 \tag{5.19}$$

Substituting Equation (5.14) into Equation (5.19) and solving for torque $\mathbf{T}_b$ produces

$$\mathbf{T}_b = \overrightarrow{b_0b_1} \times \frac{\left|\overrightarrow{a_1q} \times \mathbf{F}\right|}{\left|\overrightarrow{a_1c_1} \times \overrightarrow{b_1c_1}\right|} \overrightarrow{b_1c_1} \tag{5.20}$$

In Equations (5.18) and (5.20)

$$\mathbf{F} = \begin{pmatrix} f_x \\ f_y \\ 0 \end{pmatrix}, \overrightarrow{a_1q} = \mathbf{q}_i - [\mathbf{D}_{1i}]\mathbf{a}_1, \overrightarrow{a_0a_1} = [\mathbf{D}_{1i}]\mathbf{a}_1 - \mathbf{a}_0, \overrightarrow{b_1c_1} = [\mathbf{D}_{1i}]\mathbf{c}_1 - [\mathbf{D}(\delta\phi)_{1i}]\mathbf{b}_1 \text{ and}$$

$\overrightarrow{a_1c_1} = [\mathbf{D}_{1i}]\mathbf{c}_1 - [\mathbf{D}_{1i}]\mathbf{a}_1$.

As mentioned earlier, the intermediate gear is the designated driver in this work. Neglecting power loss, the static equilibrium driver torque is

$$\mathbf{T} = k_1^{-1}\mathbf{T}_a + k_2^{-1}\mathbf{T}_b \tag{5.21}$$

where

$k_1 = \frac{r_a}{r}$ and $k_2 = \frac{r_b}{r}$ .Variables r_a, r_b and r are the pitch radii of the gears centered at $\mathbf{a}_0$, $\mathbf{b}_0$, and $\mathbf{o}$, respectively (Figure 5.3). Equation (5.21) calculates the five-bar mechanism driver static torque for a given rigid-body load. Expressing Equation (5.21) as an inequality constraint to limit the maximum driver static torque for N prescribed rigid-body positions yields

$$(\mathbf{T}_i)^T(\mathbf{T}_i) < \tau_{max}^2 \tag{5.22}$$

where $i = 1, 2, 3, \ldots, N$.

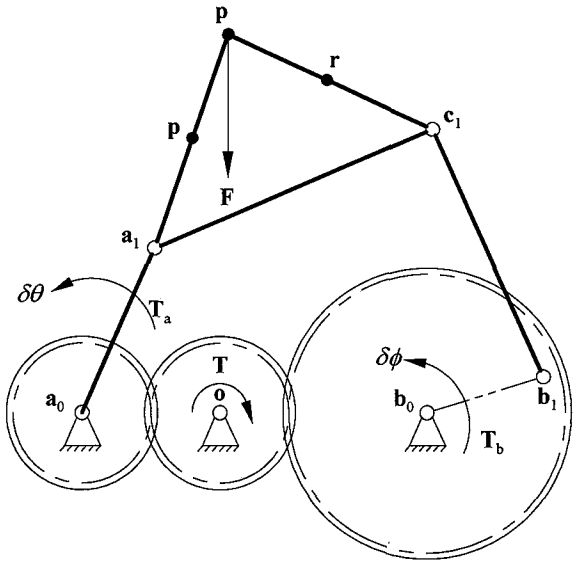

Figure 5.3 Geared five-bar mechanism in static equilibrium.

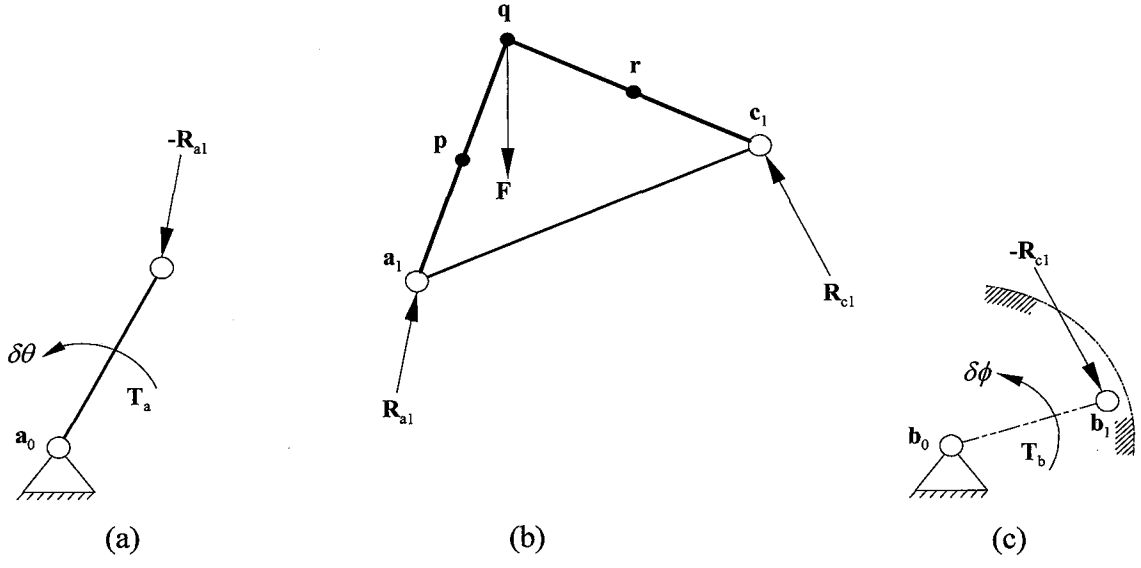

Figure 5.4 Geared five-bar mechanism link (a) $\mathbf{a}_0\mathbf{a}_1$ (b) rigid-body and (c) link $\mathbf{b}_0\mathbf{b}_1$ in static equilibrium.

5.5 Link Buckling and Elastic Deflection Constraints

As previously discussed, the link $\mathbf{b}_1\mathbf{c}_1$ is under columnar loading only because it is a two-force member. The Euler formula for critical buckling load for a column with pinned ends [5] is

$$P_{cr} = \frac{\pi^2 EI}{L^2} \tag{5.23}$$

where variables E, I and L are the modulus of elasticity, moment of inertia and effective column length, respectively. The scalar columnar load R_c in the link $\mathbf{b}_1\mathbf{c}_1$ is expressed in Equation (5.13). Expressing Equation (5.3) as an inequality constraint to prevent link $\mathbf{b}_1\mathbf{c}_1$ buckling for N prescribed rigid-body positions yields

$$\left([\mathbf{D}_{1i}]\mathbf{c}_1 - [\mathbf{D}(\delta\phi)_{1i}]\mathbf{b}_1\right)^T \left([\mathbf{D}_{1i}]\mathbf{c}_1 - [\mathbf{D}(\delta\phi)_{1i}]\mathbf{b}_1\right) < \frac{\pi^2 EI}{R_c} \tag{5.24}$$

where the right-side term is L^2 in Equation (5.23).

Unlike the link $\mathbf{b}_1\mathbf{c}_1$, link $\mathbf{a}_0\mathbf{a}_1$ is not a two-force member. As shown in Figure 5.2 and Figure 5.4a, this link is a fixed-end cantilevered beam under a load with a transverse component. Because the constraint and loading conditions on link $\mathbf{a}_0\mathbf{a}_1$ make link deflection a common occurrence, constraining the deflection of the link $\mathbf{a}_0\mathbf{a}_1$ is critical. The Euler formula for the deflection of a fixed-end cantilevered beam [5] is

$$\delta = \frac{PL^3}{3EI} \tag{5.25}$$

where variables P, L, E and I are the free-end transverse load, beam length, modulus of elasticity and moment of inertia, respectively. Equation (5.16) is the total load on the moving pivot $\mathbf{a}_1$. The transverse component of this load is

$$\overrightarrow{R_{a_{trans}}} = \left(-\frac{\left|\overrightarrow{a_1 q} \times \mathbf{F}\right|}{\left|\overrightarrow{a_1 c_1} \times \overrightarrow{b_1 c_1}\right|} \overrightarrow{b_1 c_1} - \mathbf{F} \right) \times \frac{\overrightarrow{a_0 a_1}}{\left|\overrightarrow{a_0 a_1}\right|} \tag{5.26}$$

Expressing Equation (5.1) as an inequality constraint to limit crank deflection for N prescribed rigid-body positions yields

$$\left([\mathbf{D}_{1i}]\mathbf{a}_1 - \mathbf{a}_0\right)^T \left([\mathbf{D}_{1i}]\mathbf{a}_1 - \mathbf{a}_0\right) < \left(\frac{3\delta EI}{\left|\overrightarrow{R_{a_{trans}}}\right|} \right)^{\frac{2}{3}} \tag{5.27}$$

where the right-side term is L^2 in Equation (5.25).

5.6 Motion Generation Goal Program

Formulating Equations (5.1) and (5.3) into a single objective function (that accommodates an indefinite number of N prescribed rigid-body positions) to be minimized yields

$$\begin{aligned} f(\mathbf{X}) = \sum_{i=1}^{N} \Bigg\{ & \left[\left([\mathbf{D}_{1i}]\mathbf{a}_1 - \mathbf{a}_0\right)^T \left([\mathbf{D}_{1i}]\mathbf{a}_1 - \mathbf{a}_0\right) - R_l^{\,2} \right]^2 \\ & + \left[\left([\mathbf{D}_{1i}]\mathbf{c}_1 - [\mathbf{D}(\delta\phi)_{1i}]\mathbf{b}_1\right)^T \left([\mathbf{D}_{1i}]\mathbf{c}_1 - [\mathbf{D}(\delta\phi)_{1i}]\mathbf{b}_1\right) - R_3^{\,2} \right]^2 \Bigg\} \end{aligned} \tag{5.28}$$

where $\mathbf{X} = \left(a_{1x}, a_{1y}, R_1, c_{1x}, c_{1y}, R_3\right)^T$.

- The Driver link static torque constraint

$$\left[k_1^{-1} \left(\overrightarrow{a_0 a_1} \times \left(-\frac{\left|\overrightarrow{a_1 q} \times \mathbf{F}\right|}{\left|\overrightarrow{a_1 c_1} \times \overrightarrow{b_1 c_1}\right|} \overrightarrow{b_1 c_1} - \mathbf{F} \right) \right) + k_2^{-1} \left(\overrightarrow{b_0 b_1} \times \frac{\left|\overrightarrow{a_1 q} \times \mathbf{F}\right|}{\left|\overrightarrow{a_1 c_1} \times \overrightarrow{b_1 c_1}\right|} \overrightarrow{b_1 c_1} \right) \right]^2 - T^2 \le 0$$

- The Buckling constraint of the follower

$$\left([\mathbf{D}_{1i}]\mathbf{c}_1 - [\mathbf{D}(\delta\phi)_{1i}]\mathbf{b}_1\right)^T \left([\mathbf{D}_{1i}]\mathbf{c}_1 - [\mathbf{D}(\delta\phi)_{1i}]\mathbf{b}_1\right) - \frac{\pi^2 \times E_{b_1c_1} \times I_{b_1c_1}}{\frac{\left|\overrightarrow{a_1q} \times \mathbf{F}\right|}{\left|\overrightarrow{a_1c_1} \times \overrightarrow{b_1c_1}\right|}} < 0$$

- The deflection constraint of the crank

$$\left([\mathbf{D}_{1i}]\mathbf{a}_1 - \mathbf{a}_0\right)^T \left([\mathbf{D}_{1i}]\mathbf{a}_1 - \mathbf{a}_0\right) - \left(\frac{3 \times E_{Crank} \times I_{Crank} \times \delta}{\left| \left(-\frac{\left|\overrightarrow{a_1q} \times \mathbf{F}\right|}{\left|\overrightarrow{a_1c_1} \times \overrightarrow{b_1c_1}\right|} \overrightarrow{b_1c_1} - \mathbf{F} \right) \times \frac{\overrightarrow{a_0a_1}}{\left|\overrightarrow{a_0a_1}\right|} \right|} \right)^{\frac{2}{3}} < 0$$

where i = 1, 2, ..N and N is the number of prescribed positions

Equation (5.28) and inequality constraints (5.22), (5.24) and (5.27) constitute a goal program from which mechanism solutions that approximate the prescribed rigid-body positions and satisfy maximum static torque, maximum elastic deflection and buckling conditions are calculated. The algorithm employed for solving this goal program uses Quasi-Newton approach.

The algorithm employed for solving this goal program (a nonlinear constraints problem) is SQP (Sequential Quadratic Programming) which uses Quasi-Newton approach to solve its QP (Quadratic Programming) subproblem and line search approach to determine iteration step. The merit function used by Han [45] and Powell [46] is used in the following form:

$$\Psi(\mathbf{X}) = f(\mathbf{X}) + \sum_{k=1}^{m} r_k \max\left[0, g_k(\mathbf{X})\right] \tag{5.29}$$

where $g_k(\mathbf{X})$ represents each inequality constraint, m is the total number of inequality constraints and the inequality constraint penalty parameter is

$$(r_{l+1})_k = \max_k \left\{ \lambda_k, \frac{1}{2}\left((r_l)_k + \lambda_k\right) \right\} \tag{5.30}$$

In Equation (5.30) λ_k are estimates of the Lagrange multipliers and l is the iteration index for calculating the penalty parameter r_k for each inequality constraint (l=0, 1, 2, 3,...). After specifying initial guesses for the unknown variables in the goal program $(\mathbf{X})$, the following SQP steps were employed to calculate the unknown variables:

1. calculate λ_k and $(r_{l+1})_k$, (where l=0 and k=1...m)

2. solve Equation (5.29) using Quasi-Newton method

3. calculate $(r_{l+1})_k$ using Equation (5.30) (where l=l+1 and k=1...m)

4. repeat step 2 with newly-calculated r_k

Steps 2 through 4 constitute a loop that is repeated until the penalty term in Equation (5.29), $\sum_{k=1}^{m} r_k \max\left[0, g_k(\mathbf{X})\right]$, is less than a specified penalty term residual ε.

5.7 Example Problem

5.7.1 Optimization Analysis and Mechanism Synthesis

Table 5.1 includes the x and y-coordinates (in inches) of eight prescribed rigid-body positions. This is twice the maximum number of prescribed positions available with the conventional motion generation method included in this work [1-3]. The maximum allowed driver torque is τ_{max} = 6350in-lbs and the rigid-body load at **q** is $\mathbf{F} = (0, -1000, 0)^T$ lbs.

Table 5.1 Prescribed Rigid-body Positions

	p	**q**	**r**
Pos 1	9.8106, 9.2729	12.6931, 14.5459	17.9459, 16.0227
Pos 2	8.7314, 10.8201	11.8060, 15.9834	17.1097, 17.2659
Pos 3	5.4750, 12.6794	8.8795, 17.6313	14.2555, 18.5655
Pos 4	2.8301, 12.8348	6.3575, 17.6999	11.7551, 18.4993
Pos 5	-0.4749, 11.7950	3.0503, 16.6618	8.4476, 17.4636
Pos 6	-3.7115, 9.0759	-0.4948, 14.1519	4.8424, 15.2867
Pos 7	-5.5256, 5.4763	-3.0512, 10.9525	2.0746, 12.8233
Pos 8	-5.0223, 0.3189	-4.3877, 6.2947	-0.1059, 9.6768

The gear pitch radii r_a, r_b, and r of 5, 10, and 5 inches, respectively. Link $\mathbf{a}_0\mathbf{a}_1$ and $\mathbf{b}_1\mathbf{c}_1$ shall be constructed of solid rectangular steel tubing ($E = 29*10^6$psi) of 1/2" (deep) x 3/4" (wide) and 1/2" x 1/2", respectively. For each prescribed rigid-body position, the maximum deflection of link $\mathbf{a}_0\mathbf{a}_1$ shall not exceed 0.31 inch and preventing the buckling of link $\mathbf{b}_1\mathbf{c}_1$ is critical. Using the motion generation goal program (where N=8 results in m=24 in Equation (5.29)) with prescribed values of $\mathbf{a}_0$ = (0, 0), $\mathbf{b}_0$ = (25, 0), $\mathbf{b}_1$ = (33, 6), and R_2 = 10, and initial guesses of $\mathbf{a}_1$ = (10, 5),

$R_1 = 10$, $\mathbf{c}_1 = (20, 20)$, and $R_3 = 15$. The calculated solution is $\mathbf{a}_1 = (6.9002, 4.2070)$, $R_1 = 8.0815$, $\mathbf{c}_1 = (22.3731, 17.9572)$, and $R_3 = 15.9274$. Table 5.2 includes the achieved positions before applying the principles discussed in Section 5.3. In other words, positions achieved assuming all links of the synthesized mechanism are rigid.

Table 5.2 Rigid-body Positions Achieved by Rigid Links Synthesis

	p	**q**	**r**
Pos 1	9.8106, 9.2729	12.6931, 14.5459	17.9459, 16.0227
Pos 2	8.6778, 10.8016	11.7621, 15.9591	17.0681, 17.2316
Pos 3	5.4615, 12.5440	8.8795, 17.4970	14.2580, 18.4164
Pos 4	2.8087, 12.6882	6.3575, 17.5378	11.7586, 18.3133
Pos 5	-0.4749, 11.6411	3.0800, 16.4862	8.4821, 17.2549
Pos 6	-3.7114, 8.9172	-0.4564, 13.9686	4.8892, 15.0631
Pos 7	-5.4797, 5.4763	-2.9221, 10.9142	2.2316, 12.7067
Pos 8	-5.1260, 0.3189	-4.4007, 6.2844	-0.0680, 9.6012

Because link $\mathbf{a}_0\mathbf{a}_1$ and link $\mathbf{b}_1\mathbf{c}_1$ are flexible, the deflections of these links simultaneously compromise the accuracy of the rigid-body positions achieved by the synthesized mechanism. Table 5.3 includes the rigid-body positions calculated after incorporating the parameters of the synthesized mechanism in the geared five-bar mechanism deflection model in Section 5.3. Rigid-body positions 1 through 8 correspond to $\mathbf{a}_0\mathbf{a}_1$ angles of $\theta_1 =$ 31.3702, 46.3962, 75.3991, 95.2591, 119.9135, 149.7264, 178.2751 and 222.5464 degrees, respectively. Figure 5.5 illustrates the synthesized geared five-bar motion generator. As illustrated in this figure, the moving pivot $\mathbf{b}_1$ is on the pitch circle of the gear centered at the fixed pivot $\mathbf{b}_0$.

Table 5.3 Rigid-body Positions Achieved by Elastic Links Synthesis

	p	q	r
Pos 1	9.8040, 9.1572	12.6865, 14.4296	17.9393, 15.9070
Pos 2	8.6450, 10.7478	11.7291, 15.9050	17.0353, 17.1778
Pos 3	5.4674, 12.5421	8.8854, 17.4951	14.2639, 18.4145
Pos 4	2.8847, 12.6469	6.4339, 17.4962	11.8346, 18.2720
Pos 5	-0.3300, 11.4869	3.2257, 16.3313	8.6270, 17.1007
Pos 6	-3.8492, 8.6411	-0.5949, 13.6911	4.7514, 14.7870
Pos 7	-5.5445, 5.1906	-2.9873, 10.6270	2.1668, 12.4210
Pos 8	-5.0879, 0.1648	-4.3624, 6.1295	-0.0299, 9.4471

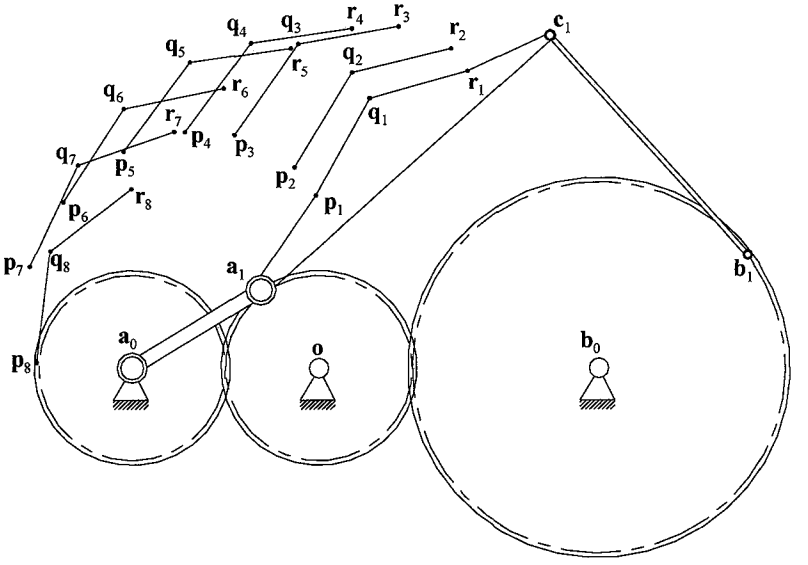

Figure 5.5 Synthesized geared five-bar motion generator.

Tables 5.4 and 5.5 includes the resulting static torque and deflection of the crank link as well as the resulting columnar loads for link $\mathbf{b}_1\mathbf{c}_1$. The buckling load for this link is 411 pounds.

Table 5.4 Crank Static Torques, Reaction Loads and Deflections

	Crank Static Torque [in-lb]	Force $_{a1}$ (lbf)			Crank Deflection [in]
		x	y	Resultant	
Pos 1	6070	-186	-791	812	0.1996
Pos 2	4658	-198	-776	800	0.1352
Pos 3	1327	-236	-763	799	0.0126
Pos 4	1067	-268	-770	815	0.1166
Pos 5	3703	-312	-796	856	0.2305
Pos 6	5727	-322	-850	909	0.3084
Pos 7	6339	-257	-905	940	0.3097
Pos 8	5242	-70	-973	976	0.2310

Table 5.5 Follower Reaction Loads and Columnar Loads

	Force$_{b1}$ (lbf)			
	x	y	Resultant	$P_{cr\_Follower}$ (lbf)
Pos 1	186	-209	280	411
Pos 2	198	-224	299	411
Pos 3	236	-237	335	411
Pos 4	268	-230	354	411
Pos 5	312	-204	373	411
Pos 6	322	-150	355	411
Pos 7	257	-95	274	411
Pos 8	70	-27	75	411

The direction of reaction forces of the crank and the link $\mathbf{b}_1\mathbf{c}_1$ is illustrated in Figure 5.6. ADAMS is also used to attain the force vectors and trace the trajectory of points **p**, **q**, and **r** on the coupler during the operation of the mechanism.

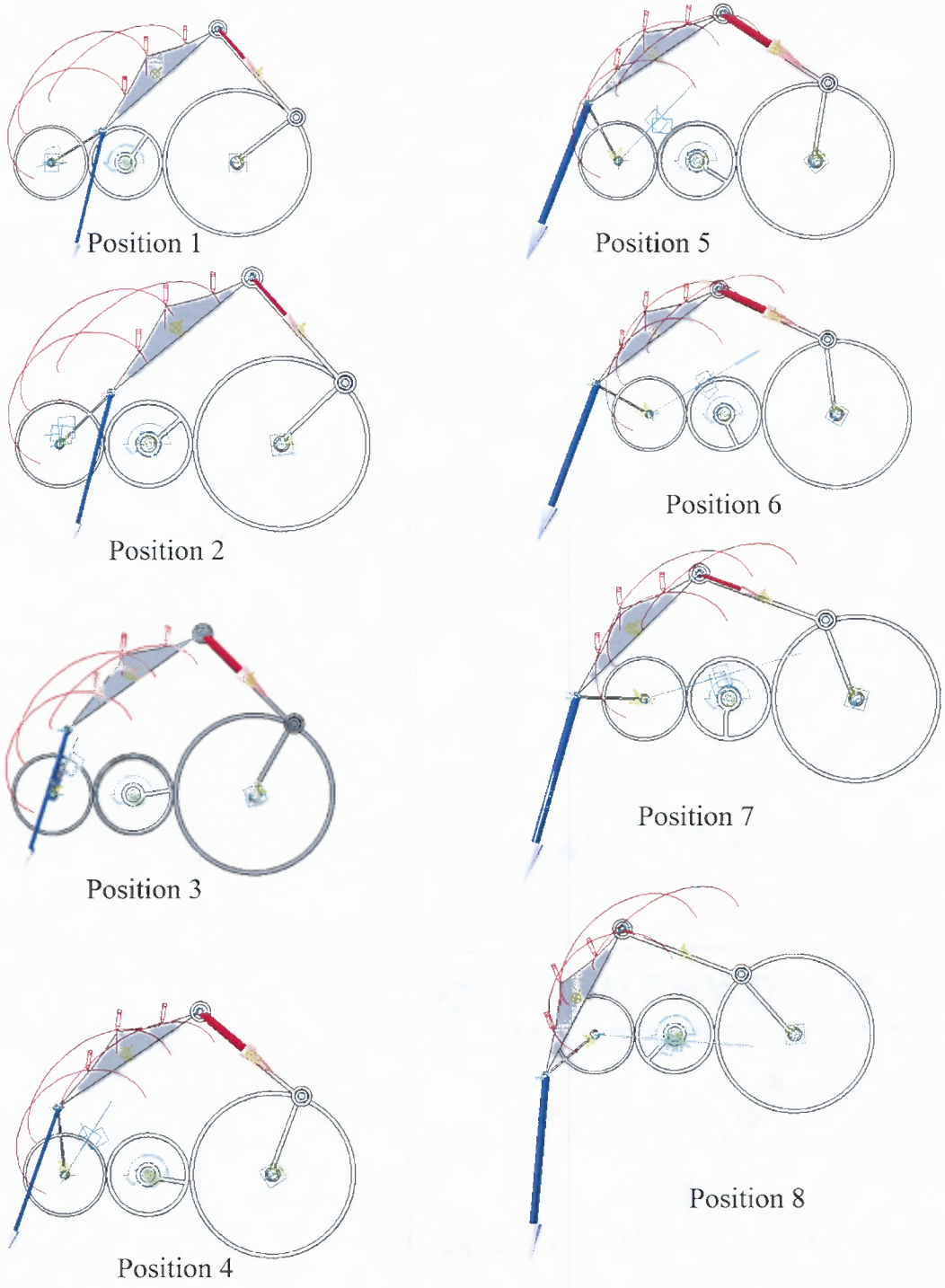

Figure 5.6 The reaction load $\mathbf{R}_A$, the external load **F** and reaction loads $\mathbf{R}_B$.

ADAMS is used to extract the magnitude of the driver torque and reaction forces for the entire operation of the synthesized mechanism. The reaction load $\mathbf{R}_A$, reaction load $\mathbf{R}_B$ and driving torque **T** are shown in Figures 5.7, 5.8 and 5.9, respectively.

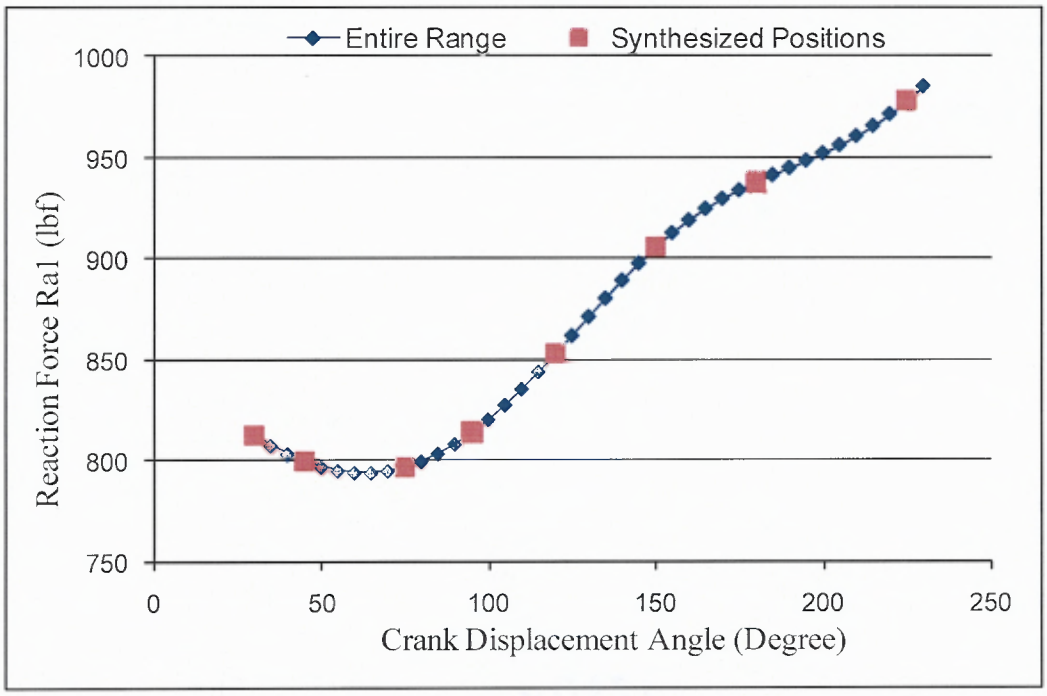

Figure 5.7 Magnitude of the reaction load $\mathbf{R}_A$ as a function of crank rotation.

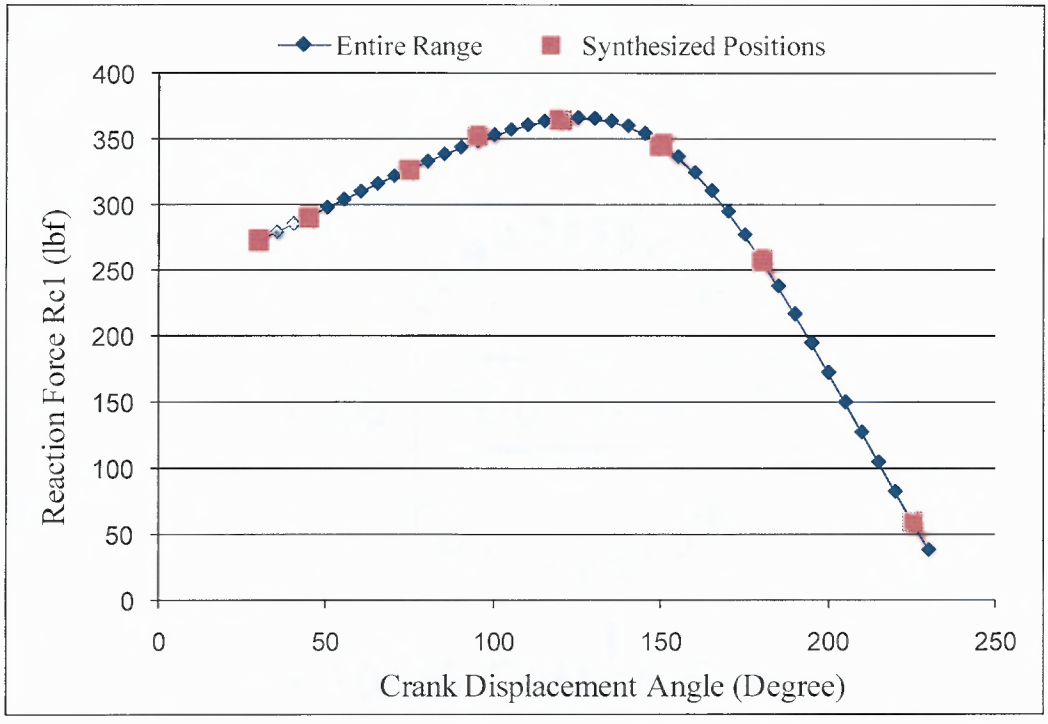

Figure 5.8 Magnitude of the reaction load $\mathbf{R}_C$ as a function of crank rotation.

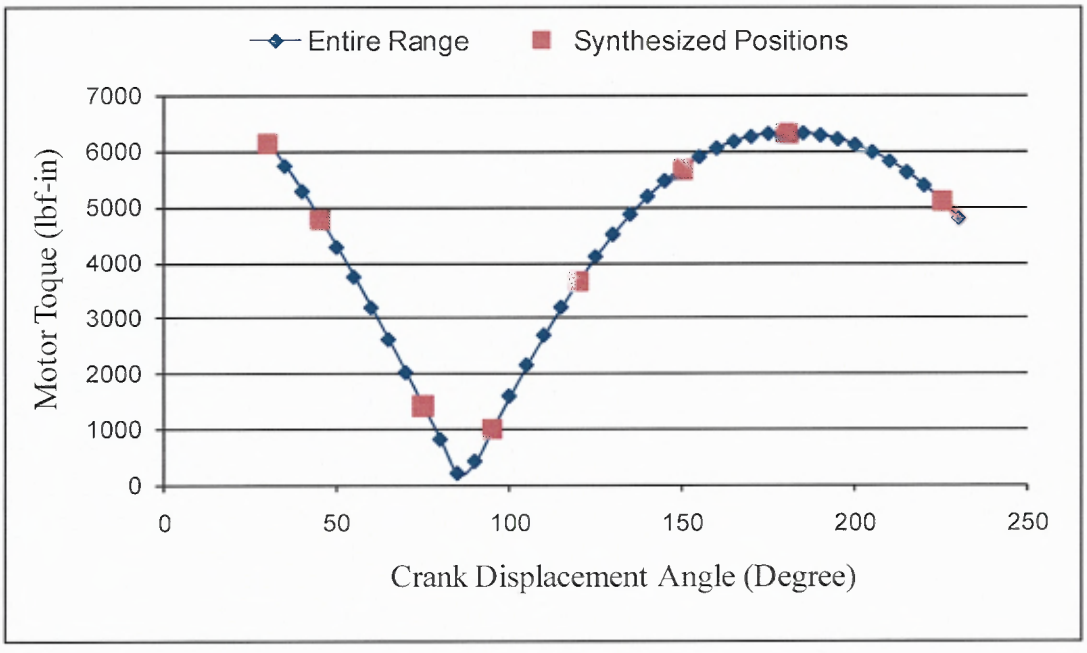

Figure 5.9 Magnitude of the driving static torque **T** as a function of crank rotation.

5.7.2 Calculation Sample and Verification

In this section, the calculations are presented to verify the results obtained by ADAMS, these calculations are done for the initial position of the synthesized mechanism, and the goal of this calculation is to find the result of the driving static torque, reaction loads and the crank deflection. Calculations for other positions were performed similarly as part of verification process. The units for the reaction loads is lbf , the torque is in lbf-in, and for the deflection is inches. The calculations are performed in MathCAD.

Figure 5.10 illustrates geared five-bar mechanism with load **W** applied on the coupler point **q**, the middle gear is the driving gear and translates the required torque to achieve static equilibrium through gear train as shown. Since the mechanism is in static equilibrium, each piece will be analyzed individually, and free body diagram (FBD) for each mechanism member will be shown.

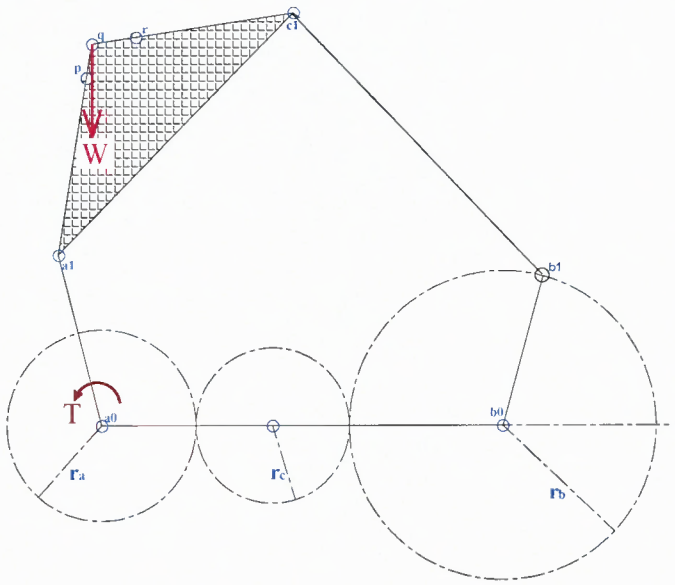

Figure 5.10 Schematic Diagram for geared five-bar mechanism.

- **Input Values**

==========

INITIAL POSITION

==========

$\theta := 31.3702\text{deg} \quad r_a := 5 \quad r_c := 5 \quad r_b := 10$

$$a0 := \begin{pmatrix} 0 \\ 0 \\ 1 \end{pmatrix} \quad a1 := \begin{pmatrix} 6.9002 \\ 4.207 \\ 1 \end{pmatrix} \quad b0 := \begin{pmatrix} 25 \\ 0 \\ 1 \end{pmatrix} \quad b1 := \begin{pmatrix} 32.9579 \\ 6.0558 \\ 1 \end{pmatrix} \quad c1 := \begin{pmatrix} 22.3731 \\ 17.9572 \\ 1 \end{pmatrix} \quad q := \begin{pmatrix} 12.6931 \\ 14.5459 \\ 1 \end{pmatrix} \quad W := \begin{pmatrix} 0 \\ -1000 \\ 0 \end{pmatrix}$$

- **Analysis of Coupler**

Since Link $\mathbf{c}_1\mathbf{b}_1$ is a two force member, Force $\mathbf{R}_c$ is always collinear to link $\mathbf{c}_1\mathbf{b}_1$

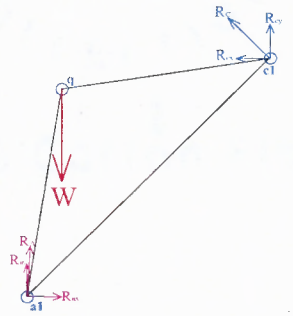

Figure 5.11 Free body diagram for coupler with rigid-body load W and reaction loads $\mathbf{R}_A$ and $\mathbf{R}_B$.

Use Equation (5.14) to find the columnar load in the follower.

$$\Sigma M_{a1} = 0 \qquad R_{C1} := \frac{\left|\overrightarrow{qa1} \times \vec{W}\right|}{\left|\overrightarrow{c1a1} \times \overrightarrow{c1b1}\right|} \cdot \overrightarrow{c1b1} \qquad \overrightarrow{R_{C1}} = \begin{pmatrix} -186 \\ 209 \\ 0 \end{pmatrix} \qquad \left|\overrightarrow{R_{C1}}\right| = 280$$

$$-\overrightarrow{R_{C1}} = \begin{pmatrix} 186 \\ -209 \\ 0 \end{pmatrix}$$

Use Equation (5.16) to find the load $\mathbf{R}_A$ on the crank.

$$\Sigma F = 0 \qquad R_A := -\overrightarrow{R_{C1}} - \vec{W} \qquad R_A := -\left(\frac{\left|\overrightarrow{qa1} \times \vec{W}\right|}{\left|\overrightarrow{c1a1} \times \overrightarrow{c1b1}\right|} \cdot \overrightarrow{c1b1} \right) - \vec{W} \qquad \vec{R_A} = \begin{pmatrix} 186 \\ 791 \\ 0 \end{pmatrix} \qquad \left|\vec{R_A}\right| = 812$$

$$-\vec{R_A} = \begin{pmatrix} -186 \\ -791 \\ 0 \end{pmatrix}$$

- **Driver Link Static Torque**

Torque is a result of perpendicular Force to the arm times the arm length. Use Equation (5.18) and (5.21) to find T_A and T_{motor}.

$$T_A := \overrightarrow{a1a0} \times \vec{R_A} \qquad T_A := \overrightarrow{a1a0} \times \left[-\left(\frac{\left|\overrightarrow{qa1} \times \vec{W}\right|}{\left|\overrightarrow{c1a1} \times \overrightarrow{c1b1}\right|} \cdot \overrightarrow{c1b1} \right) - \vec{W} \right] \qquad T_A = \begin{pmatrix} 0 \\ 0 \\ 4675 \end{pmatrix}$$

$$T_{motor} := \frac{1}{\frac{r_a}{r_c}} \cdot \overrightarrow{a1a0} \times \left[-\left(\frac{\left|\overrightarrow{qa1} \times \vec{W}\right|}{\left|\overrightarrow{c1a1} \times \overrightarrow{c1b1}\right|} \cdot \overrightarrow{c1b1} \right) - \vec{W} \right] + \frac{1}{\frac{r_b}{r_c}} \cdot \overrightarrow{b1b0} \times \left(\frac{\left|\overrightarrow{qa1} \times \vec{W}\right|}{\left|\overrightarrow{c1a1} \times \overrightarrow{c1b1}\right|} \cdot \overrightarrow{c1b1} \right)$$

$$T_{motor} = \begin{pmatrix} 0 \\ 0 \\ 6070 \end{pmatrix}$$

- **Crank Deflection**

Crank Link is link $\mathbf{a_1a_0}$, the forces acting on crank is same as $\mathbf{R_A}$ but opposite direction.

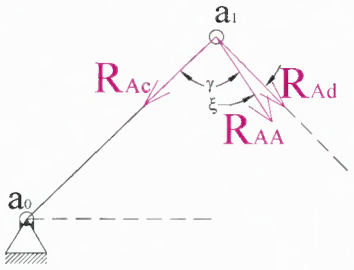

Figure 5.12 Crank with reaction load $\mathbf{R_{AA}}$.

$$\delta_W = \frac{Wl^3}{3EI} \qquad \left| \frac{R_{Ad} \cdot L_1^{\,3}}{3 \cdot E \cdot I_{a\_Crank}} \right| \qquad \delta_{Crank} := \left| \frac{\left[\left[-\left(\frac{\left| \overrightarrow{qa1} \times \vec{W} \right|}{\left| \overrightarrow{c1a1} \times \overrightarrow{c1b1} \right|} \cdot \overrightarrow{c1b1} \right) - \vec{W} \right] \times \frac{\overrightarrow{a1a0}}{\left| \overrightarrow{a1a0} \right|} \right| \cdot \left(\left| \overrightarrow{a1a0} \right| \right)^3}{3 \cdot E \cdot I_{Crank}} \right|$$

$$\delta_{Crank} = 0.1996$$

- **Follower Link Buckling**

The force acting on the link $\mathbf{c}_1\mathbf{b}_1$ (Figure 5.10) is same as $\mathbf{R}_{c1}$ but opposite direction, which will be compressive force $\mathbf{R}_{Cc}$

$$\overrightarrow{R_{Cc}} := -\overrightarrow{R_{C1}} \qquad \overrightarrow{R_{Cc}} = \begin{pmatrix} 185.982 \\ -209.115 \\ 0 \end{pmatrix} \qquad \left| \overrightarrow{R_{Cc}} \right| = 280$$

$$E := 29000000 \qquad I_{Link} := \left(\frac{1}{12} \right) (0.28)(0.25)^3 \qquad I_{Link} = 0.000365$$

$$P_{cr} := \frac{\pi^2 \cdot E \cdot I_{Link}}{\left(\left| \overrightarrow{c1b1} \right| \right)^2} \qquad P_{cr} = 411$$

5.8 Discussion

Equations (5.18), (5.20) and subsequently (5.21) become invalid when the pivots $\mathbf{a}_1$, $\mathbf{b}_1$ and $\mathbf{c}_1$ are collinear. Such a state is possible when the five-bar mechanism reaches a "lock-up" or binding position. When pivots $\mathbf{a}_1$, $\mathbf{b}_1$ and $\mathbf{c}_1$ are collinear, the denominator in Equations (5.18) and (5.20) become zero (making these equations and subsequent driver torque constraint invalid). The specific geared five-bar mechanism design considered in this work is one where $\mathbf{a}_0$ $\mathbf{a}_1$ is a link attached to the gear centered at $\mathbf{a}_0$ and $\mathbf{b}_1$ is a moving pivot on the gear centered at $\mathbf{b}_0$.

If the moving pivot $\mathbf{a}_1$ is to be mounted directly to the gear centered at $\mathbf{a}_0$, the deflection constraint (Equation (5.27)) can be excluded from the goal program since the gears are considered rigid. Different types of gear-to-link attachments change the mechanism elastic behavior (Equation (5.6)) and subsequent deflection constraints (Equations (5.27)). The mathematical analysis software MathCAD was used to codify and solve the formulated goal program.

This verification of deflection of moving pivot $\mathbf{a}_1$ is performed for the first position using two methods which they are a formulation of global stiffness matrix. Stiffness model for each position is built using the approach discussed in Section 5.3. Table 3.6 illustrates the deflection of points $\mathbf{a}_1$, $\mathbf{q}$ and $\mathbf{b}_1$. Figure 5.12 shows the global stiffness matrix for the mechanism in position 1, other positions are constructed in the same manner discussed in Section 5.3.

The second method is finite element analysis performed using COSMOS Designer 2007 to verify the deflection of the moving pivot $\mathbf{a}_1$ Figure 5.14. The results from both methods are very close to the deflection of the crank using Euler deflection equation at the moving pivot $\mathbf{a}_1$.

The deflection of the moving pivot $\mathbf{a}_1$ using global stiffness matrix approach discussed in Section 5.3 is 0.199575 inch, while the deflection of the same pivot using FEA method is 0.199576 inch. Finally, the deflection of the moving pivot $\mathbf{a}_1$ using Euler equation, assuming the crank is a cantilever beam with force at the free end, is 0.199648 inch. These results are shown in Table 5.7

$[K_{global}] =$

1	0	0	0	0	0	0	0	0	0	0	0	0	0	0
0	1	0	0	0	0	0	0	0	0	0	0	0	0	0
0	0	1	0	0	0	0	0	0	0	0	0	0	0	0
0	0	0	3608033547	6411149699	0	-3607051501	-6410552723	-157208948	0	0	0	0	0	0
0	0	0	6411149699	11456816540	0	-6410552723	-11456449673	88084498	0	0	0	0	0	0
0	0	0	0	0	1	0	0	0	0	0	0	0	0	0
0	0	0	-3607051501	-6410552723	0	19066247529	11850227373	77350168	-15459196028	-5439674650	0	0	0	0
0	0	0	-6410552723	-11456449673	0	11850227373	13396837641	138525199	-5439674650	-1940387969	0	0	0	0
0	0	0	-157208948	88084498	0	77350168	138525199	4601640185	79858780	-226609697	0	0	0	0
0	0	0	0	0	0	-15459196028	-5439674650	79858780	15459252336	5439611347	0	0	0	0
0	0	0	0	0	0	-5439674650	-1940387969	-226609697	5439611347	1940459155	0	0	0	0
0	0	0	0	0	0	0	0	0	0	0	1	0	0	0
0	0	0	0	0	0	0	0	0	0	0	0	1	0	0
0	0	0	0	0	0	0	0	0	0	0	0	0	1	0
0	0	0	0	0	0	0	0	0	0	0	0	0	0	1

Figure 5.13 Global stiffness matrix for the synthesized mechanism in the first position.

Table 5.6 Deflection of Joints $\mathbf{a}_1$, **q**, and $\mathbf{b}_1$ Using Stiffness Matrix Approach

Position 1								
Joint a_1 Deflection			**Joint q Deflection**			**Joint b_1 Deflection**		
Ux	Uy	δ	Ux	Uy	δ	Ux	Uy	δ
0.1035	-0.1706	0.1996	0.0066	-0.1163	0.1165	-0.0254	-0.0255	0.0360
Position 2								
Joint a_1 Deflection			**Joint q Deflection**			**Joint b_1 Deflection**		
Ux	Uy	δ	Ux	Uy	δ	Ux	Uy	δ
0.0975	-0.0936	0.1351	0.0330	-0.0541	0.0634	0.0136	0.0085	0.0161
Position 3								
Joint a_1 Deflection			**Joint q Deflection**			**Joint b_1 Deflection**		
Ux	Uy	δ	Ux	Uy	δ	Ux	Uy	δ
-0.0123	0.0026	0.0126	-0.0059	-0.0019	0.0062	-0.0044	-0.0085	0.0096
Position 4								
Joint a_1 Deflection			**Joint q Deflection**			**Joint b_1 Deflection**		
Ux	Uy	δ	Ux	Uy	δ	Ux	Uy	δ
-0.1169	-0.0113	0.1174	-0.0764	-0.0416	0.0870	-0.0674	-0.0843	0.1080
Position 5								
Joint a_1 Deflection			**Joint q Deflection**			**Joint b_1 Deflection**		
Ux	Uy	δ	Ux	Uy	δ	Ux	Uy	δ
-0.1990	-0.1150	0.2298	-0.1457	-0.1549	0.2127	-0.1339	-0.2114	0.2502
Position 6								
Joint a_1 Deflection			**Joint q Deflection**			**Joint b_1 Deflection**		
Ux	Uy	δ	Ux	Uy	δ	Ux	Uy	δ
-0.1554	-0.2664	0.3084	-0.1385	-0.2775	0.3102	-0.1339	-0.2943	0.3234
Position 7								
Joint a_1 Deflection			**Joint q Deflection**			**Joint b_1 Deflection**		
Ux	Uy	δ	Ux	Uy	δ	Ux	Uy	δ
-0.0096	-0.3095	0.3097	-0.0652	-0.2872	0.2945	-0.0859	-0.2379	0.2530
Position 8								
Joint a_1 Deflection			**Joint q Deflection**			**Joint b_1 Deflection**		
Ux	Uy	δ	Ux	Uy	δ	Ux	Uy	δ
0.1557	-0.1704	0.2308	0.0383	-0.1549	0.1596	-0.0291	-0.0777	0.0830

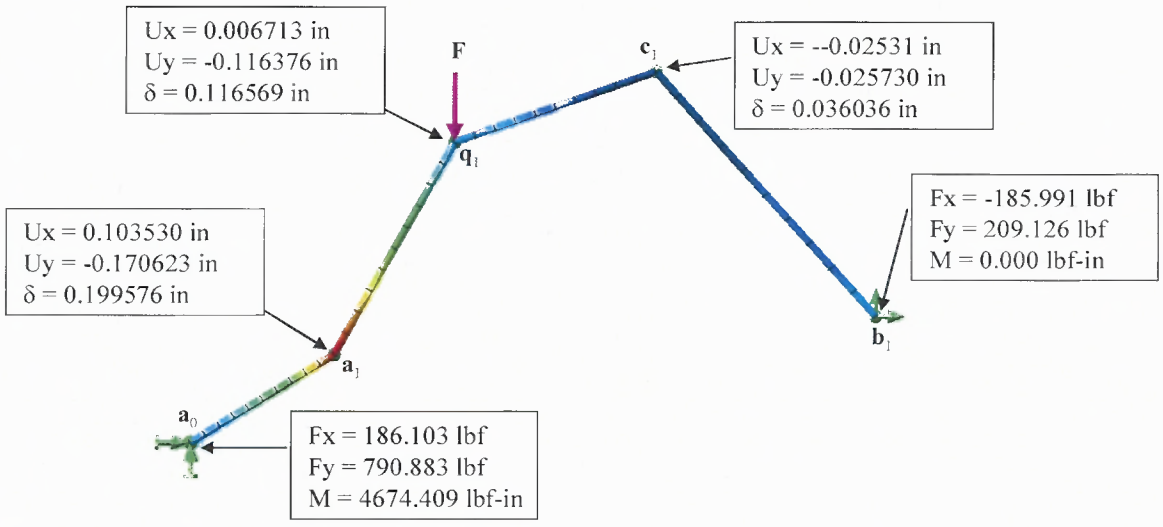

Figure 5.14 Deflections and reaction loads using FEA CosmosDesigner.

Table 5.7 Comparison of Stiffness Matrix Approach Vs FEA for the First Position

Joint a_1 Deflection					
Stiffness Matrix Approach			FEA Approach		
Ux	Uy	δ	Ux	Uy	δ
0.1035	-0.1706	0.1996	0.1035	-0.1706	0.1996
Joint q Deflection					
Stiffness Matrix Approach			FEA Approach		
Ux	Uy	δ	Ux	Uy	δ
0.0066	-0.1163	0.1165	0.0067	-0.1164	0.1166
Joint b_1 Deflection					
Stiffness Matrix Approach			FEA Approach		
Ux	Uy	δ	Ux	Uy	δ
-0.0254	-0.0255	0.0360	-0.0253	-0.0257	0.0360
Joint a_0 Reaction Loads					
Stiffness Matrix Approach			FEA Approach		
Fx	Fy	Moment	Fx	Fy	Resultant
185.771	790.697	4674.407	186.103	790.883	4674.409
Joint b_0 Reaction Loads					
Stiffness Matrix Approach			FEA Approach		
Fx	Fy	Moment	Fx	Fy	Resultant
-185.771	209.303	0.000	-185.991	209.126	0.0000

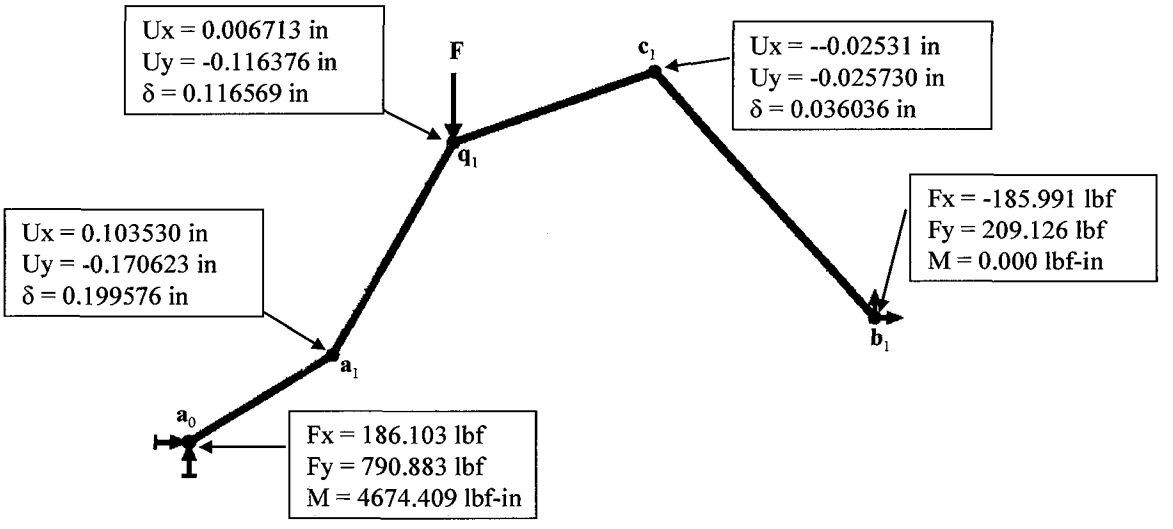

Figure 5.14 Deflections and reaction loads using FEA CosmosDesigner.

Table 5.7 Comparison of Stiffness Matrix Approach Vs FEA for the First Position

Joint a_1 Deflection					
Stiffness Matrix Approach			FEA Approach		
Ux	Uy	δ	Ux	Uy	δ
0.1035	-0.1706	0.1996	0.1035	-0.1706	0.1996
Joint q Deflection					
Stiffness Matrix Approach			FEA Approach		
Ux	Uy	δ	Ux	Uy	δ
0.0066	-0.1163	0.1165	0.0067	-0.1164	0.1166
Joint b_1 Deflection					
Stiffness Matrix Approach			FEA Approach		
Ux	Uy	δ	Ux	Uy	δ
-0.0254	-0.0255	0.0360	-0.0253	-0.0257	0.0360
Joint a_0 Reaction Loads					
Stiffness Matrix Approach			FEA Approach		
Fx	Fy	Moment	Fx	Fy	Resultant
185.771	790.697	4674.407	186.103	790.883	4674.409
Joint b_0 Reaction Loads					
Stiffness Matrix Approach			FEA Approach		
Fx	Fy	Moment	Fx	Fy	Resultant
-185.771	209.303	0.000	-185.991	209.126	0.0000

CHAPTER 6

CONCLUSIONS AND FUTURE WORK

The driver link static torque constraint formulated in this work. When incorporated into a conventional planar four-bar motion generation model, the resulting model was demonstrated to be effective in calculating planar four-bar and five-bar motion generator solutions that approximate the prescribed rigid-body positions and satisfy driver link static torque and coupler load constraints. For the design of four-bar traveler braking mechanisms, prescribed rigid-body motion, braking normal force and driver static torque are critical design considerations. It was also demonstrated that the torque constraint could be used with the conventional planar five-bar motion generation model and solved using a commercial goal program solver.

A model to synthesize planar four-bar motion generators that also includes static torque, elastic deflection and buckling was formulated and demonstrated in this work. Given a set of rigid-body positions and rigid-body load, maximum driver torque and deflection values and Young's modulus and moment of inertia data for the crank and follower, a planar four-bar mechanism was synthesized using the model formulated in this work.

A model to synthesize geared five-bar motion generators that also includes static torque, elastic deflection and buckling constraints was formulated and demonstrated in this work. Given a set of rigid-body positions, a rigid-body load, maximum driver torque and deflection values and Young's modulus and moment of

inertia data for links $\mathbf{a}_0\mathbf{a}_1$ and $\mathbf{b}_1\mathbf{c}_1$, a geared five-bar mechanism was synthesized using the goal program formulated in this work.

Based on the discussed topics the following topics are recommended as future work. The work performed was for motion generation for planar four-bar and five-bar mechanisms, the same procedure will be applied to path and function generation formulation as well as spatial mechanism synthesis. Different features will be integrated with previous work and will be focused on mechanism synthesis with position tolerances and rigid body guidance as well as extend the work done by Martin et al. [12] to be integrated with structural constraints for planar mechanisms performed in Chapter 4. Another interesting field which will be integrated to the formulated structural constraints is a formulation of stress-strain constraints and add to the goal program in order to make the solution more robust and comprehensive.

REFERENCES

1. Suh, C. H., Radcliffe C.W, (1978). Kinematics and Mechanism Design, John Wiley and Sons, Inc., New York.

2. Sandor G.N., Erdman A.G., (1984). Advanced Mechanism Design Analysis and Synthesis, Prentice-Hall, Englewood Cliffs.

3. Moaveni, S., (1999). Finite Element Analysis, Theory and Application with ANSYS, Prentice-Hall, Englewood Cliffs.

4. Knight, C.E., (1993). The Finite Element Method in Mechanical Design, PWS-KENT, Boston.

5. Pilkey, W.D., (1994). Formulas for Stress, Strain, and Structural Matrices, John Wiley and Sons, Inc., New York.

6. Ghali, A., Neville, A.M., Brown, T.G. (2003). Structural Analysis, A Unified Classical and Matrix Approach, Spon Press, New York.

7. Al-Widyan, K., Angeles, J., Cervantes-Sánchez, J.J., (2002). The robust synthesis of planar four-bar linkages for motion generation, Proceedings of the ASME Design Engineering Technical Conference, 5 A, 627-633.

8. Caracciolo, R., and Trevisani, A., (2001). Simultaneous rigid-body motion and vibration control of a flexible four-bar linkage, Mechanism and Machine Theory, 36, 2, 221-243.

9. Danieli, G. A., Mundo, D., Sciarra, V., (2001). Use of Burmester's circular theory in the determination of the optimal four-bar link reproducing actual tibia-femur relative motion, ASME Bioengineering Division, BED 51, 97-98.

10. Goehler, C. M., Stanisic, M. M. and Perez, V. P., (2004). A generalized parameterization of T_1 motion and its applications to the synthesis of planar mechanisms, Mechanism and Machine Theory, 39, 11, 1223-1241.

11. Hong, B. and Erdman, A.G., (2005). A method for adjustable planar and spherical four-bar linkage synthesis, ASME Journal of Mechanical Design, 127, 3, 456-463.

12. Martin, P. J., Russell, K.,Sodhi, R. S., (2007). On mechanism design optimization for motion generation, Mechanism and Machine Theory, 42, 10, 1251-1263.

13. Sodhi, R. S. and Russell, K., (2004). Kinematic synthesis of planar four-bar mechanisms for multi-phase motion generation with tolerances, Mechanics Based Design of Structures and Machines, 32, 2, 215-233.

14. Yao, J. and Angeles, J., (2000). Computation of all optimum dyads in the approximate synthesis of planar linkages for rigid-body guidance, Mechanism and Machine Theory, 35, 8, 1065-1078.

15. Zhixing, W., Hongying, Y. Dewei, T., Jiansheng, L. (2002). Study on rigid-body guidance synthesis of planar linkage, Mechanism and Machine Theory, 37, 7, 673-684.

16. Zhou, H., and Cheung, E. H. M., (2004). Adjustable four-bar linkages for multi-phase motion generation, Mechanism and Machine Theory, 39, 3, 261-279.

17. Lee, W.T., Russell, K., Shen, Q., Sodhi, R.S., (2008). On adjustable spherical four-bar motion generation for expanded prescribed positions, Mechanism and Machine Theory, In Press.

18. Huang, C., and Roth, R., (1993). Dimensional synthesis of closed-loop linkages to match force and position specifications, Journal of Mechanical Design, 115, 194-198.

19. Senft, J.R., (2004). Force linear mechanisms, Mechanism and Machine Theory, 39, 281-298.

20. Rundgren, B.T. (2001). Optimized Synthesis of A Dynamically Based Force Generating Planar Four-bar Mechanism, M.Sc. Thesis, Virginia Polytechnic Institute and State University.

21. Mehta, Y. B. and Bagci, C., (1974). Force and torque analysis of constrained space mechanisms and plane mechanisms with offset links by matrix displacement-direct element method, Mechanism and Machine Theory, 9, Issues 3-4, 385-403.

22. Hac, M., (1995). Dynamics of flexible mechanisms with mutual dependence between rigid body motion and longitudinal deformation of links, Mechanism and Machine Theory, 30, 6 837-847.

23. Fallahi, B., (1996). A nonlinear finite element approach to kino-static analysis of elastic beams, Mechanism and Machine Theory, 31, 3, 353-364.

24. Yang, K., and Park, Y., (1998). Dynamic stability of a flexible four-bar mechanism and its experimental investigation, Mechanism and Machine Theory, 33, 3, 307-320.

25. Caracciolo, R., and Trevisani, A. (2001). Simultaneous rigid-body motion and vibration control of a flexible four-bar linkage, Mechanism and Machine Theory, 36, 2, 221-243.

26. Mayo, J. and Dominguez, J., (1996). Geometrically non-linear formulation of flexible multibody systems in terms of beam elements: Geometric Stiffness, Computer and Structures, 59, 6, 1039-1050.

27. Sriram, B.R., and Mruthyunjaya, T.S., (1995). Synthesis of path generating flexible-link mechanisms, Computer and Structures, 56, 4, 657-666.

28. Mohammad H.F.D., (2005). Limit position synthesis and analysis of compliant 4-bar mechanism with specified energy levels using parametric pseudo-rigid-body model, Mechanism and Machine Theory, Vol. 40, 977-992.

29. Venanzi, S., Giesen, P., Parenti-Castelli, V., (2005). A novel technique for position analysis of planar compliant mechanisms, Mechanism and Machine Theory, 40, 1224-1239.

30. Sönmez, Ü., (2007). Introduction to compliant long dwell mechanism designs using buckling beams and arcs, Journal of Mechanical Design, 129, 8, 831-843.

31. Plaut, R.H., Alloway, L.A. and Virgin, L.N., (2003). Nonlinear oscillations of a buckled mechanism used as a vibration isolator, Proceedings of the IUTAM Symposium, 122, 241-250.

32. Wang, A. and Tian, W., (2007). Mechanism of buckling development in elastic bars subjected to axial impact, International Journal of Impact Engineering, 34, 2, 232-252.

33. Russell, K. and Sodhi, R.S., (2004). Kinematic synthesis of adjustable planar five-bar mechanisms for multi-phase motion generation, JSME International Journal, 47, 1, Series C, 345-349.

34. Musa, M.H., Russell, K., Sodhi, R.S., (2006). Multi-phase motion generation of five-bar mechanisms with prescribed rigid-body tolerances, CSME Transactions, 30, 4, 459-472.

35. Balli, S.S., and Chand, S., (2002). Five-bar motion and path generators with variable topology for motion between extreme positions, Mechanism and Machine Theory, 37, 11, 1435-1445.

36. Balli, S.S., and Chand, S., (2004). Synthesis of a five-bar mechanism for variable topology type with transmission angle control, Journal of Mechanical Design, 126, 1, 128-134.

37. Nokleby, S.B., and Podhorodeski, R.P., (2001). Optimization-based synthesis of grashof geared five-bar mechanisms, Journal of Mechanical Design, 123, 4, 529-534.

38. Wang, A. and Yan, H., (1991). Rigid-body guidance of planar five-bar linkages for five precision positions, Journal of the Chinese Society of Mechanical Engineers, 12, 2, 159-165.

39. Basu, P.S. and Farhang, K., (1992). Kinematic analysis and design of two-input, five-bar mechanisms driven by relatively small cranks, 22nd Biennial Mechanisms Conference, Scottsdale, Arizona.

40. Dou, X., and Ting, K., (1996). Branch identification in geared five-bar chains, Journal of Mechanical Design, 118, 3, 384-389.

41. Lin, C., and Chaing, C.H., (1992). Synthesis of planar and spherical geared five-bar function generators by the pole method, Mechanism and Machine Theory, 27, 2, 131-141.

42. Ge, W., and Chen, Z., (1999). Study of geared five-bar curves based on computer mechanism simulation with variable parameters, Mechanical Science and Technology, 18, 3, 435-437.

43. Ge, W., and Chen, Z., (1997). Application oriented study of characteristics of joint loci of geared five-bar linkage, Journal of Northwestern Polytechnic University, 15, 4, 542-546.

44. Li, T., and Dao, W., (1999). Kinematic synthesis of geared linkage mechanism for body guidance with input timing, Mechanical Science and Technology, 17, 6, 869-870.

45. Han, S.P., (1977). A globally convergent method for nonlinear programming, J. Optimization Theory and Applications, 22, 297.

46. Powell, M.J.D., (1978). A fast algorithm for nonlinearly constrained optimization calculations, G.A.Watson ed., Lecture Notes in Mathematics, Springer Verlag, 630.

47. Russell K., (2004). Lecture Notes in Mechanism Design, New Jersey Institute of Technology, New Jersey.

48. Mott, R.C., (1992). Machine Elements in Mechanical Design, Merrill-Macmillan publishing co., New York.

49. Mallik, A.K., Ghosh, A., and Dittrich, D., (1994). Kinematic Analysis and Synthesis of Mechanisms, CRC Press, New York.